PhD Research Notes

Michael Virgato

May 26, 2025

Contents

Chapter 1

Brown Dwarfs

1.1 Internal Structure

Structure equations of hydrostatic equilibrium:

$$\frac{dm}{dr} = 4\pi r^2 \rho \tag{1.1.1}$$

$$\frac{dP}{dr} = -\frac{Gm\rho}{r^2} \tag{1.1.2}$$

To obtain the radial profiles for temperature, we solve the above together with

$$\frac{dT}{d\rho} = \frac{T}{\rho^2}\frac{\left(\frac{\partial P}{\partial T}\right)}{\left(\frac{\partial u}{\partial T}\right)} \tag{1.1.3}$$

This can be rewritten in a more usable form as

$$\frac{dT}{d\rho} = \frac{dT}{dP}\frac{dP}{d\rho} \tag{1.1.4}$$

$$= \frac{dT}{dm}\frac{dm}{dP}\frac{dP}{d\rho} \tag{1.1.5}$$

$$\implies \frac{dT}{dr} = \frac{1}{\left(\frac{dr}{dP}\right)\left(\frac{dP}{d\rho}\right)}\frac{dT}{d\rho} \tag{1.1.6}$$

$$= -\frac{Gm\rho}{r^2}\frac{T}{\rho^2}\frac{1}{\left(\frac{\partial P}{\partial \rho}\right)}\frac{\left(\frac{\partial P}{\partial T}\right)}{\left(\frac{\partial u}{\partial T}\right)} \tag{1.1.7}$$

where $\rho = \rho(P, T)$. The initial conditions are then set by 2 parameters, $P(0)$ and $T(0)$, as well as $m(0) = 0$.

For a mixture of X H and and Y He, the total density and pressure is

$$\frac{1}{\rho_{mix}} = \frac{X}{\rho_H} + \frac{Y}{\rho_{He}} + \frac{Z}{\rho_Z} \tag{1.1.8}$$

$$u_{mix}(P, T) = X u_H(P, T) + Y u_{He}(P, T) + Z u_Z(P, T) \tag{1.1.9}$$

$$P_{mix} = P_H(\rho_H) + P_{He}(\rho_{He}) + P_Z(\rho_Z) \tag{1.1.10}$$

From these, the relevant derivatives can be evaluated with

$$\frac{1}{\rho_{mix}^2} d\rho_{mix} = \frac{X}{\rho_H^2} d\rho_H + \frac{Y}{\rho_{He}^2} d\rho_{He} + \frac{Z}{\rho_Z^2} d\rho_Z \tag{1.1.11}$$

$$\frac{\partial P_{mix}}{\partial \rho_{mix}} = \frac{\partial \rho_H}{\partial \rho_{mix}}\frac{\partial P_H}{\partial \rho_H} + \frac{\partial \rho_{He}}{\partial \rho_{mix}}\frac{\partial P_{He}}{\partial \rho_{He}} + \frac{\partial \rho_Z}{\partial \rho_{mix}}\frac{\partial P_Z}{\partial \rho_Z} \tag{1.1.12}$$

$$= \frac{1}{X}\frac{\rho_H^2}{\rho_{mix}^2}\frac{\partial P_H}{\partial \rho_H} + \frac{1}{Y}\frac{\rho_{He}^2}{\rho_{mix}^2}\frac{\partial P_{He}}{\partial \rho_{He}} + \frac{1}{Z}\frac{\rho_Z^2}{\rho_{mix}^2}\frac{\partial P_Z}{\partial \rho_Z} \tag{1.1.13}$$

The heavy elements are described by a scaled Helium EoS such that

$$\rho_Z(P, T) = 4\rho_{He}(P, T) \tag{1.1.14}$$

$$u_Z(P, T) = u_{He}(P, T)/4 \tag{1.1.15}$$

1.2 Review

1.2.1 Brown Dwarf/Jovian Planets

1. SIDM [24, 33]. These papers call the DM SIMPs, but really they mean DM with interactions stronger than that of WIMPS, not the $3 \to 2$ freeze-out DM.

- Ref. [33] (0408341) use Uranus' small heat production to constrain the SIDM annihilation cross section. They assume a constant SI scattering cross section for capture, with the DM-proton cross left as a free parameter. Captured SIDM are assume to be in local thermal equilibrium with the nuclei. Evaporation is calculated from the flux of SIDM that come from one interaction length beneath the planet's surface. For a given SIDM mass, there a minimum proton cross section for which limits on the annihilation rate, $\sigma v = a + b/3$ can be placed. For $\sigma_p > \sigma_{crit}$, the upper limit on a reaches a maximum value. They argue that as it is expected that the s-wave cross section should not differ from the elastic cross section by more than a few orders of magnitude, cross sections larger than σ_{crit} are ruled out.
- Ref. [24] (link to paper) study heating of Jupiter, Saturn, Neptune and Uranus. They assume the DM-proton cross section is large enough such that capture occurs in the geometric limit, with $m_\chi \sim 3\times10^6 - 10^7$ GeV. The captured DM is assumed to rapidly thermalise and have an isothermal distribution with temperature T_c. The DM is taken to be self annihilating. As the DM is very heavy, eventually it will begin to self gravitate and collapse. They study the heating produced depending on whether or not the DM reaches an equilibrium. For Saturn and Jupiter, the DM must be in a steady state to produce the heat flux, while in Neptune and Uranus it must not. They then discuss a class of hadronic axion models, with the DM being a bound state of the new fermion they introduce which is charged under $SU(3)_c$.

2. **Ref. [2] (0808.2823)** consider planetary heating due to DM accretion. They calculate (I think) the local DM density required to produce the observed heat flux from planets in the solar system.

3. **Ref. [45] (1110.5919)** looks at asymmetric DM lengthening the cooling times of BDs. They model the stellar evolution incorporating DM capture and heat transfer within MESA.

Ref.s [29, 30, 28] considered WIMPs in BDs/Jovian planets, with ref. [30] also considering a Co-SIMP DM.

Other less interesting/relevant papers on solar system constraints [27, 19].

Chapter 2

Compact Objects

2.1 Equations of State

2.1.1 Distribution Functions

The number density in phase space for a given particle species is related to the dimensionless phase space distribution function through

$$\frac{d\mathcal{R}}{d^3x d^3p} = \frac{g}{(2\pi)^3} f \tag{2.1.1}$$

Then the number density is related to these quantities through

$$\frac{dn}{d^3p} = \frac{d\mathcal{R}}{d^3x d^3p} = \frac{g}{(2\pi)^3} f \tag{2.1.2}$$

For an ideal gas in equilibrium, the distribution function is given by

$$f(E) = \frac{1}{\exp\left[(E-\mu_F)/T\right] \pm 1}. \tag{2.1.3}$$

where the $\pm$ refers to Fermi-Dirac and Bose-Einstein statistics respectively. These reduce to a simple Maxwell-Boltzmann form of

$$f(E) \approx \exp\left((\mu_F - E)/T\right) \tag{2.1.4}$$

for sufficiently low densities or and high temperatures. In the case of fermions, in the $T \to 0$ limit, μ_F is called the Fermi energy and all states bellow this level are occupied.

[M: Needs to be continued]

2.2 Beta-Equilibrium

An important process in the stability of compact objects in that of inverse β-decay,

$$e^- + p \to n + \nu \tag{2.2.1}$$

in which protons capture and electron and is converted into a neutron with the release of a neutrino, which is assumed to escape the star. This process can occur when the electrons have energy greater than the mass gap between the protons and neutrons, $m_n - m_p \sim 1.29$ MeV. This process will be an effective means of converting protons to neutrons so long as β-decay does not occur, i.e.

$$n \to e^- + p + \nu. \tag{2.2.2}$$

If the density is high enough such that all of the electron energy levels are already occupied, up to the energy of the outgoing electron, then this reaction is largely suppressed, and so we can define a critical density for which inverse β-decay dominates. Above this density, nuetron rich nuclei are stable against β-decay.

The condition for the system to be in equilibrium is given by

$$\mu_{F,e} + \mu_{F,p} = \mu_{F,n}, \tag{2.2.3}$$

we we effectively take the number density of the neutrinos vanish.

2.3 Structure Equations and Equations of State

2.3.1 Non-relativistic Structure Equations

The immense gravitational pressures within stars are balanced by an outward force leaving the medium in hydrostatic equilibrium. Consider a shell of thickness dr, which will have a mass

$$dm = 4\pi r^2 \rho(r) dr \tag{2.3.1}$$

for a spherically symmetric medium. The gravitational force experienced by this shell due to the enclosed mass, $m(r)$, will be

$$dF_g = \frac{Gm(r)dm}{r^2} \tag{2.3.2}$$

$$= 4\pi G m(r)\rho(r)dr \tag{2.3.3}$$

This will be supported by the by the difference in the pressure above and below the shell,

$$(P(r) - P(r+dr))(4\pi r^2) = 4\pi G m(r)\rho(r)dr \tag{2.3.4}$$

$$\implies -\frac{dP}{dr}r^2 dr = 4\pi G m(r)\rho(r)dr \tag{2.3.5}$$

$$\implies \frac{dP}{dr} = -\frac{Gm(r)\rho(r)}{r^2} \tag{2.3.6}$$

We can replace the mass density with the energy density through

$$\rho(r) = \epsilon(r)/c^2. \tag{2.3.7}$$

With this we can write

$$\frac{dm}{dr} = \frac{4\pi r^2 \epsilon(r)}{c^2}, \tag{2.3.8}$$

$$\frac{dP}{dr} = -\frac{G\epsilon(r)m(r)}{c^2 r^2}. \tag{2.3.9}$$

These are the coupled DEs one must solve, with $m(0) = 0$, $P(0) = P_0$. The integration ends once $P(r) = 0$, which sets the star's radius.

2.3.2 TOV Equations

The equations of hydrostatic equilibrium get modified in the framework of GR into the TOV equations

$$\frac{dP}{dr} = -\frac{Gm(r)}{r^2}\left[\rho(r) + \frac{P(r)}{c^2}\right]\left[1 + \frac{4\pi r^2 P(r)}{m(r)c^2}\right]\left[1 - \frac{2Gm(r)}{c^2 r^3}\right]^{-1} \tag{2.3.10}$$

$$\frac{dm}{dr} = 4\pi r^2 \rho(r) \tag{2.3.11}$$

These equations need to be coupled with an equation of state to relate the pressure and density of the system. Such EoSs are typically parameterised by the baryon number density n_b and specific entropy $s = S/V$ with the latter [M: why do we drop s again?...]. However is may be favourable to choose a different parameterisation of the EoS (i.e. choosing the dimensionless Fermi momentum for Fermi gasses), and so to remain somewhat general we instead choose an arbitrary parameterisation $P(\xi)$ and $\rho(\xi)$. Then the TOV equation can be written in terms of this parameter ξ. We also rescale the problem such that $r = \bar{R}x$, $m = \bar{M}u$, and demand that these scaling factors force the overall numerical factors of the two structure equations to be unity. These lead to the simplified equations

$$\frac{d\xi}{dx} = -\frac{1}{P'(\xi)}\frac{u(x)}{x^2}\left[\rho(x) + \frac{P(x)}{c^2}\right]\left[1 + \frac{x^3 P(x)}{u(x)c^2}\right]\left[1 - \frac{2u(x)}{c^2 x}\right]^{-1} \tag{2.3.12}$$

$$\frac{du}{dx} = x^2 \rho(x) \tag{2.3.13}$$

$$\bar{M} = \frac{1}{2\sqrt{G_N^3 \pi}} \tag{2.3.14}$$

$$\bar{R} = \frac{1}{2\sqrt{G_N \pi}} \tag{2.3.15}$$

where we have assumed that the exact form of $P'(\xi)$ is unknown. If it is the case that one can obtain a closed form expression for $P'(\xi)$, then the scaling factors will need to be recalculated. [M: just add $P'(\xi)$, not the other scalings]

Chapter 3

White Dwarfs

3.1 Background

The crusts[M: ?] of white dwarf (WD) stars are composed primarily of carbon and oxygen, with an interior consisting of a degenerate electron gas [38]. Hydrostatic equilibrium is maintained through the electron degenerate pressure. This arises from the Pauli exclusion principle, stating that no two fermions can occupy the same quantum state. This implies that no more than two electrons (due to them being spin-1/2) can occupy the same phase space. The phase space is then filled from the lowest energy states to the highest, with the electron velocity increasing. These high velocities lead to high pressures which counter balance the pull of gravity. As electrons have the lightest mass, they will become degenerate earliest in the dense matter. The contribution to the pressure from the carbon and oxygen nuclei can be neglected in the regions of density considered

3.2 TOV and EoS

3.2.1 General Setup

Coupling the EoS to the TOV equations results in the coupled set of ODEs we need to solve,

$$\frac{dm}{dr} = 4\pi r^2 \frac{\epsilon(\xi)}{c^2} \tag{3.2.1}$$

$$\frac{d\xi}{dr} = \frac{-1}{p'(\xi)} \frac{G}{c^2} \frac{\epsilon(\xi) + p(\xi)}{r(r - \frac{2G}{c^2} m(r))} \left[m(r) + \frac{4\pi}{c^2} p(\xi) r^3 \right] \tag{3.2.2}$$

where $p'(\xi) = dp/d\xi$. Note that this is general for any parameterization of the EoS so long as the parameter ξ's radial dependence is known

3.2.2 Ideal Case: Relativistic Fermi Gas

$$\frac{dm}{dr} = 4\pi \frac{32\mu M_u K}{3mc^2} r^2 \sinh^3\left(\frac{\xi}{4}\right) f(\xi) \tag{3.2.3}$$

$$\frac{d\xi}{dr} = \frac{-32G\mu M_u}{mc^2 \left(\cosh(\xi) - 4\cosh\left(\frac{\xi}{2}\right) + 3\right) r} \left[\sinh^3\left(\frac{\xi}{4}\right) f(\xi) + \frac{m}{32\mu M_u} \left(\sinh(\xi) - 8\sin\left(\frac{\xi}{2}\right) + 3\xi \right) \right] \times \left[m(r) + \frac{4\pi K \left(\sinh(\xi) - 8\sinh\left(\frac{\xi}{2}\right) + 3\xi \right) r^3}{3c^2} \right] \left[r - \frac{2Gm(r)}{c^2} \right]^{-1} \tag{3.2.4}$$

Scale the variables ($r = R_s x, m = M_s u$) such that the numerical pre-factors are of order 1

$$M_s = \sqrt{\frac{3}{G^3 K \pi}} \frac{c^4 m^2}{2048 M_u^2 \mu^2} = 3.17044 \times 10^{28} \mu^{-2} \text{kg} \tag{3.2.5}$$

$$R_s = \sqrt{\frac{3}{GK\pi}} \frac{c^2 m}{64 M_u \mu} = 1.37339 \times 10^6 \mu^{-1} \text{m} \tag{3.2.6}$$

These values are slightly different than the scales given in Matthew

3.2.3 Newtonian Case

$$\frac{du}{dx} = x^2 \sinh^3\left(\frac{\xi}{4}\right) f(\xi) \tag{3.2.7}$$

$$\frac{d\xi}{dx} = -\frac{u(x) \sinh^3\left(\frac{\xi}{4}\right)}{\left(\cosh(\xi) - 4\cosh\left(\frac{\xi}{2}\right) + 3\right) x^2} \tag{3.2.8}$$

3.2.4 Results

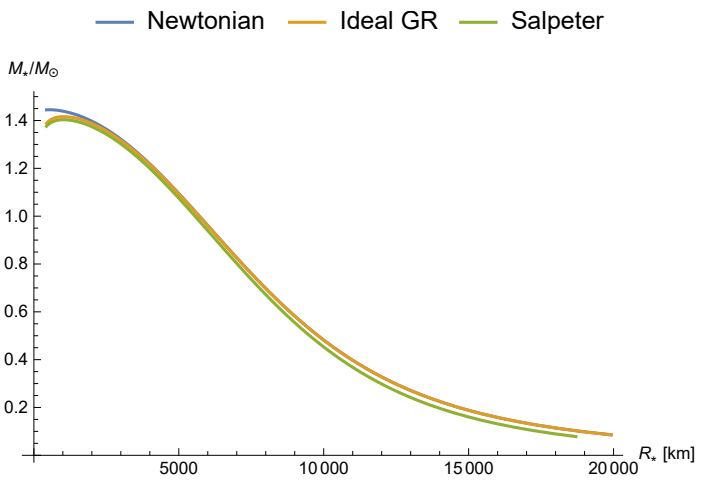

Figure 3.1: Mass-Radius relationship for Newtonian (blue), Ideal (orange) and Salpeter EoS (green) cases

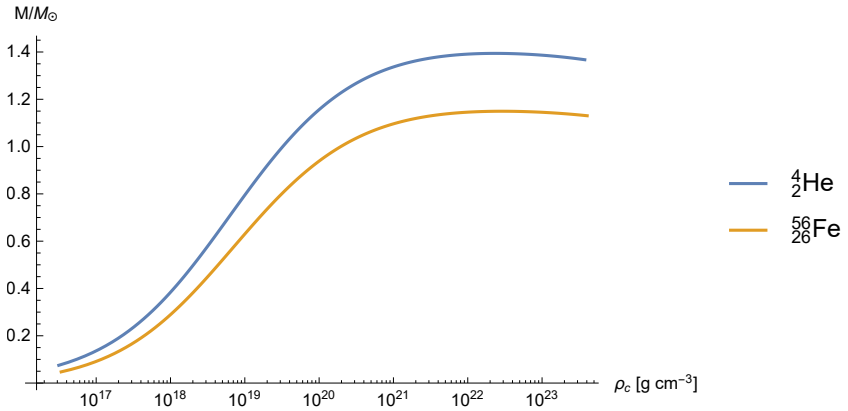

Figure 3.2: Maximum mass as a function of central density for the TOV equations coupled to the Salpeter EoS for $^{4}_{2}$He and $^{56}_{26}$Fe .

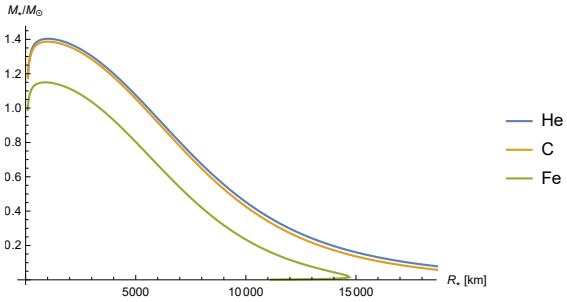

Figure 3.3: Mass-Radius relation for $^{4}_{2}$He, $^{12}_{6}$C and $^{56}_{26}$Fe white dwarfs from TOV with Salpeter EoS.

	$M_c/M_\odot$	ρ_c (2×10^{10} g cm $^{-3}$)
$^{4}_{2}$He	1.39412	1.17072
$^{12}_{6}$C	1.38638	1.17921
$^{16}_{8}$O	1.37945	1.1869
$^{20}_{10}$Ne	1.37306	1.19406
$^{24}_{12}$Mg	1.36707	1.20084
$^{28}_{14}$Si	1.36138	1.20735
$^{32}_{16}$S	1.35594	1.21355
$^{56}_{26}$Fe	1.14943	1.44658

Table 3.1: List of critical mass and central densities for white dwarf stars of various composotions using the Salpeter EoS

3.3 Feynman-Metropolis-Teller EoS

3.3.1 Zero Temperature Limit

The relativistic condition for equilibrium is stated in terms of the Fermi energy is

$$E_e^F = \sqrt{c^2(p_f^F)^2 + m_e^2c^4} - m_ec^2 - V(r) = \text{constant} > 0 \tag{3.3.1}$$

where $V(r)$ is the Coulomb potential. To avoid this expression leading to a non-integrable result for the electron density at the origin, the notion of a point like nucleus must be abandoned. To this end, the protons are assumed uniformly distributed within a radius of

$$R_c = \Delta\lambda_\pi Z^{1/3}, \tag{3.3.2}$$

where λ_π is the pion Compton wavelength and $\Delta \approx (r_0/\lambda_\pi)(A/Z)^{1/3}$, with $r_0 \approx 1.2$ fm. The proton number density can then be expressed as

$$n_p = \frac{(p_p^F)^3}{3\pi^2\hbar^3} = \frac{3Z}{4\pi R_c^3}\theta(R_c - r) = \frac{3}{4\pi}\left(\frac{1}{\Delta\lambda_\pi}\right)^3\theta(R_c - r) \tag{3.3.3}$$

The number density of electrons in the cell is

$$n_e = \frac{(p_e^F)^3}{3\pi^2\hbar^3} = \frac{1}{3\pi^2\hbar^3}\left[\hat{V}^2(r) + 2m_ec^2\hat{V}(r)\right]^{3/2} \tag{3.3.4}$$

$$n_0 = \frac{3Z}{4\pi R_{ws}^3} \tag{3.3.5}$$

where

$$\hat{V}(r) = eV(r) + E_e^F. \tag{3.3.6}$$

and n_0 is the average electron number density. The Coulomb potential satisfies the Poisson equation

$$\nabla^2 V(r) = -4\pi e\left[n_p(r) - n_e(r)\right], \tag{3.3.7}$$

with the conditions $dV/dr|_{r=R_{WS}} = 0$ and $V(R_{WS}) = 0$ due to the global charge neutrality of the cell. We introduce the dimensionless quantities $x = r/\lambda_\pi$ and $\beta(r) = r\hat{V}(r)/(\hbar c)$, giving $x_c = R_c/\lambda_\pi$, $x_{WS} = R_{WS}/\lambda_\pi$. Combining the above, the Laplace equation to

$$\frac{1}{3x}\frac{d^2\beta}{dx^2} = -\frac{\alpha}{\Delta^3}\theta(x_c - x) + \frac{4\alpha}{9\pi}\left[\frac{\beta^2(x)}{x^2} + 2\frac{m_e}{m_\pi}\frac{\beta(x)}{x}\right]^{3/2} \tag{3.3.8}$$

subject to the boundary conditions

$$\beta(0) = 0 \tag{3.3.9}$$

$$d\beta/dx|_{x_{WS}} = \beta(x_{WS})/x_{WS} \tag{3.3.10}$$

along with $\beta(x_{WS}) \geq 0$. Once the solution is found, $\hat{V}(r)$ is straightforwardly obtained. From this, one can obtain the electron number density and Fermi momentum. In order to obtain the Coulomb potential, we first need the need the electron's Fermi energy. As E_F is constant throughout the cell, we evaluate Eq. 3.3.1 at x_{WS} where $V(x_{WS}) = 0$. Using this result in Eq. 3.3.6 gives the Coulomb energy.

3.3.2 Finite Temperature Extension

The extension to finite temperatures is made by reintroducing the temperature dependence in the Fermi-Dirac distributions. Now, the electron chemical potential is no longer simply the Fermi energy of the system, but will have thermal corrections. Define the finite temperature Fermi-Dirac integrals as

$$F_k(\eta, \beta) = \int_0^\infty \frac{t^k\sqrt{1 + (\beta/2)t}}{1 + e^{t-\eta}}dt \tag{3.3.11}$$

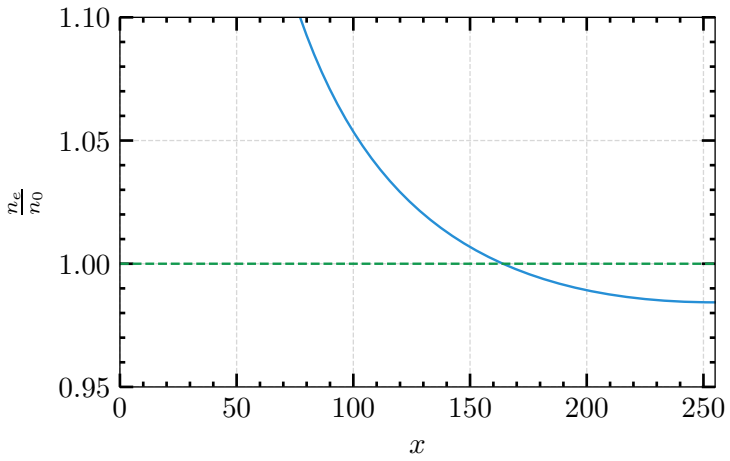

Figure 3.4: Electron number density n_e in units of the average number density n_0. Seems to agree with Ref. [37] Fig. 1.

where we define the dimensionless quantities

$$t = \frac{E_e - m_e c^2}{k_B T} \tag{3.3.12}$$

$$\eta = \frac{\mu_e}{k_B T} \tag{3.3.13}$$

$$\beta = \frac{k_B T}{m_e c^2} \tag{3.3.14}$$

and μ_e is the electron chemical potential minus the rest mass. The Thomas-Fermi equilibrium condition is given by

$$\mu_e(r) - eV(r) = k_B T \eta(r) - eV(r) = constant \tag{3.3.15}$$

with the Coulomb potential vanishing at the boundary of the cell. Now taking $\chi/r = \mu_e/(\hbar c)$, the Poisson equation Eq. 3.3.7 becomes

$$\frac{d^2\chi}{dx^2} = -4\pi\alpha x \left[\frac{3}{4\pi\Delta^3}\theta(x_c - x) - \frac{\sqrt{2}}{\pi^2}\left(\frac{m_e}{m_\pi}\right)^2 \left[F_{1/2}(\eta,\beta) + \beta F_{3/2}(\eta,\beta)\right] \right] \tag{3.3.16}$$

$$\eta = \left(\frac{\hbar c}{\lambda_\pi k_B T}\right)\frac{\chi}{x}. \tag{3.3.17}$$

Converting to a the non-linear system needed to apply Newton's method, we have the following required equations

$$\frac{d\chi}{dx} = \omega \tag{3.3.18}$$

$$\frac{d\omega}{dx} = -4\pi\alpha x \left[\frac{3}{4\pi\Delta^3}\theta(x_c - x) - \frac{\sqrt{2}}{\pi^2}\left(\frac{m_e}{m_\pi}\right)^2 \left[F_{1/2} + \beta F_{3/2}\right] \right] \tag{3.3.19}$$

$$\frac{d\xi}{dx} = \gamma \tag{3.3.20}$$

$$\frac{d\gamma}{dx} = \frac{4\sqrt{2}\alpha x}{\pi}\left(\frac{m_e}{m_\pi}\right)^3 \beta^{3/2}\left[\frac{\partial F_{1/2}}{\partial\chi} + \beta\frac{\partial F_{3/2}}{\partial\chi}\right]\xi \tag{3.3.21}$$

with the numerical procedure requiring

$$\frac{\partial \chi'}{\partial x} = 0 \tag{3.3.22}$$

$$\frac{\partial \omega'}{\partial x} = -\frac{3\alpha}{\Delta^3}\theta(x_c - x) + \frac{4\sqrt{2}\alpha}{\pi}\left(\frac{m_e}{m_\pi}\right)^3 \beta^{3/2}\left[F_{1/2} + \beta F_{3/2} + x\left(\frac{\partial F_{1/2}}{\partial x} + \beta\frac{\partial F_{3/2}}{\partial x}\right)\right] \tag{3.3.23}$$

$$\frac{\partial \xi'}{\partial x} = 0 \tag{3.3.24}$$

$$\frac{\partial \gamma'}{\partial x} = \frac{4\sqrt{2}\alpha}{\pi}\left(\frac{m_e}{m_\pi}\right)^3 \beta^{3/2}\left[\frac{\partial F_{1/2}}{\partial \chi} + \beta\frac{\partial F_{3/2}}{\partial \chi} + x\left(\frac{\partial^2 F_{1/2}}{\partial \chi \partial x} + \beta\frac{\partial^2 F_{3/2}}{\partial \chi \partial x}\right)\right]\xi \tag{3.3.25}$$

3.3.3 Thomas-Fermi Digression

To understand this, we first attempt to solve the simpler Thomas-Fermi equation,

$$\frac{d^2\phi}{dx^2} = \frac{\phi^{3/2}(x)}{\sqrt{x}} \tag{3.3.26}$$

with the conditions

$$\phi(0) = 1 \tag{3.3.27}$$

$$x_{WS}\left.\frac{d\phi}{dx}\right|_{x_{WS}} = \phi(x_{WS}) \tag{3.3.28}$$

This last condition is a statement that the line tangent to the point $(x_{WS}, \phi(x_{WS})$, i.e. the edge of the Wigner-Seitz cell, passes through the origin.

The solutions are obtained by varying the initial value of the derivative and checking if the solution satisfies the end BC up to a certain tolerance, such that

$$a(x_{WS}) = |\beta(x_{WS}) - x_{WS}\beta'(x_{WS})| \tag{3.3.29}$$

$$a < 1 \times 10^{-7} \tag{3.3.30}$$

The tolerance may be changed, depending on the accuracy we want.

Thomas Fermi Equation

Found solutions for $x_{WS} \lesssim 15$. Can go higher, need to change the increment size of $\phi'(0) = \phi_0$. Larger values of x_{WS} become more and more sensitive to the value of ϕ_0 as the solution begins to asymptote.

3.3.4 Nonlinear Shooting with Newton's method

Demonstration of nonlinear shooting method applied to the Feynman-Metropolis-Teller equation of state for white dwarf stars.

$$y'' = f(x, y, y'), \quad a \le x \le b, \tag{3.3.31}$$

where we take

$$f(x, y, y') = -\frac{3x\alpha}{\Delta^3}\theta(x_c - x) + \frac{4x\alpha}{3\pi}\left[\frac{y^2(x)}{x^2} + 2\frac{m_e}{m_\pi}\frac{y(x)}{x}\right]^{3/2}, \quad 0 \le x \le x_{WS} \tag{3.3.32}$$

with boundary conditions

$$a_0 y(a) - a_1 y'(a) = \gamma. \tag{3.3.33}$$

$$b_0 y(b) + b_1 y'(b) = \beta. \tag{3.3.34}$$

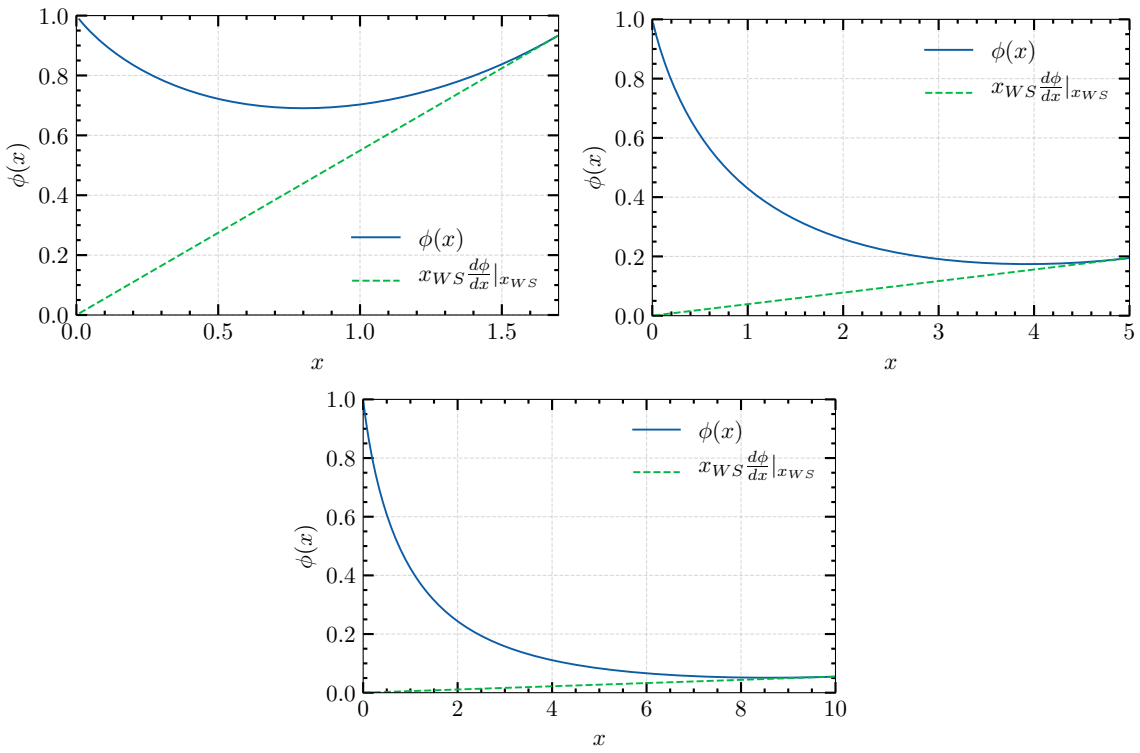

Figure 3.5: TF solution for $x_{WS} = 1.7,\ 5,\ 10$

In the present case we have

$$a_0 = 1, \quad a_1 = 0, \quad b_0 = 1, \quad b_1 = -x_{WS}, \quad \gamma = 0, \quad \beta = 0 \tag{3.3.35}$$

The related IVP is then given by

$$u'' = f(x, u, u') \tag{3.3.36}$$

with initial conditions parameterised by s given by

$$u(a) = a_1 s - c_1\gamma \tag{3.3.37}$$
$$u'(a) = a_0 s - c_0\gamma \tag{3.3.38}$$

where the coefficients c_0 and c_0 are any constants such that

$$a_1 c_0 - a_0 c_1 = 1. \tag{3.3.39}$$

Hence we have $c_1 = -1$, and c_0 is a free parameter (set to 0?), leaving

$$u(0) = 0 \tag{3.3.40}$$
$$u'(0) = s - c_0. \tag{3.3.41}$$

The solution to the IVP now depends on the value of s, so we write it as $u(x; s)$. Then this solution to the IVP will also satisfy the BVP if s is a root of

$$\phi(s) = b_0 u(b; s) + b_1 u'(b; s) - \beta = 0 \tag{3.3.42}$$
$$\implies \phi(s) = u(x_{WS}; s) - x_{WS} u'(x_{WS}; s) = 0 \tag{3.3.43}$$

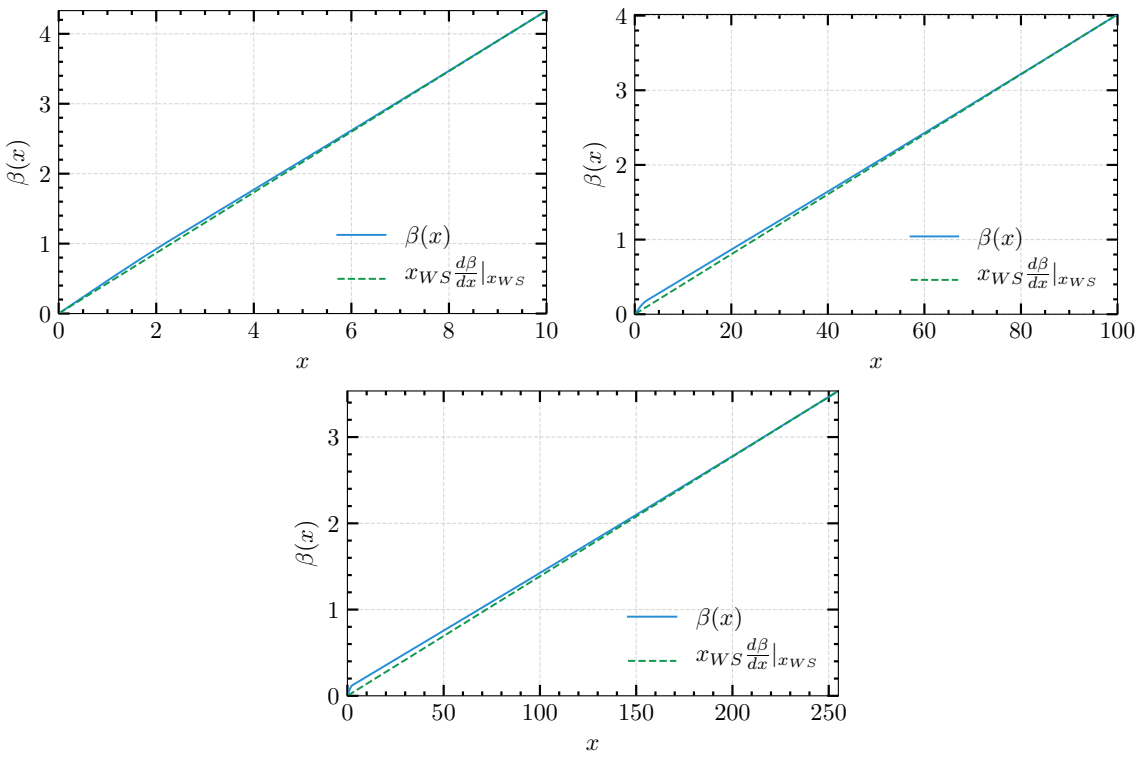

Figure 3.6: Solutions of Eq. 3.3.8 for $x_{WS} = 10,\ 100,\ 255$.

To solve the IVP we set up the system of equations

$$u' = v \tag{3.3.44}$$
$$v' = f(x, u, v) \tag{3.3.45}$$

with the conditions

$$u(a) = a_1 s - c_0 \gamma \tag{3.3.46}$$
$$v(a) = a_0 s - c_0 \gamma \tag{3.3.47}$$

which gives

$$u(0) = 0 \tag{3.3.48}$$
$$v(0) = s - c_0 \tag{3.3.49}$$

and denote the solutions as $u(x; s)$ and $v(x; s)$, leaving

$$\phi(s) = b_0 u(b; s) + b_1 v(b; s) - \beta = 0 \tag{3.3.50}$$
$$\implies \phi(s) = u(x_{WS}; s) - x_{WS} v(x_{WS}; s) = 0 \tag{3.3.51}$$

To find the root we apply Newton's method to obtain

$$s_{i+1} = s_i - \frac{\phi(s_i)}{\dot{\phi}(s_i)} \tag{3.3.52}$$

where

$$\dot{\phi}(s) = \frac{\partial \phi}{\partial s}. \tag{3.3.53}$$

We now need to find $\dot{\phi}(s)$. This is done by defining

$$\xi(x) = \frac{\partial u(x;s)}{\partial s} \tag{3.3.54}$$

$$\eta(x) = \frac{\partial v(x;s)}{\partial s} \tag{3.3.55}$$

which gives the resulting additional system of ODEs

$$\xi' = \eta \tag{3.3.56}$$

$$\eta' = p(x;s)\eta + q(x;s)\xi \tag{3.3.57}$$

with the initial conditions are

$$\xi(a) = a_1 \tag{3.3.58}$$

$$\eta(a) = a_0 \tag{3.3.59}$$

The coefficents are defined as

$$p(x;s) = \frac{\partial f}{\partial v} \tag{3.3.60}$$

$$q(x;s) = \frac{\partial f}{\partial u} \tag{3.3.61}$$

For our example we have

$$p(x;s) = 0 \tag{3.3.62}$$

$$q(x;s) = \frac{4\alpha}{\pi}\left[\frac{u^2}{x^2} + 2\frac{m_e}{m_\pi}\frac{u}{x}\right]^{1/2}\left[\frac{u}{x} + \frac{m_e}{m_\pi}\right] \tag{3.3.63}$$

thus we can write

$$\dot{\phi}(s) = b_0\xi(b;s) + b_1\eta(b;s) \tag{3.3.64}$$

$$\implies \dot{\phi}(s) = \xi(x_{WS};s) - x_{WS}\eta(x_{WS};s) \tag{3.3.65}$$

The system we need to solve is then

$$u' = v, \tag{3.3.66}$$

$$v' = -\frac{3x\alpha}{\Delta^3}\theta(x_c - x) + \frac{4x\alpha}{3\pi}\left[\frac{u^2}{x^2} + 2\frac{m_e}{m_\pi}\frac{u}{x}\right]^{3/2}, \tag{3.3.67}$$

$$\xi' = \eta \tag{3.3.68}$$

$$\eta' = \frac{4\alpha}{\pi}\left[\frac{u^2}{x^2} + 2\frac{m_e}{m_\pi}\frac{u}{x}\right]^{1/2}\left[\frac{u}{x} + \frac{m_e}{m_\pi}\right]\xi \tag{3.3.69}$$

with the conditions

$$u(0) = 0, \quad v(0) = s \tag{3.3.70}$$

$$\xi(0) = 0, \quad \eta(0) = 1 \tag{3.3.71}$$

where s is determined through

$$s_{i+1} = s_i - \frac{u(x_{WS};s_i) - x_{WS}v(x_{WS};s_i)}{\xi(x_{WS};s_i) - x_{WS}\eta(x_{WS};s_i)} \tag{3.3.72}$$

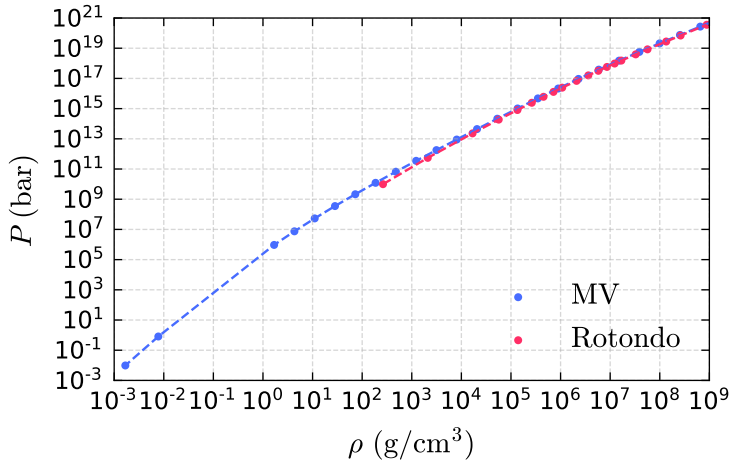

Figure 3.7: Comparison with Rotondo

with s_0 arbitrary, but should be somewhat close to the true value. The Jacobian matrix is

$$J = \begin{pmatrix} 0 & 1 & 0 & 0 \\ \frac{4\alpha}{\pi}\left[\frac{u^2}{x^2} + 2\frac{m_e}{m_\pi}\frac{u}{x}\right]^{1/2}\left[\frac{u}{x} + \frac{m_e}{m_\pi}\right] & 0 & 0 & 0 \\ 0 & 0 & 0 & 1 \\ \frac{8\alpha\xi}{\pi x}\frac{\left(\frac{u^2}{x^2}+2\frac{m_e u}{m_\pi x}+\frac{m_e^2}{2m_\pi^2}\right)}{\left(\frac{u^2}{x^2}+2\frac{m_e}{m_\pi}\frac{u}{x}\right)^{1/2}} & 0 & \frac{4\alpha}{\pi}\left[\frac{u^2}{x^2} + 2\frac{m_e}{m_\pi}\frac{u}{x}\right]^{1/2}\left[\frac{u}{x} + \frac{m_e}{m_\pi}\right] & 0 \end{pmatrix} \tag{3.3.73}$$

with

$$\frac{\partial}{\partial x}\begin{pmatrix} u' \\ v' \\ \xi' \\ \eta' \end{pmatrix} = \begin{pmatrix} 0 \\ -\frac{3\alpha}{\Delta^3}\theta(x_c - x) - \frac{8\alpha}{3\pi}\left[\frac{u^2}{x^2} + 2\frac{m_e}{m_\pi}\frac{u}{x}\right]^{1/2}\left[\frac{u^2}{x^2} + \frac{m_e}{2m_\pi}\frac{u}{x}\right] \\ 0 \\ -\frac{8\alpha\xi}{\pi x^2}\frac{\left(\frac{u^2}{x^2}+2\frac{m_e u}{m_\pi x}+\frac{m_e^2}{2m_\pi^2}\right)}{\left(\frac{u^2}{x^2}+2\frac{m_e}{m_\pi}\frac{u}{x}\right)^{1/2}} \end{pmatrix} \tag{3.3.74}$$

System is highly dependent on the initial gradient used to start the shooting, with the accuracy increasing with x_{WS}. To deal with this, the system must be solved sequentially, with the previous successful initial gradient used to solve the system for the next x_{WS}. [M: There are still pathological points for $x_{WS} > 1 \times 10^4$ where the integrator breaks down. This is because the Newton's method does not increment the initial gradient within the required accuracy. When this happens, shifting the initial gradient by a small amount so that a solution is found enables Newton's method to converge on a solution.]

3.3.5 TOV Solutions from FMT EoS

Parameterize the EoS with the Wigner-Seitz cell radius x_{WS}, giving the TOV equations in the form

$$\frac{dm}{dr} = 4\pi r^2 \rho(x_{WS}) \tag{3.3.75}$$

$$\frac{dx_{WS}}{dr} = \frac{-G}{p'(x_{WS})}\frac{\rho(x_{WS}) + p(x_{WS})/c^2}{r(r - \frac{2G}{c^2}m(r))}\left[m(r) + \frac{4\pi}{c^2}p(x_{WS})r^3\right] \tag{3.3.76}$$

The resulting mass-radius relation is shown in Fig. 3.9. The required x_{WS} range was $x_c = 1.94055$ tp 1×10^4.

Critical mass and density are $M_\star = 1.38705 M_\odot$ and $\rho_c = 2.29059 \times 10^{10} g/cm^3$

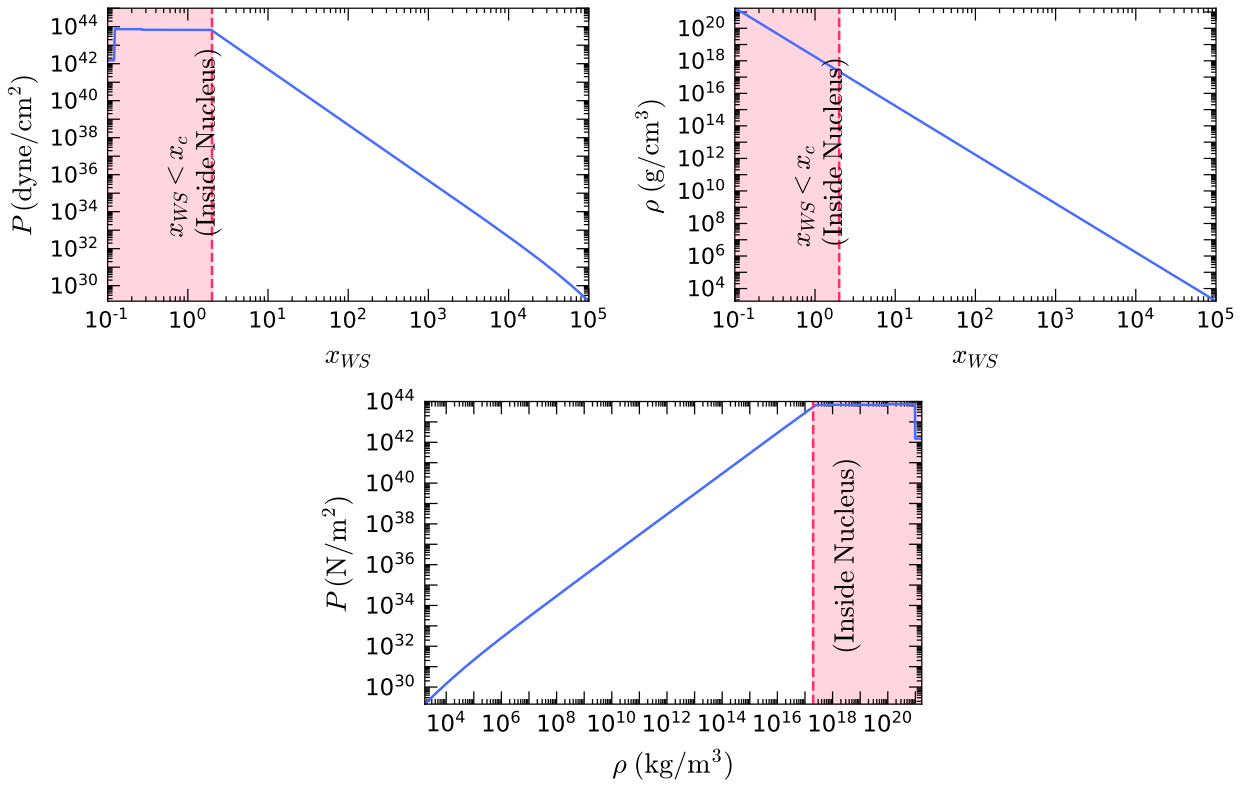

Figure 3.8: Pressure and density as a function of the Wigner-Seitz cell radius and the pressure-density relation for Carbon white dwarfs.

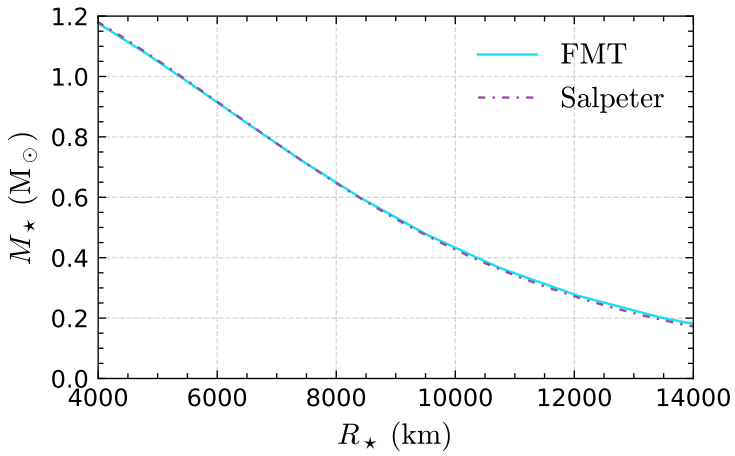

Figure 3.9: Mass radius relationship for Carbon white dwarf using the FMT EoS.

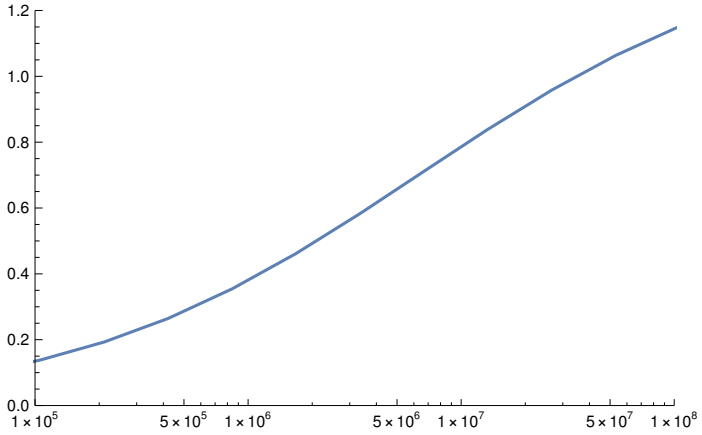

Figure 3.10: Mass-central density relation

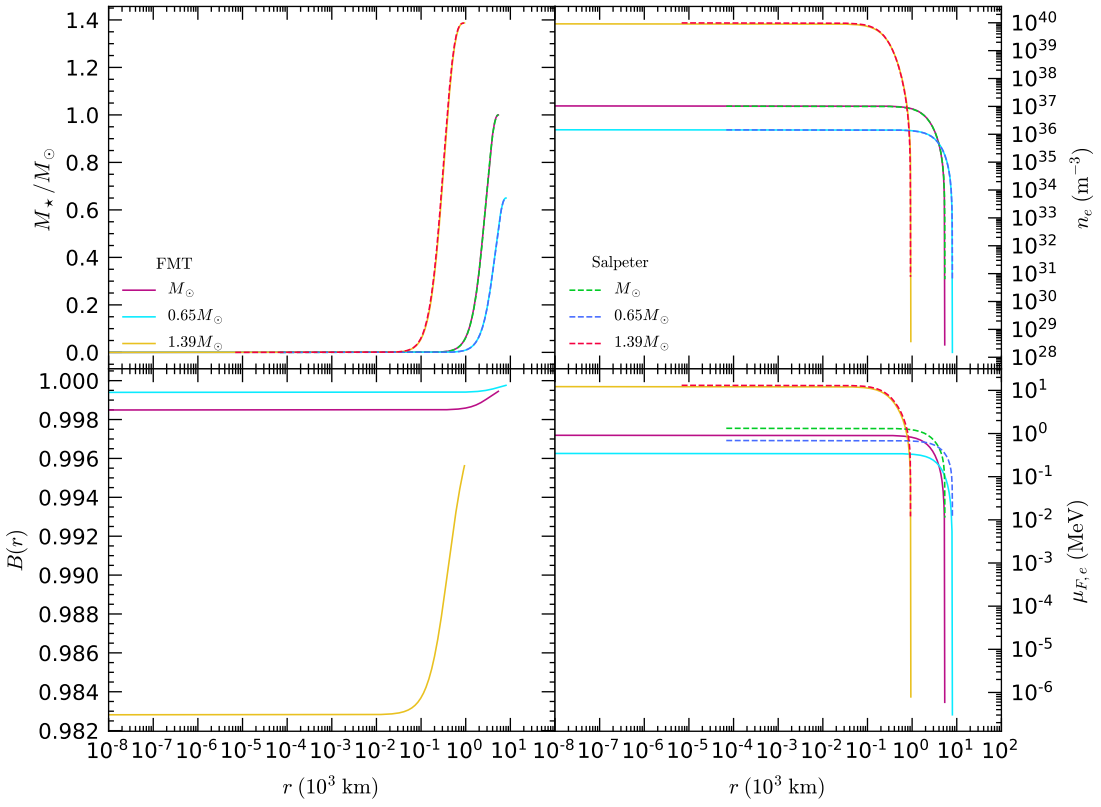

Figure 3.11: Radial profiles of EOS dependent variables for white dwarfs of mass $1.39M_\odot$, $1M_\odot$, $0.65M_\odot$

The electron number density is calculated as the average number density of the Wigner-Seitz cell at given radius,

$$n_e(x_{WS}(r)) = \frac{3Z}{4\pi(x_{WS}(r)\lambda_\pi)^3} \tag{3.3.77}$$

[M: Should be changed to the value of the number density at the edge of the cell] The electron chemical potential, $\mu_{F,e}$, must be calculated alongside the solution to the relativistic Thomas-Fermi equation for each x_{WS} via Eqn. 3.3.1.

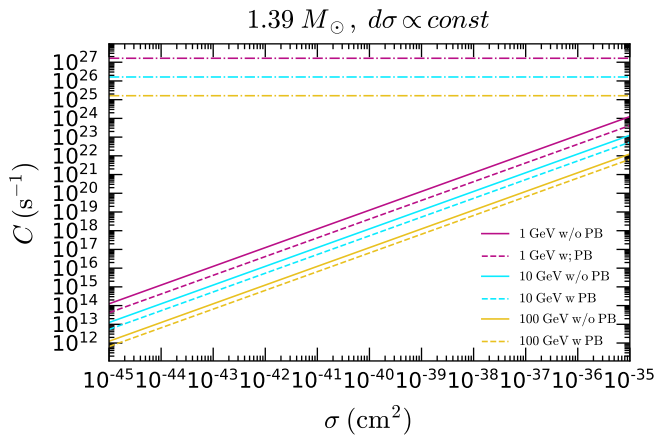

Figure 3.12: Caption

3.4 Capture on Electrons

Unlike neutron stars, the boost to the DM velocity due to the WD's potential well is not substantial enough to justify neglecting the initial velocity at infinity, u_χ, hence we cannot simply integrate over it. Reintroducing this integral, the capture rate is then given by

$$C = 4\pi \frac{\rho_\chi}{m_\chi} \int_0^{R_\star} dr\, \zeta(r) \frac{\sqrt{1-B(r)}}{B(r)} r^2 \int_0^\infty du_\chi\, \frac{f_{MB}(u_\chi)}{u_\chi} \Omega^-(r) \tag{3.4.1}$$

$$\Omega^-(r) = \int dE_e\, ds\, dt \frac{d\sigma}{d\cos\theta_{cm}} \frac{E_e}{2\pi^2 m_\chi} \sqrt{\frac{B(r)}{1-B(r)}} \frac{s}{\beta(s)\gamma(s)} f_{FD}(E_e, r)(1 - f_{FD}(E_e^{'}, r)) \tag{3.4.2}$$

$$f_{MB}(u_\chi) = \frac{u_\chi}{v_\star v_d} \sqrt{\frac{3}{2\pi}} \left[e^{-\frac{3(u_\chi - v_\star)^2}{2v_d^2}} - e^{-\frac{3(u_\chi + v_\star)^2}{2v_d^2}} \right] \tag{3.4.3}$$

The full capture rate is then given by

$$C = \frac{2}{\pi} \frac{\rho_\chi}{m_\chi^2 v_s v_d} \sqrt{\frac{3}{2\pi}} \int_0^{R_\star} dr\, \frac{\zeta(r)}{\sqrt{B(r)}} r^2 \int_0^\infty du_\chi\, \frac{f_{MB}(u_\chi)}{u_\chi} \int dt\, dE_e\, ds \frac{d\sigma}{d\cos\theta_{cm}} \frac{E_e s}{\beta(s)\gamma(s)} \times f_{FD}(E_e)(1 - f_{FD}(E_e^{'})) \tag{3.4.4}$$

We must also modify the DM energy and momentum so be

$$E_\chi = \frac{m_\chi}{\sqrt{B(r)}} \left(1 + \frac{1}{2} u_\chi^2\right) \tag{3.4.5}$$

$$p_\chi = \frac{m_\chi}{\sqrt{B}} \sqrt{(1 + \frac{1}{2} u_\chi^2)^2 - B} \tag{3.4.6}$$

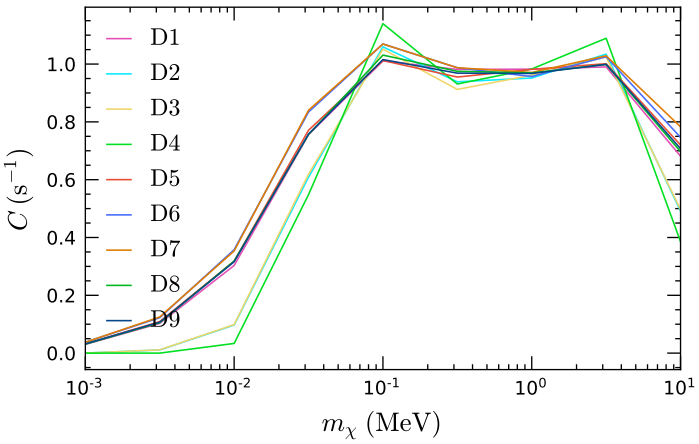

Figure 3.13: y-axis should be Girogio's/my results

and the limits of integration

$$t_{max} = 0 \tag{3.4.7}$$

$$t_{min} = -\frac{\gamma^2(s)}{s} \tag{3.4.8}$$

$$s_{max} = m_e^2 + m_\chi^2 + 2\frac{m_\chi}{\sqrt{B(r)}}\left(1+\frac{1}{2}u_\chi^2\right)E_e + 2\frac{m_\chi}{\sqrt{B}}\sqrt{(1+\frac{1}{2}u_\chi^2)^2 - B}\sqrt{E_e^2 - m_e^2} \tag{3.4.9}$$

$$s_{min} = m_e^2 + m_\chi^2 + 2\frac{m_\chi}{\sqrt{B(r)}}\left(1+\frac{1}{2}u_\chi^2\right)E_e - 2\frac{m_\chi}{\sqrt{B}}\sqrt{(1+\frac{1}{2}u_\chi^2)^2 - B}\sqrt{E_e^2 - m_e^2} \tag{3.4.10}$$

$$E_{e,min} = m_e \tag{3.4.11}$$

$$E_{e,max} = m_e + \mu_{F,e} \tag{3.4.12}$$

For DM masses below $10^{-6} \lesssim m_\chi \lesssim \mu_{F,e}/m_e$, the kinetic energy on impact is not great enough to expel an electron from the Fermi sea in the interior of the star, and so capture only occurs at the surface, significantly reducing the capture rate in this region.

3.5 Evaporation

[M: This is outdated, it uses non-relativistic formalism] Focusing on the isothermal component on the DM distribution,

$$n_{\chi,iso} = \frac{e^{-r^2/r_\chi^2}}{\int_0^{R_\star} 4\pi r^2 e^{-r^2/r_\chi^2} dr} = N_{iso} e^{-r^2/r_\chi^2} \tag{3.5.1}$$

$$r_\chi = \sqrt{\frac{3T_{\star,c}}{2\pi G \rho_c m_\chi}} \tag{3.5.2}$$

where $T_{\star,c}$, ρ_c are the central temperature and density of the star. The evaporation rate in the non-relativistic formalism is given by

$$E = \int_0^{R_\star} dr\ 4\pi r^2 \int_0^{v_{esc}(r)} dw\ 4\pi w^2 f_{MB}^{evap}(r,w)\ \Omega^+(w) \tag{3.5.3}$$

$$\Omega^+(w) = \int_{v_{esc}(r)}^{\infty} dv\ R^+(w \to v) \tag{3.5.4}$$

$$R^+(w \to v) = \frac{32\mu_+^4}{\sqrt{\pi}} \frac{v}{w} k^3 n_r(r) \int_0^\infty ds \int_0^\infty dt\ t e^{-k^2 u_e^2} \frac{d\sigma}{d\cos\theta} \Theta(t+s-v)\Theta(w-|t-s|) \tag{3.5.5}$$

$$f_{MB}^{evap}(r,w) = n_{\chi,iso}(r) \left(\frac{m_\chi}{2\pi T_\star}\right)^{3/2} e^{-\frac{m_\chi w^2}{T_\star}} \tag{3.5.6}$$

$$\mu = \frac{m_\chi}{m_e} \tag{3.5.7}$$

$$\mu_\pm = \frac{1 \pm \mu}{2} \tag{3.5.8}$$

$$k^2 = \frac{m_e}{2T_\star} \tag{3.5.9}$$

$$u_e^2 = 2\mu\mu_+ t^2 + 2\mu_+ s^2 - \mu w^2 \tag{3.5.10}$$

$$v_{esc}^2(r) = 1 - B(r) \tag{3.5.11}$$

For simplicity I have assumed the DM is at the same temperature as the star. The complete expression for the evaporation rate in this approximation is

$$E = 128\sqrt{\pi}\mu_+^4 k^3 N_{iso} \int_0^{R_\star} dr \int_0^{v_{esc}(r)} dw \int_{v_{esc}(r)}^\infty dv \int_0^\infty ds \int_0^\infty dt\ r^2 n_e(r) \frac{vt}{w} e^{-r^2/r_\chi^2}\ e^{-m_\chi w^2/T_\star}\ e^{-k^2 u_e^2} \times \frac{d\sigma}{d\cos\theta} \Theta(t+s-v)\Theta(w-|t-s|) \tag{3.5.12}$$

Need to add the local thermal equilibrium (LTE) component of the DM distribution, which requires the calculation of transport quantities for WDs.

Chapter 4

Interaction Rates Including Pauli Blocking

4.1 Differential Interaction Rate

We write the differential interaction rate following ref. [11] as

$$\Gamma = \int \frac{d^3k^{'}}{(2\pi)^3} \frac{1}{(2E_\chi)(2E^{'}_\chi)(2m_n)(2m_n)} \Theta(E^{'}_\chi - m_\chi)\Theta(\pm q_0) S(q_0, q) \tag{4.1.1}$$

$$\begin{aligned} S(q_0, q) = 2 \int \frac{d^3p}{(2\pi)^3} \int \frac{d^3p^{'}}{(2\pi)^3} \frac{m_n^2}{E_n E^{'}_n} \left|\overline{\mathcal{M}}\right|^2 (2\pi)^4 \delta^4 \left(k_\mu + p_\mu - k^{'}_\mu - p^{'}_\mu\right) \\ \times f_{FD}(E_n)(1 - f_{FD}(E^{'}_n))\Theta(E_n - m_n)\Theta(E^{'}_n - m_n) \end{aligned} \tag{4.1.2}$$

Integrating over $d^3p^{'}$ using the delta function leaves

$$S(q_0, q) = \frac{1}{2\pi^2} \int d^3p \, \frac{m_n^2}{E_n E^{'}_n} \left|\overline{\mathcal{M}}\right|^2 \delta\left(q_0 + E_n - E^{'}_n\right) f_{FD}(E_n)(1 - f_{FD}(E^{'}_n))\Theta(E_n - m_n)\Theta(E^{'}_n - m_n) \tag{4.1.3}$$

After this, the final state neutron energy is fixed to

$$E^{'}_n(E_n, q, \theta) = \sqrt{m_n^2 + (\vec{p} + \vec{q})^2} = \sqrt{E_n^2 + q^2 + 2qp\cos\theta} > m_n, \quad \forall p, q, \theta, |\cos\theta| < 1, \tag{4.1.4}$$

where θ is the angle between the neutron initial momentum and the transferred momentum, defined below. To perform the remaining integrals, we write $d^3p = pE_n dE_n \, d\cos\theta \, d\phi$. For the EFT operators we are considering we need to consider polynomials in s and t, such that

$$|\mathcal{M}|^2 = \sum_{n,m} \alpha_{n,m} t^n s^m \tag{4.1.5}$$

Writing $s = m_\chi^2 + m_n^2 + 2E_\chi E_n - 2\vec{p}\cdot\vec{k}$ where the quantity $\vec{k}\cdot\vec{p}$ is obtained from kinematics. We choose to work in the frame where the momentum transfer $\vec{q}$ lies on the z-axis

$$\vec{k} = (k\sin\theta_\chi, 0, k\cos\theta_\chi) \tag{4.1.6}$$

$$\vec{p} = (p\sin\theta\cos\phi, p\sin\theta\sin\phi, p\cos\theta) \tag{4.1.7}$$

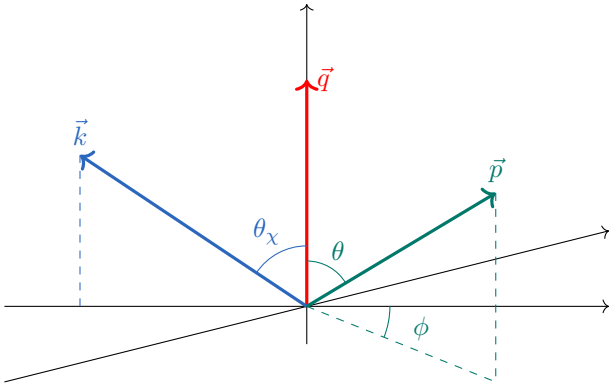

Figure 4.1: Schematic of kinematics

The angles can be written in terms of the other kinematic quantities such that

$$E'_\chi = \sqrt{m_\chi^2 + (\vec{k} - \vec{q})} \tag{4.1.8}$$

$$\implies (E_\chi - q_0)^2 = m_\chi^2 + (k^2 + q^2 - 2kq\cos\theta_\chi) \tag{4.1.9}$$

$$\implies \cos\theta_\chi = \frac{q^2 - q_0^2 + 2E_\chi q_0}{2q\sqrt{E_\chi^2 - m_\chi^2}} \tag{4.1.10}$$

$$E'_n = \sqrt{m_n^2 + (\vec{p} + \vec{q})} \tag{4.1.11}$$

$$\implies (E_n + q_0)^2 = m_n^2 + (p^2 + q^2 + 2pq\cos\theta) \tag{4.1.12}$$

$$\implies \cos\theta = \frac{q_0^2 - q^2 + 2E_n q_0}{2q\sqrt{E_n^2 - m_n^2}} \tag{4.1.13}$$

From these we get

$$\vec{k}\cdot\vec{p} = kp\sin\theta_\chi\sin\theta\cos\phi + kp\cos\theta_\chi\cos\theta \tag{4.1.14}$$

$$= kp\left[\sqrt{1 - \frac{(q^2 - q_0^2 + 2E_\chi q_0)^2}{4q^2(E_\chi^2 - m_\chi^2)}}\sqrt{1 - \frac{(q_0^2 - q^2 + 2E_n q_0)^2}{4q^2(E_n^2 - m_n^2)}}\cos\phi + \frac{(q^2 - q_0^2 + 2E_\chi q_0)(q_0^2 - q^2 + 2E_n q_0)}{4q^2\sqrt{E_\chi^2 - m_\chi^2}\sqrt{E_n^2 - m_n^2}}\right] \tag{4.1.15}$$

$$= \frac{(q^2 - q_0^2 + 2E_\chi q_0)(q_0^2 - q^2 + 2E_n q_0)}{4q^2} \tag{4.1.16}$$

$$+ \sqrt{E_\chi^2 - m_\chi^2 - \frac{(q^2 - q_0^2 + 2E_\chi q_0)^2}{4q^2}}\sqrt{E_n^2 - m_n^2 - \frac{(q_0^2 - q^2 + 2E_n q_0)^2}{4q^2}}\cos\phi \tag{4.1.17}$$

We then use the remaining delta function to integrate over θ, which gives rise to a step function, leaving

$$S(q_0, q) = \alpha t^n \frac{m_n^2}{2\pi^2 q}\int dE_n d\phi s^m f_{FD}(E_n)(1 - f_{FD}(E_n + q_0))\Theta(E_n)\Theta(1 - \cos^2\theta(q, q_0, E_n)). \tag{4.1.18}$$

The ϕ integrals can be easily computed for a given power of s, and so we write the response function as

$$S(q_0, q) = \alpha t^n \frac{m_n^2}{\pi q}\int dE_n\ f_{FD}(E_n)(1 - f_{FD}(E_n + q_0))\frac{\mathcal{U}_m}{q^{2m}}\Theta(E_n)(1 - \cos^2(\theta)) \tag{4.1.19}$$

where the $\mathcal{U}_m$ are polynomials in q_0, q, E_χ and E_n, and can be written as

$$\mathcal{U}_m = \frac{q^{2m}}{2\pi}\int_0^{2\pi} d\phi\ s^m = \sum_i \mathcal{V}_{m,i}E_n^i \tag{4.1.20}$$

in order to separate out the E_n dependence. Doing this leaves integrals of interest to be

$$\int dE_n E_n^i f_{FD}(E_n)(1 - f_{FD}(E_n + q_0)) \tag{4.1.21}$$

Change variables to

$$x = \frac{E_n - \mu_F}{T_\star},\ z = \frac{q_0}{T_\star} \tag{4.1.22}$$

which we can use to write

$$\int dE_n E_n^i f_{FD}(E_n)(1-f_{FD}(E_n+q_0)) = T_\star \int dx\,(\mu_F + T_\star x)^i\, f_{FD}(x) f_{FD}(-x-z) \tag{4.1.23}$$

$$= T_\star \int dx \sum_{j=0}^{i} \binom{i}{j} T_\star^j x^j \mu_F^{i-j} f_{FD}(x) f_{FD}(-x-z) \tag{4.1.24}$$

$$= \sum_{j=0}^{i} T_\star^{j+1} \binom{i}{j} \mu_F^{i-j} \int dx x^j f_{FD}(x) f_{FD}(-x-z) \tag{4.1.25}$$

$$= \sum_{j=0}^{i} \binom{i}{j} \mu_F^{i-j} \int dE_n (E_n-\mu_F)^j f_{FD}(E_n) f_{FD}(-E_n-q_0) \tag{4.1.26}$$

$$= \sum_{j=0}^{i} \binom{i}{j} \mu_F^{i-j} (-1)^j \frac{q_0^{j+1}}{j+1} g_j\left(\frac{E_n-\mu_F}{q_0}\right) \quad \text{for} \quad T_\star \to 0 \tag{4.1.27}$$

with

$$g_j(x) = \begin{cases} 1, & x > 0 \\ 1-(-x)^{j+1}, & -1 < x < 0 \\ 0, & x < -1 \end{cases} \tag{4.1.28}$$

For $i = 1, 2$ we have

$$\int dE_n E_n f_{FD}(E_n)(1-f_{FD}(E_n+q_0)) = F_1(E_n-\mu_F, q_0) + \mu_F F_0(E_n-\mu_F, q_0) \tag{4.1.29}$$

$$\int dE_n E_n^2 f_{FD}(E_n)(1-f_{FD}(E_n+q_0)) = F_2(E_n-\mu_F, q_0) + 2\mu_F F_1(E_n-\mu_F, q_0) + \mu_F^2 F_0(E_n-\mu_F, q_0) \tag{4.1.30}$$

The integration range for E_n is obtained from the two step functions. There are two cases, $t < 0$ and $t > 0$. In the former case, the range become $E_n^{t^-} < E_n < \infty$ and for the latter $0 < E_n < E_n^{t^+}$ which can be seen from Eq. 4.1.13, and are given by

$$E_n^{t^-} = -\left(m_n + \frac{q_0}{2}\right) + \sqrt{\left(m_n+\frac{q_0}{2}\right)^2 + \left(\frac{\sqrt{q^2-q_0^2}}{2} - \frac{m_n q_0}{\sqrt{q^2-q_0^2}}\right)^2} \tag{4.1.31}$$

$$E_n^{t^+} = -\left(m_n + \frac{q_0}{2}\right) + \sqrt{\left(m_n+\frac{q_0}{2}\right)^2 - \left(\frac{\sqrt{q_0^2-q^2}}{2} + \frac{m_n q_0}{\sqrt{q_0^2-q^2}}\right)^2} \tag{4.1.32}$$

These are both the same root of Eq. 4.1.13, but with an interchange of $t \leftrightarrow -t$. We denote the response function for $t < 0$ as S^- and for $t > 0$ as S^+. For S^- we have

$$S_m^- = \alpha t^n \frac{m_n^2}{\pi q^{2m+1}} \sum_{i=0}^{m} \mathcal{V}_{m,i} \int_{E_n^{t^-}}^{\infty} dE_n E_n^i f_{FD}(E_n)(1-f_{FD}(E_n+q_0)) \tag{4.1.33}$$

$$= \alpha t^n \frac{m_n^2}{\pi q^{2m+1}} \sum_{i=0}^{m} \mathcal{V}_{m,i} \sum_{j=0}^{i} \binom{i}{j} \mu_F^{i-j} \int_{E_n^{t^-}}^{\infty} dE_n (E_n-\mu_F)^j f_{FD}(E_n) f_{FD}(-E_n-q_0) \tag{4.1.34}$$

$$= \alpha t^n \frac{m_n^2}{\pi q^{2m+1}} \sum_{i=0}^{m} \mathcal{V}_{m,i} \sum_{j=0}^{i} \binom{i}{j} \mu_F^{i-j} \frac{(-1)^j q_0^{j+1}}{j+1} \left[1 - g_j\left(\frac{E_n^{t^-}-\mu_F}{q_0}\right)\right] \tag{4.1.35}$$

$$= \alpha t^n \frac{m_n^2}{\pi q^{2m+1}} \sum_{i=0}^{m} \mathcal{V}_{m,i} \sum_{j=0}^{i} \binom{i}{j} \mu_F^{i-j} \frac{(-1)^j q_0^{j+1}}{j+1} h_j\left(\frac{E_n^{t^-}-\mu_F}{q_0}\right) \tag{4.1.36}$$

while for S^+ the logic is

$$S_m^+ = \alpha t^n \frac{m_n^2}{\pi q^{2m+1}} \sum_{i=0}^{m} \mathcal{V}_{m,i} \int_0^{E_n^{t^+}} dE_n E_n^i f_{FD}(E_n)(1 - f_{FD}(E_n + q_0)) \tag{4.1.37}$$

$$= \alpha t^n \frac{m_n^2}{\pi q^{2m+1}} \sum_{i=0}^{m} \mathcal{V}_{m,i} \sum_{j=0}^{i} \binom{i}{j} \mu_F^{i-j} \int_0^{E_n^{t^+}} dE_n (E_n - \mu_F)^j f_{FD}(E_n) f_{FD}(-E_n - q_0) \tag{4.1.38}$$

$$= \alpha t^n \frac{m_n^2}{\pi q^{2m+1}} \sum_{i=0}^{m} \mathcal{V}_{m,i} \sum_{j=0}^{i} \binom{i}{j} \mu_F^{i-j} \frac{(-1)^j q_0^{j+1}}{j+1} \left[g_j \left(\frac{E_n^{t^+} - \mu_F}{q_0} \right) - g_j \left(\frac{-\mu_F}{q_0} \right) \right] \tag{4.1.39}$$

$$= -\alpha t^n \frac{m_n^2}{\pi q^{2m+1}} \sum_{i=0}^{m} \mathcal{V}_{m,i} \sum_{j=0}^{i} \binom{i}{j} \mu_F^{i-j} \frac{(-1)^j q_0^{j+1}}{j+1} h_j \left(\frac{E_n^{t^+} - \mu_F}{q_0} \right) \quad \text{for } q_0 < 0 \tag{4.1.40}$$

with

$$h_j(x) = \begin{cases} 0, & x > 0 \\ (-x)^{j+1}, & -1 < x < 0 \\ 1, & x < -1 \end{cases} \tag{4.1.41}$$

The final step of the S^+ calculation holds only for up-scattering of the DM, i.e. $q_0 < 0$. For matrix elements that are polynomials in s and t, we can instead write

$$S^- = \sum_{n,m} \alpha_{n,m} t^n \frac{m_n^2}{\pi q^{2m+1}} \sum_{i=0}^{m} \mathcal{V}_{m,i} \sum_{j=0}^{i} \binom{i}{j} \mu_F^{i-j} \frac{(-1)^j q_0^{j+1}}{j+1} h_j \left(\frac{E_n^{t^-} - \mu_F}{q_0} \right) \tag{4.1.42}$$

$$S^+ = -\sum_{n,m} \alpha_{n,m} t^n \frac{m_n^2}{\pi q^{2m+1}} \sum_{i=0}^{m} \mathcal{V}_{m,i} \sum_{j=0}^{i} \binom{i}{j} \mu_F^{i-j} \frac{(-1)^j q_0^{j+1}}{j+1} h_j \left(\frac{E_n^{t^+} - \mu_F}{q_0} \right) \tag{4.1.43}$$

4.1.1 Down Scattering

In terms of the interaction rate we have

$$\Gamma^- = \int \frac{d\cos\theta k'^2 dk'}{64\pi^3 E_\chi E'_\chi} \Theta(E_\chi - q_0 - m_\chi)\Theta(q_0) \sum_{n,m} \frac{\alpha_{n,m} t^n}{q^{2m+1}} \sum_{i=0}^{m} \mathcal{V}_{m,i} \sum_{j=0}^{i} \binom{i}{j} \mu_F^{i-j} \frac{(-1)^j q_0^{j+1}}{j+1} h_j \left(\frac{E_n^{t^-} - \mu_F}{q_0} \right) \tag{4.1.44}$$

Change variables to q_0 and q through

$$q_0 = E_\chi - \sqrt{k'^2 + m_\chi^2} \tag{4.1.45}$$

$$q^2 = k^2 + k'^2 - 2kk'\cos\theta \tag{4.1.46}$$

$$\implies dk' d\cos\theta = \frac{E'_\chi q}{kk'^2} dq_0 dq \tag{4.1.47}$$

To further simplify we introduce $t_E = -t = q^2 - q_0^2$, $dq = dt_E/(2q)$,

$$\implies dk' d\cos\theta = \frac{E'_\chi}{2kk'^2} dq_0 dt_E \tag{4.1.48}$$

giving the interaction rate as

$$\Gamma^- = \frac{1}{128\pi^3 E_\chi k}\int_0^{E_\chi - m_\chi} dq_0 \int dt_E \sum_{n,m}\frac{\alpha_{n,m}(-1)^n t_E^n}{(t_E+q_0^2)^{m+\frac{1}{2}}}\sum_{i=0}^{m}\mathcal{V}_{m,i}\sum_{j=0}^{i}\binom{i}{j}\mu_F^{i-j}\frac{(-1)^j q_0^{j+1}}{j+1}h_j\left(\frac{E_n^{t^-}-\mu_F}{q_0}\right) \tag{4.1.49}$$

$$= \sum_{n,m}\frac{(-1)^n\alpha_{n,m}}{128\pi^3 E_\chi k}\int_0^{E_\chi - m_\chi} dq_0 \int \frac{dt_E t_E^n}{(t_E+q_0^2)^{m+\frac{1}{2}}}\sum_{i=0}^{m}\mathcal{V}_{m,i}\sum_{j=0}^{i}\binom{i}{j}\mu_F^{i-j}\frac{(-1)^j q_0^{j+1}}{j+1}h_j\left(\frac{E_n^{t^-}-\mu_F}{q_0}\right) \tag{4.1.50}$$

with the $\mathcal{V}_{m,i} = \mathcal{V}_{m,i}(t_E, q_0, E_\chi)$

There are then two main cases to consider; when $h_j(x)$ is unity or not. We then denote the t_E integrand in the former case as f_1 and f_2 for the latter, i.e.

$$f_1^{(m,n)}(t_E) = \frac{t_E^n}{(t_E+q_0^2)^{m+\frac{1}{2}}}\sum_{i=0}^{m}\mathcal{V}_{m,i}\sum_{j=0}^{i}\binom{i}{j}\mu_F^{i-j}\frac{(-1)^j q_0^{j+1}}{j+1} \tag{4.1.51}$$

$$f_2^{(m,n)}(t_E) = \frac{-t_E^n}{(t_E+q_0^2)^{m+\frac{1}{2}}}\sum_{i=0}^{m}\mathcal{V}_{m,i}\sum_{j=0}^{i}\binom{i}{j}\mu_F^{i-j}\frac{1}{j+1}\left(E_n^{t^-}-\mu_F\right)^{j+1} \tag{4.1.52}$$

where we suppress the explicit dependence on the other variables for brevity. We encode the integrals over t_E within an operator

$$\mathcal{I}_{n,m}(f^{(m,n)}(t), t_1^+, t_2^+, t_1^-, t_2^-) = \sum_{i=1,2}\sum_{j=1,2}\left(F^{(m,n)}(t_i^+) - F^{(m,n)}(t_j^-)\right)\Theta\left(t_{3-i}^+ - t_i^+\right)\Theta\left(t_i^+ - t_j^-\right) \times \Theta\left(t_j^- - t_{3-j}^-\right), \tag{4.1.53}$$

$$F^{(m,n)}(t) = \int dt\, f^{(m,n)}(t), \tag{4.1.54}$$

The full interaction rate is then written as

$$\begin{aligned}\Gamma^-(E_\chi) = \sum_{n,m}\frac{(-1)^n\alpha_{n,m}}{128\pi^3 E_\chi k}\int_0^{E_\chi - m_\chi} dq_0 \Big[&\mathcal{I}_{n,m}\left(f_1^{(m,n)}(t), t_E^+, t_{\mu^-}^+, t_E^-, t_{\mu^-}^-\right)\Theta(\mu_{F,n}-q_0) \\ &+\mathcal{I}_{n,m}\left(f_2^{(m,n)}(t), t_E^+, t_{\mu^+}^+, t_E^-, t_{\mu^-}^+\right)\Theta(\mu_{F,n}-q_0) \\ &+\mathcal{I}_{n,m}\left(f_2^{(m,n)}(t), t_E^+, t_{\mu^-}^-, t_E^-, t_{\mu^+}^-\right)\Theta(\mu_{F,n}-q_0) \\ &+\mathcal{I}_{n,m}\left(f_2^{(m,n)}(t), t_E^+, t_{\mu^+}^+, t_E^-, t_{\mu^+}^-\right)\Theta(q_0-\mu_{F,n})\Big],\end{aligned} \tag{4.1.55}$$

where the t_E integration limits are

$$t_E^\pm = 2\left[E_\chi(E_\chi - q_0) - m_\chi^2 \pm k\sqrt{(E_\chi-q_0)^2 - m_\chi^2}\right], \tag{4.1.56}$$

$$t_{\mu^+}^\pm = 2\left[\mu_{F,n}(\mu_{F,n}+q_0) + m_n(2\mu_{F,n}+q_0) \pm \sqrt{\left(\mu_{F,n}(\mu_{F,n}+q_0) + m_n(2\mu_{F,n}+q_0)\right)^2 - m_n^2 q_0^2}\right], \tag{4.1.57}$$

$$t_{\mu^-}^\pm = 2\left[\mu_{F,n}(\mu_{F,n}-q_0) + m_n(2\mu_{F,n}-q_0) \pm \sqrt{\left(\mu_{F,n}(\mu_{F,n}-q_0) + m_n(2\mu_{F,n}-q_0)\right)^2 - m_n^2 q_0^2}\right], \tag{4.1.58}$$

4.1.2 Inelastic Case

For $t > 0$, we instead have

$$\Gamma^{+} = -\int \frac{d\cos\theta k^{'2} dk^{'}}{64\pi^3 E_\chi E_\chi^{'}} \Theta(E_\chi - q_0 - m_\chi)\Theta(-q_0) \sum_{n,m} \frac{\alpha_{n,m} t^n}{q^{2m+1}} \sum_{i=0}^{m} \mathcal{V}_{m,i} \sum_{j=0}^{i} \binom{i}{j} \mu_F^{i-j} \frac{(-1)^j q_0^{j+1}}{j+1} h_j \left(\frac{E_n^{t^+} - \mu_F}{q_0} \right). \tag{4.1.59}$$

Again we change integration variables to q and q_0 as above, but instead we make the substitution $q^2 = q_0^2 - t$, such that $dq = -dt/(2q)$,

$$\implies dk' d\cos\theta = -\frac{E'_\chi}{2kk'^2} dq_0 dt \tag{4.1.60}$$

giving the interaction rate as

$$\Gamma^{+} = \sum_{n,m} \frac{\alpha_{n,m}}{128\pi^3 E_\chi k} \int_0^{E_\chi - m_\chi} dq_0 \int \frac{dt\, t^n}{(q_0^2 - t)^{m+\frac{1}{2}}} \sum_{i=0}^{m} \mathcal{V}_{m,i} \sum_{j=0}^{i} \binom{i}{j} \mu_F^{i-j} \frac{(-1)^j q_0^{j+1}}{j+1} h_j \left(\frac{E_n^{t^+} - \mu_F}{q_0} \right) \tag{4.1.61}$$

with the $\mathcal{V}_{m,i} = \mathcal{V}_{m,i}(t_E, q_0, E_\chi)$ Again we need to consider the two cases when h_j is unity or not, with the two integrands being

$$f_1^{(m,n)}(t) = \frac{t^n}{(q_0^2 - t)^{m+\frac{1}{2}}} \sum_{i=0}^{m} \mathcal{V}_{m,i} \sum_{j=0}^{i} \binom{i}{j} \mu_F^{i-j} \frac{(-1)^j q_0^{j+1}}{j+1} \tag{4.1.62}$$

$$f_2^{(m,n)}(t) = \frac{t^n}{(q_0^2 - t)^{m+\frac{1}{2}}} \sum_{i=0}^{m} \mathcal{V}_{m,i} \sum_{j=0}^{i} \binom{i}{j} \mu_F^{i-j} \frac{1}{j+1} \left(E_n^{t^+} - \mu_F \right)^{j+1} \tag{4.1.63}$$

where we suppress the explicit dependence on the other variables for brevity. In general the integration limits on t are given by combining the definitions of q and q_0 with that of t, and are given by

$$t^{\pm} = 2\left[m_\chi^2 - E_\chi(E_\chi - q_0) \pm k\sqrt{(E_\chi - q_0)^2 - m_\chi^2} \right] \tag{4.1.64}$$

[M: Remove $q_0 < 0$, make it > 0] We now consider how to split the integral over the ranges of $h_j(x)$. For the case $h_j(x) = 0$, we require $E_n^{t^+} - \mu_F < 0$, as $q_0 < 0$, which translates to

$$\frac{(2m_n q_0 + t)^2}{4t} + (2m_n + q_0)\mu_F + \mu_F^2 < 0 \tag{4.1.65}$$

As $t > 0$, this is the case when t is between the two roots of Eq. 4.1.65, given by

$$t_\mu^{'\pm} = -2\left[\mu_F(q_0 + \mu_F) + m_n(q_0 + 2\mu_F) \pm \sqrt{(\mu_F(q_0 + \mu_F) + m_n(q_0 + 2\mu_F))^2 - m_n^2 q_0^2} \right] \tag{4.1.66}$$

If we look at the region $0 < h_j(x) < 1$, we require

$$E_n^{t^+} - \mu_F < 0 \tag{4.1.67}$$

$$E_n^{t^+} - \mu_F + q_0 > 0 \tag{4.1.68}$$

which requires

$$-\frac{m_n^2 q_0^2}{t} - \frac{t}{4} + m_n(q_0 - 2\mu_F) + (q_0 - \mu_F)\mu_F > 0 \tag{4.1.69}$$

As $q_0 < 0$, this is never possible, and so we are never in this region.

4.2 Interaction Rate for Low Energies

Need to consider the case where $T_\chi = E_\chi - m_\chi < \mu_F$, with $0 < q_0 < T_\chi < \mu_F$. Then the t_E integration limits follow the hierarchy; $t^+_{\mu^+} \sim t^+_{\mu^-} \geq t^-_{\mu^-} \sim t^-_{\mu^+} \gtrsim 0$, and $t^+_{\mu^-} \gg t^+_E \geq t^-_E \gg t^-_{\mu^-}$. Then the only term in 4.1.55 that remains is the first term, and only the $i = j = 1$ term contributes, leaving

$$\Gamma^-(E_\chi) = \sum_{n,m} \frac{(-1)^n \alpha_{n,m}}{128\pi^3 E_\chi k} \int_0^{E_\chi - m_\chi} dq_0 \int_{t^-_E}^{t^+_E} dt_E \; f_1^{(m,n)}(t_E) \tag{4.2.1}$$

At first order in q_0 and T_χ, we have the following approximations

$$E_\chi \approx m_\chi \tag{4.2.2}$$

$$k \approx \sqrt{2 m_\chi T_\chi} \tag{4.2.3}$$

$$t^\pm_E \approx 4 m_\chi T_\chi \left[1 - \frac{q_0}{2T_\chi} \pm \sqrt{1 - \frac{q_0}{T_\chi}}\right] \tag{4.2.4}$$

$$\Gamma^- \approx \sum_{n,m} \frac{(-1)^n \alpha_{n,m}}{128\sqrt{2}\pi^3 m_\chi^{3/2} T_\chi^{1/2}} \int_0^{T_\chi} dq_0 \int_{t^-_E}^{t^+_E} dt_E \; f_1^{(m,n)}(t_E) \tag{4.2.5}$$

For single term matrix elements such that $\left|\overline{M}\right|^2 = \alpha_{n,m}(-t)^n s^m$, the corresponding $\Gamma^-_{n,m}$ are

$$\Gamma^-_{0,0} = \frac{\alpha_{0,0}}{120\pi^3 m_\chi} T_\chi^2 \tag{4.2.6}$$

$$\Gamma^-_{1,0} = \frac{2\alpha_{1,0}}{105\pi^3} T_\chi^3 \tag{4.2.7}$$

$$\Gamma^-_{2,0} = \frac{4\alpha_{2,0} m_\chi}{63\pi^3} T_\chi^4 \tag{4.2.8}$$

$$\Gamma^-_{0,1} = \frac{\alpha_{0,1}((m_n + m_\chi)^2 + 2m_\chi \mu_F)}{120\pi^3} T_\chi^2 \tag{4.2.9}$$

$$\Gamma^-_{1,1} = \frac{2\alpha_{1,1}((m_n + m_\chi)^2 + 2m_\chi \mu_F)}{105\pi^3} T_\chi^3 \tag{4.2.10}$$

$$\Gamma^-_{0,2} = \frac{\alpha_{0,2}((m_n + m_\chi)^2 + 2m_\chi \mu_F)^2}{120\pi^3} T_\chi^2 \tag{4.2.11}$$

The $\alpha_{n,m}$ can be obtained at some reference point, taken to be the surface of the NS, from the differential cross section,

$$\frac{d\sigma}{d\cos\theta} = \frac{\alpha_{n,m}(-t)^n s^m}{32\pi(m_n + m_\chi)^2} \tag{4.2.12}$$

which gives

$$\sigma_{0,0} = \frac{\alpha_{0,0}}{16\pi(m_n + m_\chi)^2} \tag{4.2.13}$$

$$\sigma_{1,0} = \frac{\alpha_{1,0}}{32\pi(m_n + m_\chi)^2} t_{max} \tag{4.2.14}$$

$$\sigma_{2,0} = \frac{1}{3}\frac{\alpha_{2,0}}{16\pi(m_n + m_\chi)^2} t_{max}^2 \tag{4.2.15}$$

$$\sigma_{0,1} = \frac{\alpha_{0,1}}{16\pi(m_n + m_\chi)^2} s \tag{4.2.16}$$

$$\sigma_{1,1} = \frac{\alpha_{1,1}}{32\pi(m_n + m_\chi)^2} t_{max} s \tag{4.2.17}$$

$$\sigma_{0,2} = \frac{\alpha_{0,2}}{16\pi(m_n + m_\chi)^2} s^2 \tag{4.2.18}$$

where I have used

$$t = -\frac{t_{max}}{2}(1-\cos\theta) \tag{4.2.19}$$

$$t_{max} \sim \frac{4m_n^2 m_\chi^2}{(m_n^2+m_\chi^2)}\frac{1-B(R_\star)}{B(R_\star)} \tag{4.2.20}$$

$$s \sim m_n^2 + m_\chi^2 + \frac{2m_\chi(m_n+\mu_F)}{\sqrt{B(R_\star)}} [M :\sim (m_n+m_\chi)^2] \tag{4.2.21}$$

Again introducing the correction

$$\zeta = \frac{n_n}{n_{free}} \sim \frac{3\pi^2}{(2m_n\mu_F)^{3/2}} n_n \tag{4.2.22}$$

Then the interaction rates can be expressed with respect to the surface of the star as

$$\Gamma^-_{0,0}(T_\chi) = \frac{\sqrt{2}}{10}\frac{(1+\mu)^2}{\mu}\frac{m_n}{(m_n\mu_F)^{3/2}}\sigma_{surf} n_n T_\chi^2 \tag{4.2.23}$$

$$\Gamma^-_{1,0}(T_\chi) = \frac{4\sqrt{2}}{35}\frac{(1+\mu)^2(1+\mu^2)}{\mu^2}\frac{1}{(m_n\mu_F)^{3/2}}\frac{B(R_\star)}{(1-B(R_\star)}\sigma_{surf} n_n T_\chi^3 \tag{4.2.24}$$

$$\Gamma^-_{2,0}(T_\chi) = \frac{\sqrt{2}}{7}\frac{(1+\mu)^2(1+\mu^2)^2}{\mu^3}\frac{1}{m_n(m_n\mu_F)^{3/2}}\left(\frac{B(R_\star)}{(1-B(R_\star)}\right)^2\sigma_{surf} n_n T_\chi^4 \tag{4.2.25}$$

$$\Gamma^-_{0,1}(T_\chi) = \frac{\sqrt{2}}{10}\frac{(m_n(1+\mu)^2+2\mu\mu_F)}{\mu(m_n\mu_F)^{3/2}}\sigma_{surf} n_n T_\chi^2 \tag{4.2.26}$$

$$\Gamma^-_{1,1}(T_\chi) = \frac{4\sqrt{2}}{35}\frac{(m_n(1+\mu)^2+2\mu\mu_F)(1+\mu^2)}{\mu^2 m_n(m_n\mu_F)^{3/2}}\frac{B(R_\star)}{(1-B(R_\star)}\sigma_{surf} n_n T_\chi^3 \tag{4.2.27}$$

$$\Gamma^-_{0,2}(T_\chi) = \frac{\sqrt{2}}{10}\frac{(m_n(\mu+1)^2+2\mu\mu_F)^2}{\mu(\mu+1)^2 m_n(\mu_F m_n)^{3/2}}\sigma_{surf} n_n T_\chi^2 \tag{4.2.28}$$

The average energy loss per collision is given by

$$\langle\Delta T\rangle = \frac{1}{\Gamma^-}\int_0^{T_\chi} dq_0\; q_0\frac{d\Gamma^-}{dq_0} \tag{4.2.29}$$

which gives the results

$$\langle\Delta T^{0,0}\rangle = \frac{4}{7}T_\chi \sim \langle\Delta T^{0,1}\rangle \sim \langle\Delta T^{0,2}\rangle \tag{4.2.30}$$

$$\langle\Delta T^{1,0}\rangle = \frac{5}{9}T_\chi \sim \langle\Delta T^{1,1}\rangle \tag{4.2.31}$$

$$\langle\Delta T^{2,0}\rangle = \frac{28}{55}T_\chi \tag{4.2.32}$$

The DM will reach thermal equilibrium with the neutrons when $T_\chi = T_\star$. There are two stages to this process; one where the interactions are not affected by Pauli blocking which takes N_1 collisions, and the next N_2 collisions where Pauli blocking is in effect. The time it takes for thermalisation to occur is given by the sum of the average times between collisions

$$t_{th} = \sum_{n=0}^{N_2}\frac{1}{\Gamma^-(T_n)} \sim \sum_{n=N_1}^{N_2}\frac{1}{\Gamma^-(T_n)} \tag{4.2.33}$$

where T_n is the DM kinetic energy after n collisions. If Pauli blocking is in effect for the entire process, then T_n is related to the initial kinetic energy, T_0 through

$$T_n = T_0\left(1-\frac{\Delta T}{T}\right)^n. \tag{4.2.34}$$

This result implies the following relation;

$$\frac{T_N}{T_0} = \frac{T_{eq}}{T_0} = \left(1 - \frac{\Delta T}{T}\right)^N \tag{4.2.35}$$

Then for interaction rates which follow $\Gamma^- \propto (T_\chi)^p$, we have that

$$t_{th} \propto \sum_{n=N_1}^{N_2} (T_n)^{-p} \tag{4.2.36}$$

$$= \frac{1}{T_{N_1}^p} \sum_{n=N_1}^{N_2} \left(\left(1 - \frac{\Delta T}{T}\right)^{-p}\right)^n \tag{4.2.37}$$

$$= \frac{1}{T_{N_1}^p} \frac{(1-\Delta T/T)^{p(1-N_1)} - (1-\Delta T/T)^{-pN_2}}{-1 + (1-\Delta T/T)^p} \tag{4.2.38}$$

$$\sim \frac{1}{T_{N_1}^p} \frac{(1-\Delta T/T)^{-pN_2}}{1-(1-\Delta T/T)^p} \quad \text{for} \quad N_2 > N_1 \tag{4.2.39}$$

$$= \frac{1}{T_{N_1}^p} \left(\frac{T_{eq}}{T_{N_1}}\right)^{-p} \frac{1}{1-(1-\Delta T/T)^p} \tag{4.2.40}$$

$$= \frac{1}{T_{eq}^p} \frac{1}{1-(1-\Delta T/T)^p} \tag{4.2.41}$$

The resulting thermalisation times are then (setting $B(R_\star) \sim 0.5$)

$$t_{th}^{0,0} = \frac{49}{4\sqrt{2}} \frac{\mu}{(1+\mu)^2} \frac{\sqrt{m_n \mu_F^3}}{n_n \sigma_{surf} T_{eq}^2} \tag{4.2.42}$$

$$\sim 1.427 \times 10^8 \text{ yrs} \frac{\mu}{(1+\mu)^2} \left(\frac{\mu_F(0)}{0.2 \text{ GeV}}\right)^{3/2} \left(\frac{2 \times 10^{-45} \text{ cm}^2}{\sigma_{surf}}\right) \left(\frac{0.375 \text{ fm}^{-3}}{n_n(0)}\right) \left(\frac{10^3 \text{ K}}{T_{eq}}\right)^2 \tag{4.2.43}$$

$$t_{th}^{1,0} = \frac{729}{76\sqrt{2}} \frac{\mu^2}{(1+\mu)^2(1+\mu^2)} \frac{1-B(R_\star)}{B(R_\star)} \frac{(m_n \mu_F)^{3/2}}{n_n \sigma_{surf} T_{eq}^3} \tag{4.2.44}$$

$$\sim 1.217 \times 10^{18} \text{ yrs} \frac{\mu^2}{(1+\mu)^2(1+\mu^2)} \left(\frac{\mu_F(0)}{0.2 \text{ GeV}}\right)^{3/2} \left(\frac{2 \times 10^{-45} \text{ cm}^2}{\sigma_{surf}}\right) \left(\frac{0.375 \text{ fm}^{-3}}{n_n(0)}\right) \left(\frac{10^3 \text{ K}}{T_{eq}}\right)^3 \tag{4.2.45}$$

$$t_{th}^{2,0} = \frac{9150625}{1231312\sqrt{2}} \frac{\mu^3}{(1+\mu)^2(1+\mu^2)^2} \left(\frac{1-B(R_\star)}{B(R_\star)}\right)^2 \frac{\sqrt{m_n^5 \mu_F^3}}{n_n \sigma_{surf} T_{eq}^4} \tag{4.2.46}$$

$$\sim 1.027 \times 10^{28} \text{ yrs} \frac{\mu^3}{(1+\mu)^2(1+\mu^2)^2} \left(\frac{\mu_F(0)}{0.2 \text{ GeV}}\right)^{3/2} \left(\frac{2 \times 10^{-45} \text{ cm}^2}{\sigma_{surf}}\right) \left(\frac{0.375 \text{ fm}^{-3}}{n_n(0)}\right) \left(\frac{10^3 \text{ K}}{T_{eq}}\right)^4 \tag{4.2.47}$$

Using Eq. 4.15 of the thermalisation paper, I get, for $\mu_F \sim 0.2$ GeV and $\mu = 10^{-3}$

$$t_{th}^{D1} \sim \frac{3}{2} t_{th}^{0,0} \tag{4.2.48}$$
$$t_{th}^{D2} \sim t_{th}^{1,0} \tag{4.2.49}$$
$$t_{th}^{D3} \sim \frac{5}{3} t_{th}^{1,0} \sim \frac{3}{2} t_{th}^{0,0} \tag{4.2.50}$$
$$t_{th}^{D4} \sim t_{th}^{2,0} \tag{4.2.51}$$
$$t_{th}^{D5} \sim \frac{13}{8} t_{th}^{0,0} \sim \frac{3}{2} t_{th}^{0,0} \tag{4.2.52}$$
$$t_{th}^{D6} \sim 3 t_{th}^{0,0} \tag{4.2.53}$$
$$t_{th}^{D7} \sim 5 t_{th}^{0,0} \tag{4.2.54}$$
$$t_{th}^{D8} \sim \frac{3}{2} t_{th}^{0,0} \tag{4.2.55}$$
$$t_{th}^{D9} \sim \frac{8}{5} t_{th}^{0,0} \sim \frac{3}{2} t_{th}^{0,0} \tag{4.2.56}$$
$$t_{th}^{D10} \sim \frac{7}{2} t_{th}^{0,0} \tag{4.2.57}$$
$$\tag{4.2.58}$$

High mass, $\mu = 10^3$;

$$t_{th}^{D1} \sim \frac{3}{2} t_{th}^{0,0} \tag{4.2.59}$$
$$t_{th}^{D2} \sim \frac{5}{3} t_{th}^{1,0} \sim \frac{3}{2} t_{th}^{0,0} \tag{4.2.60}$$
$$t_{th}^{D3} \sim t_{th}^{1,0} \tag{4.2.61}$$
$$t_{th}^{D4} \sim t_{th}^{2,0} \tag{4.2.62}$$
$$t_{th}^{D5} \sim \frac{13}{8} t_{th}^{0,0} \sim \frac{3}{2} t_{th}^{0,0} \tag{4.2.63}$$
$$t_{th}^{D6} \sim 5 t_{th}^{0,0} \tag{4.2.64}$$
$$t_{th}^{D7} \sim 3 t_{th}^{0,0} \tag{4.2.65}$$
$$t_{th}^{D8} \sim \frac{3}{2} t_{th}^{0,0} \tag{4.2.66}$$
$$t_{th}^{D9} \sim \frac{8}{5} t_{th}^{0,0} \sim \frac{3}{2} t_{th}^{0,0} \tag{4.2.67}$$
$$t_{th}^{D10} \sim \frac{7}{2} t_{th}^{0,0} \tag{4.2.68}$$
$$\tag{4.2.69}$$

For matrix elements that are linear combinations of t^n, we have

$$\left|\overline{M}\right|^2 = a_0 + a_1 t + a_2 t^2 \tag{4.2.70}$$
$$\Gamma^- = a_0 \, \Gamma^-_{0,0}\big|_{\alpha_{0,0}=1} + a_1 \, \Gamma^-_{1,0}\big|_{\alpha_{1,0}=1} + a_2 \, \Gamma^-_{2,0}\big|_{\alpha_{2,0}=1} \tag{4.2.71}$$
$$\frac{1}{t_{th}} = \frac{a_0}{t_{th}^{0,0}}\bigg|_{\alpha_{0,0}=1} + \frac{a_1}{t_{th}^{1,0}}\bigg|_{\alpha_{1,0}=1} + \frac{a_2}{t_{th}^{2,0}}\bigg|_{\alpha_{2,0}=1} \tag{4.2.72}$$

For the operators D1-10, $a_i \propto \Lambda^{-4}$, and we set Λ such that the total cross section is equal to $\sigma_{surf} \sim 2 \times 10^{-45}$ cm^2, i.e.

$$\Lambda^4 = \frac{\sigma(\Lambda = 1)}{\sigma_{surf}} \tag{4.2.73}$$

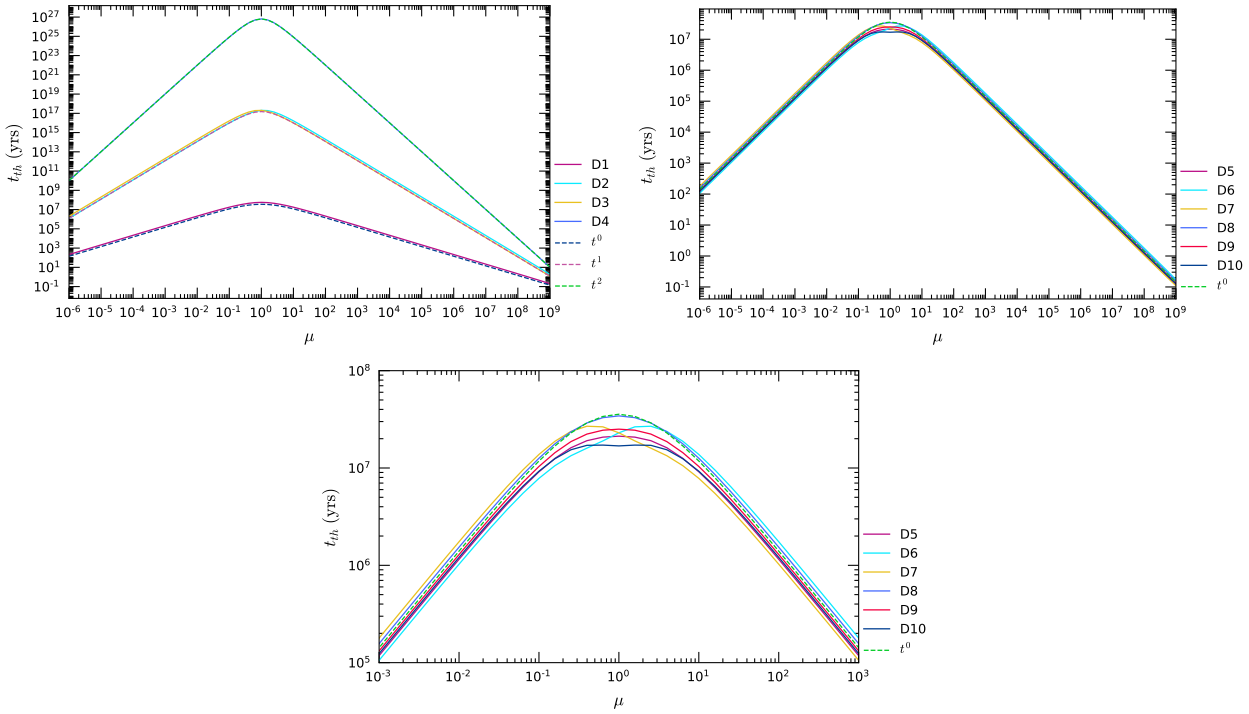

Figure 4.2: Thermalisation times using Eq. 4.2.72. Upper plots are for operators D1-4 (left) and D5-10 (right), with the lower plot highlighting a smaller mass range for operators D5-10

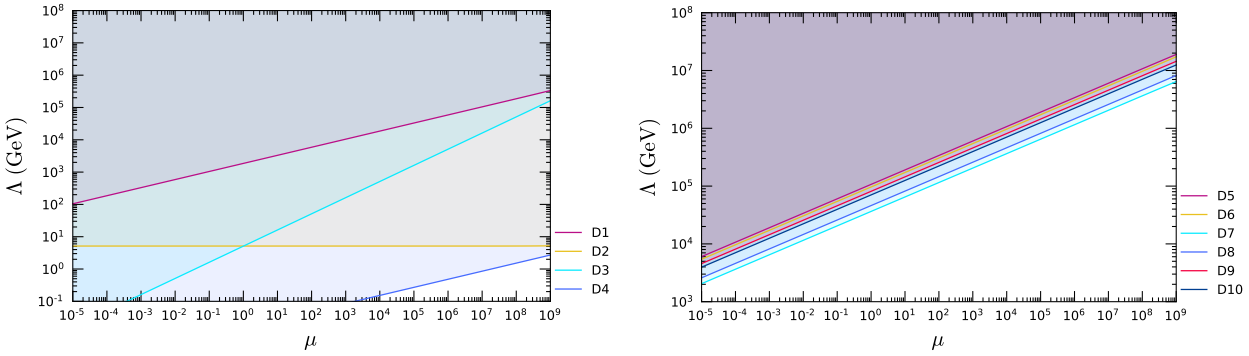

Figure 4.3: Constraints on Λ for D1-4 (left) and D5-10 (right) for thermalisation within the age of the universe

Scaling from 4.2.72 at $\mu = 10^3$:

$$t_{th}^{D1} \sim \frac{3}{2} t_{th}^{0,0} \tag{4.2.74}$$

$$t_{th}^{D2} \sim \frac{5}{3} t_{th}^{1,0} \tag{4.2.75}$$

$$t_{th}^{D3} \sim t_{th}^{1,0} \tag{4.2.76}$$

$$t_{th}^{D4} \sim t_{th}^{2,0} \tag{4.2.77}$$

$$t_{th}^{D5} \sim t_{th}^{D6} \sim t_{th}^{D7} \sim t_{th}^{D8} \sim t_{th}^{D9} \sim t_{th}^{D10} \sim t_{th}^{0,0} \tag{4.2.78}$$

4.3 Non-Degenerate Protons

For the lighter mass NSs, the protons are in a non-degenerate state, with their chemical potentials being zero. In this case, the free number density is worked out by integrating

$$\frac{dN_p}{dV} = \frac{pE_p dE_p d\cos\theta_{uw}}{2\pi^2} f_{FD}(E_p, r) \tag{4.3.1}$$

on the interval $[m_p, m_p/\sqrt{B(r)}]$, with the result

$$n_{free} = \frac{m_p^3}{3\pi^2} \left(\frac{1 - B(r)}{B(r)} \right)^{3/2} \tag{4.3.2}$$

4.4 Up-scattering Rate

We now treat the case of $q_0 < 0$ applicable to up scattering and evaporation. Focusing on s-independent matrix elements and elastic scattering, we write the response function as

$$S^-(q_0, q) = \frac{m_n^2}{\pi q} \int_{E_n^{t^-}}^{\infty} f_{FD}(E_n)(1 - f_{FD}(E_n + q_0)) \tag{4.4.1}$$

and evaluate the integral, now with $q_0 < 0$. If we attempt to take the $T_\star \to 0$ limit as before, we find that there is no overlap of the Fermi-Dirac functions, and so we need to maintain the lowest order thermal contributions. The integral is given by

$$\int f_{FD}(E)(1 - f_{FD}(E + q_0)) = \frac{T_\star e^{q_0/T_\star}}{1 - e^{q_0/T_\star}} \left(\log\left(1 + e^{(E-\mu_F)/T_\star}\right) - \log\left(1 + e^{(E+q_0-\mu_F)/T_\star}\right) \right) \tag{4.4.2}$$

and we can recognise 3 distinct regions which result in

$$\frac{-q_0 e^{q_0/T_\star}}{1 - e^{q_0/T_\star}}, \quad E > \mu_F - q_0 \tag{4.4.3}$$

$$\frac{(E - \mu_F) e^{q_0/T_\star}}{1 - e^{q_0/T_\star}}, \quad \mu_F - q_0 > E > \mu_F \tag{4.4.4}$$

$$0, \quad \mu_F > E \tag{4.4.5}$$

we write this as

$$\int f_{FD}(E)(1 - f_{FD}(E + q_0)) = -\frac{q_0 e^{q_0/T_\star}}{1 - e^{q_0/T_\star}} g_+ \left(\frac{E - \mu_F}{q_0} \right) \tag{4.4.6}$$

where

$$g_+(x) = \begin{cases} 1, & x < -1 \\ -x, & -1 < x < 0 \\ 0, & x > 0 \end{cases} \tag{4.4.7}$$

leaving the response function as

$$S_{up}^-(q_0, q) = \frac{m_n^2 q_0}{\pi q} \frac{e^{q_0/T_\star}}{e^{q_0/T_\star} - 1} \left[1 - g_+ \left(\frac{E_n^{t^-} - \mu_F}{q_0} \right) \right] \tag{4.4.8}$$

$$= \frac{m_n^2 q_0}{\pi q} \frac{e^{q_0/T_\star}}{e^{q_0/T_\star} - 1} h_+ \left(\frac{E_n^{t^-} - \mu_F}{q_0} \right) \tag{4.4.9}$$

$$h_+(x) = \begin{cases} 0, & x < -1 \\ 1 + x, & -1 < x < 0 \\ 1, & x > 0 \end{cases} \tag{4.4.10}$$

The interaction rate is then

$$\Gamma_{up}^- = \int \frac{k'^2 d\cos\theta dk'}{64\pi^2 m_n^2 E_\chi E'_\chi} \left|\overline{\mathcal{M}}\right|^2 \Theta(E_\chi - q_0 - m_\chi) \Theta(-q_0) S_{up}^-(q_0, q) \tag{4.4.11}$$

$$= \frac{(-1)^n \alpha}{128\pi^3 E_\chi k} \int_{-\infty}^{0} dq_0 \, \frac{q_0 e^{q_0/T_\star}}{e^{q_0/T_\star} - 1} \int dt_E \, \frac{t_E^n}{\sqrt{t_E + q_0^2}} h_+ \left(\frac{E_n^{t^-} - \mu_F}{q_0} \right) \tag{4.4.12}$$

where we have substituted $\left|\overline{\mathcal{M}}\right|^2 = \alpha t^n$ as the matrix element. Typically we expect to be in the regime where $h_+ = 1$, and so the differential up scattering rate is related to the previous result through

$$\frac{d\Gamma_{up}^-}{dq_0} = \frac{e^{q_0/T_\star}}{e^{q_0/T_\star} - 1} \frac{d\Gamma_{down}^-}{dq_0} \tag{4.4.13}$$

If we want the full expressions, we need to consider the three possibilities of h_+.

- For $h_+ = 0$, we require $E_n^{t^-} > \mu_F - q_0$, which translates to

$$\frac{m_n^2 q_0^2}{t_E} + \frac{t_E}{4} + m_n(q_0 - 2\mu_F) + (q_0 - \mu_F) > 0 \tag{4.4.14}$$

  and since $t_E > 0$, we look for values not between the roots of Eq. 4.4.14, which are the $t^{\pm}_{\mu^-}$ from before.

- For $h_+ = 1 + x$, we require $\mu_F - q_0 > E_n^{t^-} > \mu_F$, which requires

$$\frac{m_n^2 q_0^2}{t_E} + \frac{t_E}{4} + m_n(q_0 - 2\mu_F) + (q_0 - \mu_F) < 0 \tag{4.4.15}$$

$$\frac{m_n^2 q_0^2}{t_E} + \frac{t_E}{4} - \mu_F(q_0 + \mu_F) - m_n(q_0 + 2\mu_F) > 0 \tag{4.4.16}$$

  and so we are between the roots $t^{\pm}_{\mu^-}$ and outside the roots $t^{\pm}_{\mu^+}$.

- Finally for $h_+ = 1$, we need $E_n^{t^-} < \mu_F$, which can also be obtained as the compliment of the above regions, which is between the roots $t^{\pm}_{\mu^+}$.

We also need to consider the hierarchy the roots take. For $q_0 > -\mu_F$, all of the roots exist and are in the order $t^+_{\mu^-} \geq t^+_{\mu^+} \geq t^-_{\mu^+} \geq t^-_{\mu^-}$. For $-\mu_F - 2m_n < q_0 < -\mu_F$, the $t^{\pm}_{\mu^+}$ roots do not exist, and for $q_0 < -\mu_F - 2m_n$, they are negative, so the order becomes $t^+_{\mu^-} \geq t^-_{\mu^-}$. We also need to take into account that the absolute bounds on t_E are $t_E^+ \geq t_E \geq t_E^-(\geq 0)$. We can encode the t_E integral in the operator like before,

$$\Gamma^-_{up} = \frac{(-1)^n \alpha}{128\pi^3 E_\chi k} \int_{-\infty}^{0} dq_0 \frac{e^{q_0/T_\star}}{e^{q_0/T_\star} - 1} \Big[\mathcal{I}\left(\tilde{f}_1(t), t_E^+, t^+_{\mu^+}, t_E^-, t^-_{\mu^+}\right) \Theta(q_0 + \mu_F) \tag{4.4.17}$$

$$+ \mathcal{I}\left(\tilde{f}_2(t), t_E^+, t^+_{\mu^-}, t_E^-, t^+_{\mu^+}\right) \Theta(q_0 + \mu_F) \tag{4.4.18}$$

$$+ \mathcal{I}\left(\tilde{f}_2(t), t_E^+, t^-_{\mu^+}, t_E^-, t^-_{\mu^-}\right) \Theta(q_0 + \mu_F) \tag{4.4.19}$$

$$+ \mathcal{I}\left(\tilde{f}_2(t), t_E^+, t^+_{\mu^-}, t_E^-, t^-_{\mu^-}\right) \Theta(-q_0 - \mu_F) \Big] \tag{4.4.20}$$

$$\tilde{f}_1(t_E) = \frac{q_0 t_E^n}{\sqrt{t_E + q_0^2}} \tag{4.4.21}$$

$$\tilde{f}_2(t_E) = \frac{t_E^n}{\sqrt{t_E + q_0^2}} (E_n^{t^-} + q_0 - \mu_F) \tag{4.4.22}$$

4.4.1 Evaporation From Degenerate Media

We now apply the up scattering rate to the case of thermalised DM being evaporated from a degenerate, relativistic media. For now we work in the optically thin regime. Evaporation requires that the target transfers a minimum amount of energy such that the DM escapes the star, given by

$$q_0^{min} = E_\chi - m_\chi/\sqrt{B} = K_\chi - m_\chi \left(1/\sqrt{B} - 1\right) \tag{4.4.23}$$

where $K_\chi = E_\chi - m_\chi$ is the DM kinetic energy. Then the up scattering rate applicable to evaporation is given by

$$\Gamma^-_{evap} = \int_{-\infty}^{q_0^{min}} dq_0 \, \frac{d\Gamma^-_{up}}{dq_0} = \int_{-\infty}^{z-y} dx \frac{d\Gamma^-_{up}}{dx} \tag{4.4.24}$$

$$x = \frac{q_0}{T_\star} \tag{4.4.25}$$

$$y = \frac{m_\chi \left(1/\sqrt{B} - 1\right)}{T_\star} \tag{4.4.26}$$

$$z = \frac{K_\chi}{T_\star} \tag{4.4.27}$$

To obtain the evaporation rate, we integrate this over star's volume and the DM distribution, which we take to be isothermal and given by

$$n_{\chi,iso} = \frac{N_c}{1 + \exp\left(\frac{K_\chi - m_\chi\left(1/\sqrt{B}-1\right)}{T_\star}\right)} \sim N_c \exp\left(-\frac{K_\chi - m_\chi\left(1/\sqrt{B}-1\right)}{T_\star}\right) = N_c e^{(y-z)} \tag{4.4.28}$$

which is normalised such that the total number of DM particles is

$$N_\chi = 4\pi \int_0^{R_\star} r^2 dr \int_0^{m_\chi\left(1/\sqrt{B}-1\right)} dK_\chi \frac{N_c}{1 + \exp\left(\frac{K_\chi - m_\chi\left(1/\sqrt{B}-1\right)}{T_\star}\right)} \tag{4.4.29}$$

$$\sim 4\pi R_\star^3 N_c T_\star \int_0^1 d\tilde{r}\, \tilde{r}^2 \int_0^y dz\, e^{y-z} \tag{4.4.30}$$

$$= 4\pi R_\star^3 N_c T_\star \int_0^1 d\tilde{r}\, \tilde{r}^2 (e^y - 1) \tag{4.4.31}$$

Therefore the total evaporation rate is given by

$$E_{tot} = 4\pi \int_0^{R_\star} dr\, r^2 \int_0^{m_\chi\left(1/\sqrt{B}-1\right)} dK_\chi \, \frac{N_c}{1 + \exp\left(\frac{K_\chi - m_\chi\left(1/\sqrt{B}-1\right)}{T_\star}\right)} \int_{-\infty}^{q_0^{min}} dq_0 \, \frac{d\Gamma^-_{up}}{dq_0} \tag{4.4.32}$$

$$\sim 4\pi N_c R_\star^3 T_\star \int_0^1 d\tilde{r}\, \tilde{r}^2 \int_0^y dz\, e^{y-z} \int_{-\infty}^{z-y} dx \, \frac{d\Gamma^-_{up}}{dx} \tag{4.4.33}$$

$$\tag{4.4.34}$$

We are interested in calculating the evaporation rate per DM particle, $E_\star = E_{tot}/N_\chi$, such that the evolution of the number of DM inside the star is given by

$$\frac{dN_\chi}{dt} = C_\star - E_\star N_\chi - A_\star N_\chi^2 \tag{4.4.35}$$

This is given by

$$E_\star = \frac{\int_0^1 d\tilde{r}\, \tilde{r}^2 \int_0^y dz\, \frac{1}{1+\exp(z-y)} \int_{-\infty}^{z-y} dx \frac{d\Gamma^-_{up}}{dx}}{\int_0^1 d\tilde{r}\, \tilde{r}^2 \int_0^y dz\, \frac{1}{1+\exp(z-y)}} \tag{4.4.36}$$

$$\sim \frac{\int_0^1 d\tilde{r}\, \tilde{r}^2 \int_0^y dz\, e^{y-z} \int_{-\infty}^{z-y} dx \frac{d\Gamma^-_{up}}{dx}}{\int_0^1 d\tilde{r}\, \tilde{r}^2 (e^y - 1)} \tag{4.4.37}$$

$$\sim \frac{1}{e^y - 1} \int_0^y dz\, e^{y-z} \int_{-\infty}^{z-y} dx \frac{d\Gamma^-_{up}}{dx} \tag{4.4.38}$$

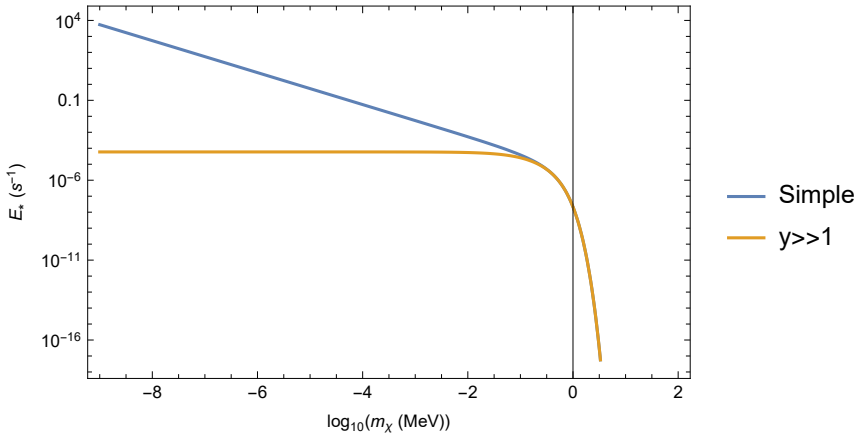

Figure 4.4: Simplified evaporation rate for WD. The $y \gg 1$ refers to replacing $(e^y - 1)^{-1} \to e^{-y}$

where in the last step we assume the DM is localised close to the centre of the star.

We can use a simplified form of the interaction rate, where we only take the $h_+ = 1$ contribution, which leads to a simplified evaporation rate for constant matrix element

$$E_\star^{simp} = \frac{(m_n^2 + m_\chi^2)\sigma_0 T_\star^2}{2\pi^2 m_\chi (e^y - 1)} \int_0^y dz\, e^{y-z} \int_{-\infty}^{z-y} dx\, \frac{x e^x}{e^x - 1} \tag{4.4.39}$$

A simple approximation for the evaporation mass is

$$E_\star(m_{evap}) t_\star \sim 1 \tag{4.4.40}$$

where $t_\star$ is the age of the star. For ages $> 10^5$ yrs the evaporation mass is ~ 1 MeV.

4.5 Kinetic Heating

The metric at any point inside or outside the NS can be written as

$$ds^2 = B(r)dt^2 - A(r)dr^2 - r^2(d\theta^2 + \sin^2\theta d\phi^2) \tag{4.5.1}$$

Along an orbit, the conserved conjugate momenta are the angular momentum per unit mass, $p_\phi = -L$ and the energy per unit mass $p_t = E_\chi$, and taking the orbit to lie in the $\theta = \pi/2$ plane leads to $p_\theta = 0$.

The equation which describes the orbit can be obtained from the square of the energy-momentum 4-vector,

$$g_{\alpha\beta}p^\alpha p^\beta - m_\chi^2 = 0 \tag{4.5.2}$$

$$\implies g^{\alpha\beta}p_\alpha p_\beta - m_\chi^2 = 0 \tag{4.5.3}$$

with

$$g^{tt} = 1/B(r), \quad g^{rr} = -1/A(r), \quad g^{\phi\phi} = -1/r^2 \tag{4.5.4}$$

$$\implies 0 = g^{tt}p_t p_t + g^{rr}p_r p_r + g^{\phi\phi}p_\phi p_\phi - m_\chi^2 \tag{4.5.5}$$

$$= \frac{E_\chi^2}{B(r)} - \frac{1}{A(r)}\left(g_{rr'}p^{r'}\right)\left(g_{rr'}p^{r'}\right) - \frac{L^2}{r^2} - m_\chi^2 \tag{4.5.6}$$

$$= \frac{E_\chi^2}{B(r)} - m_\chi^2 A(r)\left(\frac{dr}{d\tau}\right)^2 - \frac{L^2}{r^2} - m_\chi^2 \tag{4.5.7}$$

To find $dt/d\tau$, we use

$$p^t = m_\chi \frac{dt}{d\tau} = g^{tt}p_t = \frac{E_\chi}{B(r)} \tag{4.5.8}$$

$$\implies \frac{dt}{d\tau} = \frac{1}{B(r)}\frac{E_\chi}{m_\chi} \tag{4.5.9}$$

This gives

$$\left(\frac{dr}{dt}\right)^2 = \frac{B}{\tilde{E}_\chi^2 A}\left[\tilde{E}_\chi^2 - B(r)\left(1 + \frac{\tilde{L}^2}{r^2}\right)\right] \tag{4.5.10}$$

For simplicity, consider orbits that are a straight line ($\tilde{L} = 0$), which has a radial extent R. This is related to $\tilde{E}_\chi$ through

$$\tilde{E}_\chi^2 = B(R) \tag{4.5.11}$$

$$\implies R = \frac{2GM_\star}{1 - \tilde{E}_\chi^2}, \quad R > R_\star \tag{4.5.12}$$

using $B(r > R_\star) = 1 - 2GM_\star/r$.

It is important to note that E_χ so far has been the *conserved* energy along the orbit, which for the initial approach is $E_\chi = m_\chi + \frac{1}{2}m_\chi u^2 \sim m_\chi$. We now call this energy $E_\chi^{\rm orbit}$, which is related to the DM energy as seen by a distant observer, $E_\chi^{\rm int}$, and is the energy used in calculating the interaction rates, through

$$E_\chi^{\rm orbit} = \sqrt{g_{tt}}E_\chi^{\rm int} = \sqrt{B(r)}E_\chi^{\rm int} \tag{4.5.13}$$

and as $E_\chi^{\rm orbit} < m_\chi$ for all subsequent scatters after capture, eq. 4.5.12 is always positive.

These "orbits" are straight lines that pass through the star's centre and extend an amount $R - R_\star$ on either side. Due to the symmetry of the motion, the period of the orbit is then

$$T_{\rm orbit} = 4\int_0^R \frac{1}{dr/dt}dr \tag{4.5.14}$$

More relevant to this application is the time spent inside and outside the star, which is given by

$$T_{\text{inside}} = 4\int_0^{R_\star} \frac{1}{dr/dt} dr \tag{4.5.15}$$

$$T_{\text{inside}} = 4\int_{R_\star}^{R} \frac{1}{dr/dt} dr \tag{4.5.16}$$

4.5.1 Keeping Angular Dependence

For $\tilde{L} \neq 0$, we need the equation of motion for the angular coordinate ϕ,

$$\frac{d\phi}{d\tau} = g^{\phi\phi} p_\phi = \frac{\tilde{L}}{r^2} \tag{4.5.17}$$

$$\implies \frac{d\phi}{dt} = \frac{B(r)}{\tilde{E}_\chi} \frac{\tilde{L}^2}{r^2} \tag{4.5.18}$$

The maximum value of $\tilde{L}^2$ is given by

$$\tilde{L}^2_{\text{MAX}} = \frac{\tilde{E}_\chi^2 - B(r)}{B(r)} r^2 \tag{4.5.19}$$

and we parameterise the possible angular momentum along the orbit as

$$\tilde{L}^2 = y\tilde{L}^2_{\text{MAX}}, \quad 0 < y < 1. \tag{4.5.20}$$

leading to the equation for dr/dt simplifying to

$$\frac{dr}{dt} = \frac{B(r)}{\tilde{E}_\chi^2 A(r)} \left(\tilde{E}_\chi^2 - B(r)\right)(1-y) \tag{4.5.21}$$

showing that the maximum radius of the orbit does not change from the $\tilde{L} = 0$ case, only the time spent outside the star changes.

4.5.2 Checking Newtonian/Non-Relativistic Limit

In the Newtonian limit, we take

$$B - 1 \approx 2\phi \ll 1, \tag{4.5.22}$$

$$A - 1 \approx -2GM(r)/r \equiv -2V(r) \ll 1, \tag{4.5.23}$$

$$\tilde{L}^2/r^2 \ll 1, \tag{4.5.24}$$

$$\tilde{E} - 1 = \varepsilon \ll 1, \tag{4.5.25}$$

with ε the non-relativistic energy per unit mass. Then expanding Eq. 4.5.10 we get

$$\left(\frac{dr}{dt}\right)^2 = (1+2\phi)(1+2V) - (1+2\phi)^2(1+2V)(1-2\varepsilon)\left(1 + \frac{\tilde{L}^2}{r^2}\right) \tag{4.5.26}$$

$$= 1 + 2\phi + 2V - \left(1 + 4\phi + 2V + \frac{\tilde{L}^2}{r^2} - 2\varepsilon\right) \tag{4.5.27}$$

$$= -2\phi - \frac{\tilde{L}^2}{r^2} + 2\varepsilon \tag{4.5.28}$$

$$\implies \frac{1}{2}\left(\frac{dr}{dt}\right)^2 + \frac{\tilde{L}^2}{2r^2} + \phi = \varepsilon \tag{4.5.29}$$

which is the standard result for a Newtonian orbit.

4.5.3 Procedure for calculating kinetic heating time

- Select a point in the star for the DM to scatter off, $r_{\text{scatter},0}$.
- DM comes in from infinity with initial energy $E_\chi \approx m_\chi$
- Boost DM to local energy of $m_\chi/\sqrt{B(r_{\text{scatter}})}$
- Scatter the DM and calculate initial ΔE_χ
- Set local DM energy to $E_\chi \equiv p^t = m_\chi/\sqrt{B(r_{\text{scatter}})} - \Delta E_\chi$
- Calculate the new conserved energy per unit mass along the orbit as

$$\tilde{E}_\chi^{\text{orbit}} = \sqrt{B(r_{\text{scatter}})}E_\chi/m_\chi = \frac{\sqrt{B(r_{\text{scatter}})}}{m_\chi}(m_\chi/\sqrt{B(r_{\text{scatter},0})} - \Delta E_\chi) \tag{4.5.30}$$

- Use Equation 4.5.11 to solve for the maximum radius of the orbit, R_{orbit}.
- Use equations 4.5.15 and 4.5.16 to calculate $T_{\text{in}}/(T_{\text{in}} + T_{\text{out}})$
- Adjust the time interval between scatter by $dt \to dt(T_{\text{in}}/(T_{\text{in}} + T_{\text{out}}))^{-1}$
- Iterate until $R_{\text{orbit}} < R_\star$

Chapter 5

Capture in Neutron Stars

5.1 Deep Inelastic Scattering

When the energy transfer in DM-nucleon scatterings reaches above ~ 1 GeV, the DM begins to resolve the parton structure of the nucleon, and deep inelastic scattering (DIS) occurs. The reaction that takes place is then

$$\chi(k) + N(P) \to \chi(k^{'}) + X \tag{5.1.1}$$

$$\chi(k) + q_i(xP) \to \chi(k^{'}) + q_i(p^{'}) \tag{5.1.2}$$

where X is the unknown hadronic final state. At the parton level[1], the DM-parton undergo elastic scattering, with cross section $\hat{\sigma}$. The total cross section for the process eq. 5.1.1 is obtained by summing over the parton cross sections weighted by the corresponding parton distribution functions (PDFs) $f_i(x, Q^2)$,

$$\frac{d^2\sigma}{dx\, dQ^2} = \sum_i f_i(x, Q^2) \frac{d\hat{\sigma}}{dQ^2}, \tag{5.1.3}$$

where $Q^2 = -q^2 = -\hat{t}$ is the squared 4-momentum transfer, and x is the fraction of the nucleon momentum carried by the parton, $p = xP$. As we are dealing with heavy incoming particles, we follow ref. [3]. Important kinematic relations:

$$\hat{t} = 2m_\chi^2 - 2k \cdot k^{'} \tag{5.1.4}$$

$$\hat{s} = m_\chi^2 + x^2 m_n^2 + 2p \cdot k = (1-x)(m_\chi^2 - x m_n^2) + xs \tag{5.1.5}$$

$$\hat{u} = m_\chi^2 + x^2 m_n^2 - 2p \cdot k^{'} \tag{5.1.6}$$

$$\hat{s} + \hat{t} + \hat{u} = 2m_\chi + 2x^2 m_n^2 \tag{5.1.7}$$

$$s = m_\chi^2 + m_n^2 + 2P \cdot k \tag{5.1.8}$$

The Q^2 parameter is typically swapped out for the parameter y, the fractional energy lost by the DM in the nucleon rest frame

$$y = \frac{q \cdot P}{k \cdot P} = \frac{-\hat{t}}{\hat{s} - m_\chi^2 - x^2 m_n^2} \tag{5.1.9}$$

$$dQ^2 = (\hat{s} - m_\chi^2 - x^2 m_n^2) dy = x(s - m_\chi^2 - m_n^2) dy \tag{5.1.10}$$

giving the differential cross section as

$$\frac{d^2\sigma}{dx\, dy} = (\hat{s} - m_\chi^2 - x^2 m_n^2) \sum_i f_i(x, Q^2) \frac{d\hat{\sigma}}{dQ^2} = x(s - m_\chi^2 - m_n^2) \sum_i f_i(x, Q^2) \frac{d\hat{\sigma}}{dQ^2}, \tag{5.1.11}$$

The integration bounds for DIS are generically $0 < x < 1$ and $0 < y < y_{max}$, where y_{max} is set by imposing $\cos\theta \leq 1$, and in general $y_{max} \neq 1$[2]. Now, the value of y_{max} is set by

$$\begin{aligned} y_{max} &= \frac{-\hat{t}_{min}}{\hat{s} - m_\chi^2 - x^2 m_n^2} \\ &= \frac{\hat{\gamma}^2}{\hat{s}\hat{\beta}} \\ &= \frac{(\hat{s} - m_\chi^2 - x^2 m_n^2)^2 - 4x^2 m_\chi^2 m_n^2}{\hat{s}(\hat{s} - m_\chi^2 - x^2 m_n^2)} \end{aligned}$$

where $\hat{\beta} = \beta(\hat{s}, m_\chi, x m_n)$, $\hat{\gamma} = \gamma(\hat{s}, m_\chi, x m_n)$ The parton level differential cross section is given by

$$\frac{d\hat{\sigma}}{dQ^2} = \frac{2\hat{s}}{\hat{\gamma}^2} \frac{d^2\hat{\sigma}}{dx\, d\cos\theta_{CM}} = \frac{\hat{s}}{8\pi\hat{\gamma}^2} \frac{\hat{\beta}^2}{(2\hat{s}\hat{\beta}^2 - \hat{\gamma}^2)} \widehat{|\mathcal{M}|}^2 \tag{5.1.12}$$

[1] Parton level quantities will be denoted with a 'hat' to distinguish them from the nucleon level.

[2] In typical DIS calculations, e.g. neutrino-nucleon scattering, the incoming particle is treated as massless, allowing $y_{max} = 1$.

with the nucleon level being

$$\frac{d^2\sigma}{dx\,dy} = (\hat{s} - m_\chi^2)\frac{\hat{s}}{8\pi\hat{\gamma}^2}\frac{\hat{\beta}^2}{(2\hat{s}\hat{\beta}^2 - \hat{\gamma}^2)}\sum_i f_i(x,Q^2)\widehat{|\mathcal{M}_i|^2} \tag{5.1.13}$$

As the capture rate required integrating over $\hat{s}$, this must be done at the parton level, i.e. before integrating over x. Following ref. [8], we do this with

$$\hat{s}_0 = m_\chi^2 + 2xE_nE_\chi \tag{5.1.14}$$

$$\delta\hat{s} = 2xm_\chi\sqrt{E_n^2 - m_n^2}\sqrt{\frac{1-B}{B}} \tag{5.1.15}$$

$$E_n \simeq m_n + \mu_{F,n} \tag{5.1.16}$$

One should in practice integrate over E_n. The differential capture rate will then go as

$$\frac{dC}{dV} \sim \int_0^1 dx \int_{\hat{s}_0-\delta\hat{s}}^{\hat{s}_0+\delta\hat{s}} d\hat{s} \int_0^{y_{max}} dy \frac{\hat{s}(\hat{s} - m_\chi^2)}{8\pi\hat{\gamma}^2}\frac{\hat{\beta}}{(2\hat{s}\hat{\beta} - \hat{\gamma}^2)}\sum_i f_i(x,Q^2)\widehat{|\mathcal{M}_i|^2}\,\theta(Q^2-1) \tag{5.1.17}$$

$$\sim \int_0^1 dx\, 2\delta\hat{s} \int_0^{y_{max}} dy \frac{\hat{s}_0(\hat{s}_0 - m_\chi^2)}{8\pi\hat{\gamma}^2}\frac{\hat{\beta}}{(2\hat{s}_0\hat{\beta} - \hat{\gamma}^2)}\sum_i f_i(x,Q^2)\widehat{|\mathcal{M}_i|^2}\,\theta(Q^2-1) \tag{5.1.18}$$

where the step functions enforces the momentum transfer to be above 1 GeV as the PDFs are only reliable above this threshold.

Chapter 6

Annihilation

6.1 Loop Induced Two Photon Channel

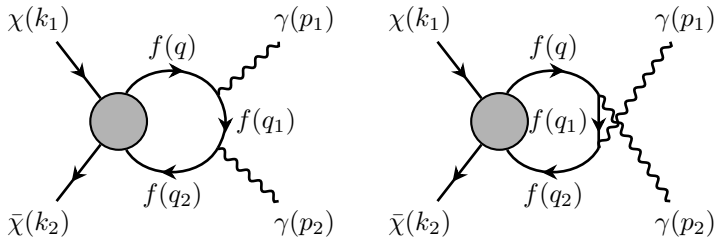

Figure 6.1: Diagrams contributing to DM annihilation to two photons

DM annihilation to two photons is induced at one loop order due to the coupling to SM fermions. The relevant diagrams are shown in fig. 6.1. The structure of the matrix elements will be

$$i\mathcal{M} = \sum_f \frac{N_c c_f^I}{\Lambda^2} \left[\bar{v}\Gamma_\chi^\alpha u\right] \epsilon_\mu^*(p_1)\epsilon_\nu^*(p_2) \int \frac{d^4q}{(2\pi)^4} \frac{\mathrm{Tr}\left[\Gamma_{f,\alpha} i(\not{q}+m_f)(-ieQ_f\gamma^\mu) i(\not{q}_1+m_f)(-ieQ_f\gamma^\nu) i(\not{q}_2+m_f)\right]}{(q^2-m_f^2)(q_1^2-m_f^2)(q_2^2-m_f^2)} + (p_1 \leftrightarrow p_2) \tag{6.1.1}$$

$$= \sum_f \frac{N_c c_f^I}{\Lambda^2} \left[\bar{v}\Gamma_\chi^\alpha u\right] \epsilon_\mu^*\epsilon_\nu^* ie^2 Q_f^2 F_\alpha^{\mu\nu} + (p_1 \leftrightarrow p_2) \tag{6.1.2}$$

with c_f^I the DM-fermion coupling for interaction types $I \in \{S, P, V, A, T\}$, N_c the fermion colour factor,

$$q_1 = q - p_1 \tag{6.1.3}$$

$$q_2 = q - p_1 - p_2 \tag{6.1.4}$$

and $F_\alpha^{\mu\nu}$ accounts for the loop integral

$$F_\alpha^{\mu\nu} = \int \frac{d^4q}{(2\pi)^4} \frac{\mathrm{Tr}\left[\Gamma_{f,\alpha}(\not{q}+m_f)\gamma^\mu(\not{q}_1+m_f)\gamma^\nu(\not{q}_2+m_f)\right]}{(q^2-m_f^2)(q_1^2-m_f^2)(q_2^2-m_f^2)} \tag{6.1.5}$$

As an estimate, take

$$F_{appx} \sim \frac{1}{16\pi^2}\Lambda_{loop}\log\left(\frac{s}{m_f^2}\right) \tag{6.1.6}$$

for some momentum cutoff $\Lambda_{loop} \sim m_f$ [M: does this makes sense? Or should we take $\Lambda_{loop} \sim \Lambda_{EFT}$?]

Then the squared matrix element goes as [M: need to deal with sum over fermions]

$$|\overline{\mathcal{M}}|^2 = \frac{e^4 Q_f^4 N_c^2}{4} \frac{(c_f^I)^2}{\Lambda^4} \mathrm{Tr}\left[(\not{k}_1+m_\chi)\Gamma_\chi^\alpha(\not{k}_2-m_\chi)\Gamma_\chi^\beta\right] F_\alpha^{\mu\nu} F_{\mu\nu\beta} \tag{6.1.7}$$

$$\sim \frac{e^4 Q_f^4 N_c^2}{4} \frac{(c_f^I)^2}{\Lambda^4} H_\chi \left[\frac{1}{16\pi^2}\Lambda_{loop}\log\left(\frac{s}{m_f^2}\right)\right]^2 \tag{6.1.8}$$

where the factor containing DM traces has been written as H_χ. To compare to annihilation to neutrinos in the low DM mass range ($m_\chi < m_e$), note that the amplitude will be of the form

$$|\mathcal{M}_f|^2 \sim \frac{(c_f^I)^2}{\Lambda^4} H_\chi H_f \sim \frac{(c_f^S)^2}{\Lambda^4} H_\chi (s - 4m_f^2) \tag{6.1.9}$$

where the last step is for operator D1. Then the ratio of the cross sections between the two channels is

$$\frac{\sigma_\gamma}{\sigma_\nu} \sim \frac{m_f^2}{m_\nu^2}\frac{1}{4m_\chi^2}\frac{e^4 Q_f^4 N_c^2}{4}\left[\frac{1}{16\pi^2}\Lambda_{loop}\log\left(\frac{s}{m_f^2}\right)\right]^2 \tag{6.1.10}$$

assuming $m_\chi \gg m_\nu$. Because the ratio m_f/m_ν is so large, this implies $\gg \mathcal{O}(10^{10})$ enhancements compared to the neutrino channel. In fact, if this estimate is to be believed, any interaction which couples to the fermion mass is dominated by the photon channel due to the top quark running in the loop, i.e. we get enhancements of factors m_t^2/m_f^2. This could be beneficial to D1-4 and maybe D8. This channel is forbidden for operators D5-6 due to the Landau-Yang theorem (check this, maybe others?).

Being more concrete, looking at D1, I evaluate the loop integral using `FeynCalc` [43, 42, 32] together with `PackageX` [36].

$$\left|\overline{\mathcal{M}}\right|^2_{D1} = \frac{e^4 Q_f^4 N_c^2 (y_f)^2}{64\pi^4\Lambda^4}\frac{m_f^2}{s^2}(s-4m_\chi^2)\left((s-4m_f^2)\log^2\left(\frac{\sqrt{s(s-4m_f^2)}-(s-2m_f^2)}{2m_f^2}\right)-4s\right)^2 \tag{6.1.11}$$

with the total annihilation cross section being

$$\frac{d\sigma_\gamma^{D1}}{d\cos\theta} = \frac{1}{32\pi s}\sqrt{\frac{s}{s-4m_\chi^2}}\left|\overline{\mathcal{M}}\right|^2_{D1} \tag{6.1.12}$$

Expanding in v_{rel} leaves,

$$\sigma_\gamma v_{rel} = \frac{2m_f^2}{v^2}\frac{e^2 Q_f^4 N_c^2 m_f^2 v_{rel}^2}{4096\pi^5 m_\chi^4}\left(4m_\chi^2+(m_f^2-m_\chi^2)\log^2\left(1+\frac{2m_\chi\left(\sqrt{m_\chi^2-m_f^2}-m_\chi\right)}{m_f^2}\right)\right) \tag{6.1.13}$$

Assuming that the loop is dominated by the top quark running in it, this channel greatly dominates over the neutrino channel by 10^9 orders of magnitude at the electron mass, down to 10^4 orders of magnitude for $m_\chi < 10^{-2}$ MeV. After $m_\chi > m_e$, the electron channel dominates by several orders of magnitude. For D5, 6, 7, 9 and 10, the loop integrals vanish.

For D8, the photon channel is hugely suppressed compared to the neutrino channel, as shown in Fig. **??**

Doing the D1 Integral

For operator D1, we need to compute the integral

$$I^{\mu\nu} = \int \frac{d^4q}{(2\pi)^4}\frac{\mathrm{Tr}\left[(\not{q}+m)\gamma^\mu(\not{q}_1+m)\gamma^\nu(\not{q}_2+m)\right]}{(q^2-m^2)(q_1^2-m^2)(q_2^2-m^2)} \tag{6.1.14}$$

First, we compute the trace in the numerator, which results in

$$\mathrm{Tr}[\cdots] = 4m\left[g^{\mu\nu}\left(m^2-q\cdot q_1+q\cdot q_2-q_1\cdot q_2\right)+q^\mu(q_1^\nu+q_2^\nu)+q_1^\mu(q^\nu+q_2^\nu)-q_2^\mu(q^\nu-q_1^\nu)\right] \tag{6.1.15}$$

$$= 4m\left[g^{\mu\nu}\left(m^2-q^2+2q\cdot k_1-k_1^2-k_1\cdot k_2\right)+4q^\mu q^\nu-4q^\mu k_1^\nu-2q^\mu k_2^\nu-2k_1^\mu q^\nu+2k_1^\mu k_1^\nu+k_1^\mu k_2^\nu+k_2^\mu k_1^\nu\right] \tag{6.1.16}$$

$$= 2m\left[g^{\mu\nu}(2m^2-2q^2+4q\cdot k_1-s)+2(4q^\mu q^\nu-4q^\mu k_1^\nu-2q^\mu k_2^\nu-2k_1^\mu q^\nu+2k_1^\mu k_1^\nu+k_1^\mu k_2^\nu+k_2^\mu k_1^\nu)\right] \tag{6.1.17}$$

where we have used the fact that the out going photons are on shell such that

$$k_1^2 = k_2^2 = 0 \tag{6.1.18}$$

$$k_1\cdot k_2 = s/2 \tag{6.1.19}$$

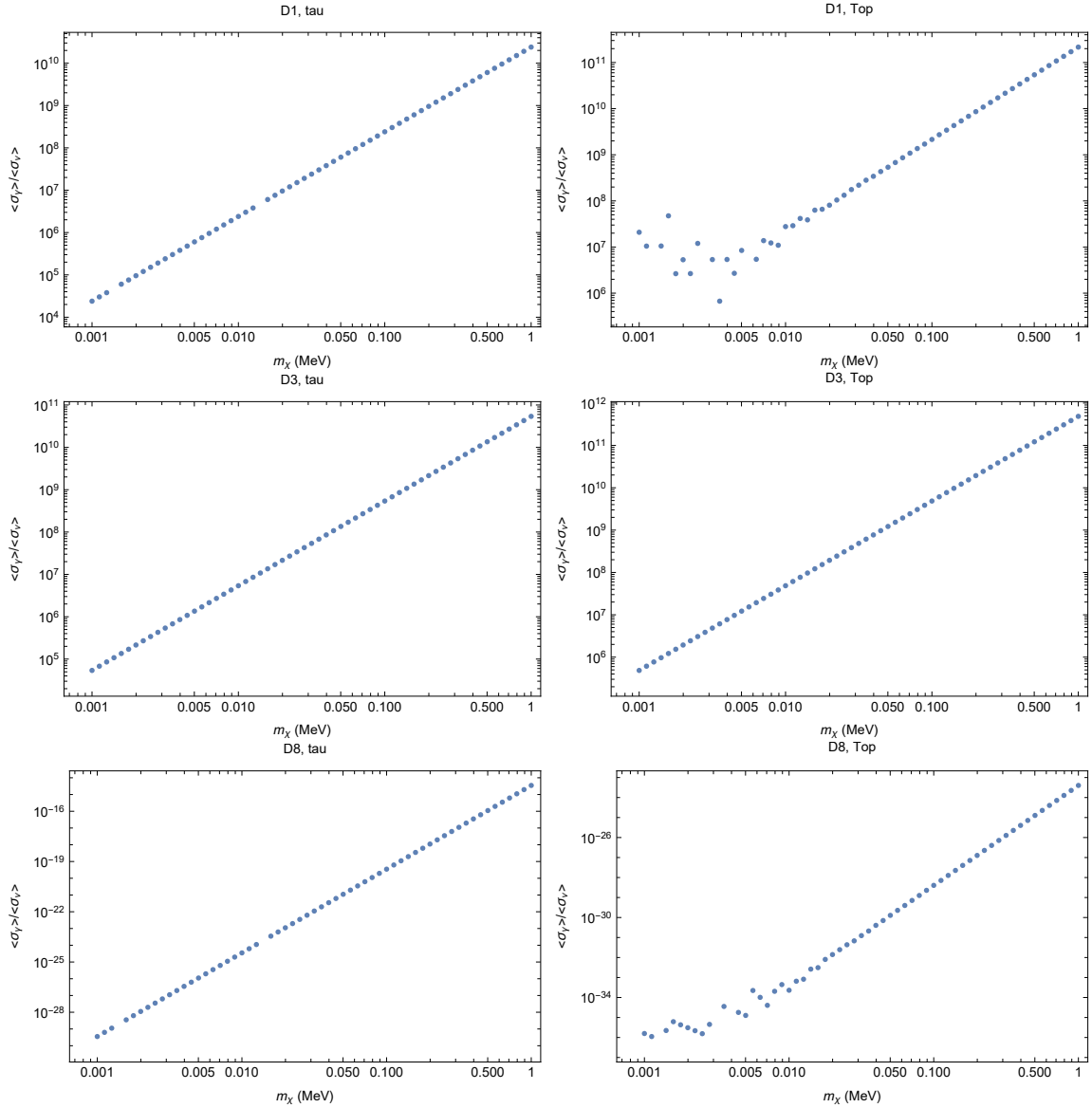

Figure 6.2: Ratio of annihilation cross section to photons and neutrinos for operators D1, 3 and 8. Left: τ running in loop, Right: top running in loop

To simplify the denominator, we introduce Feynman parameters x, y and z, and complete the square as follows;

$$\frac{1}{(q^2-m^2)(q_1^2-m^2)(q_2^2-m^2)} = \int_0^1 dx\,dy\,dz \frac{\delta(x+y+z-1)}{[x(q^2-m^2)+y(q_1^2-m^2)+z(q_2^2-m^2)]^3} \tag{6.1.20}$$

$$= \int_0^1 dx\,dy\,dz \frac{\delta(x+y+z-1)}{[(q-\delta)^2-\Delta]^3} \tag{6.1.21}$$

with

$$\delta^\mu = (1-x)k_1^\mu + (1-x-y)k_2^\mu \tag{6.1.22}$$

$$\Delta = m^2 - (1-x-y)xs \tag{6.1.23}$$

We can then shift the integration variable such that $q^\mu \to q^\mu + \delta^\mu$, and neglect terms linear in q, as the integrand is now even. This leaves

$$I^{\mu\nu} = 2m\int_0^1 dx \int_0^{1-x} dy \int \frac{d^4q}{(2\pi)^4} \frac{g^{\mu\nu}(2m^2 - s(2x(x+y-1)+1) - 2q^2) + 8q^\mu q^\nu + 2(k_1^\mu - 2\delta^\mu)(2k_1^\nu + k_2^\nu - 2\delta^\nu) + 2k_1^\mu k_2^\nu}{(q^2-\Delta)^3} \tag{6.1.24}$$

Regulate the integrals using dimensional regularisation,

$$I^{\mu\nu} = 2m\int_0^1 dx \int_0^{1-x} dy \int \frac{d^dq}{(2\pi)^d} \left(\frac{g^{\mu\nu}(2\Delta - s - (\frac{8}{d}-2)q^2)}{(q^2-\Delta)^3} \right. \tag{6.1.25}$$

$$\left. + \frac{4(x(2x-1)k_1^\mu k_1^\nu + (2x(x+y-1) - y + 1)k_1^\mu k_2^\nu + (x+y-1)(4x+2y-1)k_2^\mu k_1^\nu)}{(q^2-\Delta)^3} \right) \tag{6.1.26}$$

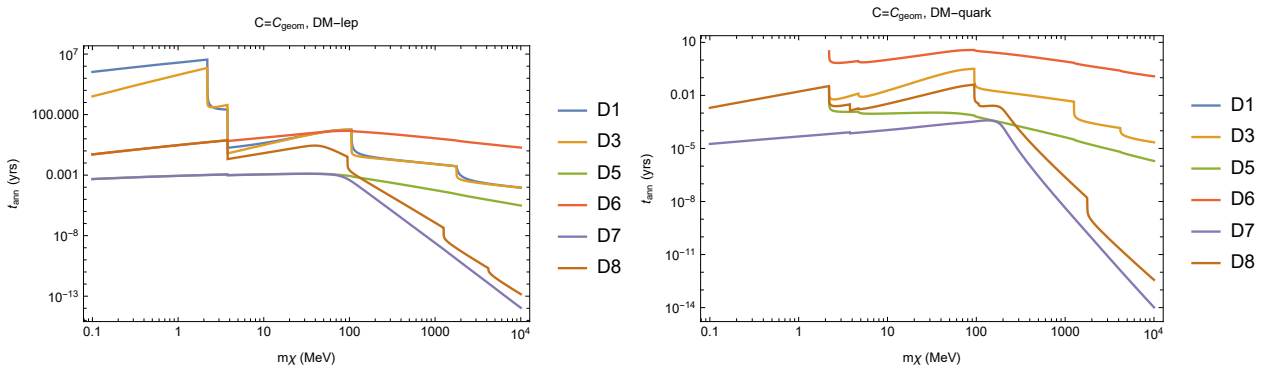

Figure 6.3: Capture-annihilation equilibrium timescales for DM with tree-level couplings to leptons (left) or quarks (right).

6.2 Annihilation to Fermions through Loops

DM which couples to quarks/leptons generate couplings to one another through photon/Z exchange at one or two loop processes. The couplings induced by photon exchange are

$$G_{\chi f}^{1,3} = \frac{Q_f^2 N_{c,L} \alpha_{em}^2}{2\pi} \sum_L G_{\chi L}^{1,3} \frac{2 m_L m_f}{4m_L^2 - m_f^2} \log\left(\frac{4m_L^2}{m_f^2}\right) \tag{6.2.1}$$

$$G_{\chi f}^{5,6} = \frac{Q_f \alpha_{em}}{3\pi} \sum_L G_{\chi L}^{5,6} N_{c,L} Q_L \log\left(\frac{m_L^2}{\lambda^2}\right) \tag{6.2.2}$$

$$\tag{6.2.3}$$

where f denotes the final state fermion and L denotes the fermion running in the loop, the $G_{\chi j}^i$ are the EFT couplings, λ is the CoM energy.

6.3 Neutrino Mean Free Path

6.3.1 Simple Approximation

As a first approximation, just consider neutrinos interacting with electrons through a 4-Fermi interaction. As we are considering centre of mass energies below the electron mass, we cannot neglect external particle masses as is typically done in neutrino scattering calculations. The charged and neutral current cross sections are then given by

$$\sigma_{CC} = \frac{G_F^2}{\pi s}(s - m_e^2)(s - m_\ell^2) \tag{6.3.1}$$

$$\sigma_{NC} = \frac{G_F^2}{12\pi s^3}((c_a - c_v)^2 m_e^8 - 2(2c_a - 5c_v)(c_a - c_v)m_e^6 s + 3(3c_a^2 - 6c_a c_v + 7c_v^2)m_e^4 s^2 \tag{6.3.2}$$

$$+ 2(c_a^2 - 11c_a c_v - 2c_v^2)m_e^2 s^3 + 4(c_a^2 + c_a c_v + c_v^2)s^4)) \tag{6.3.3}$$

where c_a and c_v are the electron axial and vector couplings to the Z boson respectively. Neglecting Pauli-blocking, the mean free path is then given by

$$\lambda_\nu(r) = \frac{1}{n_e(r)\sigma_{TOT}} \tag{6.3.4}$$

with $s = m_\chi + m_e + \mu_{F,e}(r)$ the centre of mass energy of of the neutrino-electron interaction, meaning that the cross section is implicitly dependent on the position. Only electron neutrinos will undergo charged current interactions as we are considering centre off mass energies below the muon mass.

The above neglects Pauli-blocking which will increase the mean free path.

We can then calculate the probability that a neutrino produced near the centre of the star reaches the surface without scattering is

$$P(\text{Escape}) = e^{-\tau(R_\star)} \tag{6.3.5}$$

$$\tau(R_\star) = \int_{r_0}^{R_\star} \frac{dx}{\lambda_\nu(x)} \tag{6.3.6}$$

where $r_0 \sim 0$ is the position the neutrino was produced. This assumes the neutrino travels in a straight line.

6.3.2 Including Pauli Blocking

$$\frac{1}{\lambda} = \frac{\sigma}{V} = 2\int \frac{d^3p_e}{(2\pi)^3}\frac{d^3p_\nu^{'}}{(2\pi)^3}\frac{d^3p_e^{'}}{(2\pi)^3}\frac{\left|\overline{\mathcal{M}}\right|^2(2\pi)^4\delta(p_\nu + p_e - p_\nu^{'} - p_e^{'})}{(2E_\nu)(2E_e)(2E_\nu^{'})(2E_e^{'})|\vec{v}_\nu - \vec{v}_e|}f_{FD}(E_e)(1 - f_{FD}(E_e^{'})) \tag{6.3.7}$$

$$= 2\int \frac{d^3p_e}{(2\pi)^3}dt\frac{d\cos\theta}{dt}\frac{d\sigma}{d\cos\theta}f_{FD}(E_e)(1 - f_{FD}(E_e^{'})) \tag{6.3.8}$$

$$= \frac{1}{2\pi^2}\int dt\, ds\, dE_e\, \frac{E_e s}{\gamma^2 E_\nu}\frac{d\sigma}{d\cos\theta}f_{FD}(E_e)(1 - f_{FD}(E_e^{'})) \tag{6.3.9}$$

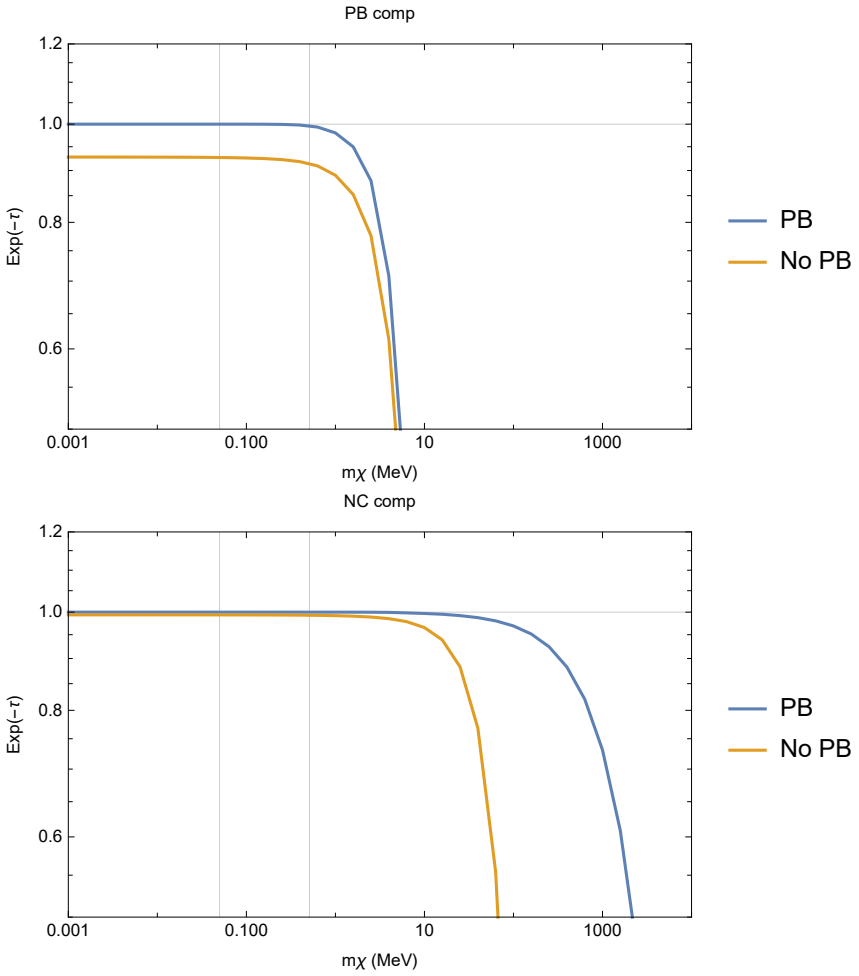

Figure 6.4: Probability of neutrino reaching the surface of the WD without interacting. Top: Including interactions with C nuclei. Bottom: Only NC electron scattering

Chapter 7

Hyperons

See refs [40, 39, 20].

7.1 Nucleon Form Factors

Following Ref. [20] and putting things in our notation, for spin-independent scattering

$$\frac{\sqrt{c_N^S}}{\Lambda^2} = \sum_{q=u,d,s} f_{T_q}^{(N)} \frac{\alpha_{3q}}{m_q} + \frac{2}{27} f_{T_G}^{(N)} \sum_{q=c,b,t} \frac{\alpha_{3q}}{m_q} \tag{7.1.1}$$

$$= \frac{\sqrt{2}}{v} \frac{1}{\Lambda^2} \left[\sum_{q=u,d,s} f_{T_q}^{(N)} + \frac{2}{9} f_{T_G}^{(N)} \right] \tag{7.1.2}$$

where I have substituted α_{3q} for the quark Yukawas y_q/Λ^2 for the EFT operators. The parameters above are defined through the nuclear matrix elements

$$m_N f_{T_q}^{(N)} = \sigma_{Bq} = \langle N | \, m_q \bar{q} q \, | N \rangle = m_q B_q^{(N)} \tag{7.1.3}$$

$$f_{T_G}^{(N)} = 1 - \sum_{q=u,d,s} f_{T_q}^{(N)} \tag{7.1.4}$$

In [40], the $f_{T_q}^{(N)}$ are denoted $\overline{\sigma}_{Bq}$. For protons and neutrons, these are related such that $B_u^{(p)} = B_d^{(n)}$, $B_d^{(p)} = B_u^{(n)}$ and $B_s^{(p)} = B_s^{(n)}$. Define the strange scalar density as

$$y = \frac{2B_s^{(N)}}{B_u^{(N)} + B_d^{(N)}} = \frac{2m_l}{m_s} \frac{\sigma_{Bs}}{\sigma_{Bl}}. \tag{7.1.5}$$

The π-nucleon sigma term, $\sigma_{\pi N}$, can be written as

$$\sigma_{\pi N} = \frac{1}{2} (m_u + m_d) \left(B_u^{(N)} + B_d^{(N)} \right) \tag{7.1.6}$$

These are also denoted as σ_{Bl}, where the B stands for any baryon. Another related quantity is

$$\sigma_0 = m_l \langle N | \, \overline{u}u + \overline{d}d - 2\overline{s}s \, | N \rangle \tag{7.1.7}$$

$$= \sigma_{Bl} - \frac{2m_l}{m_s} \sigma_{Bs} \tag{7.1.8}$$

Known:

$$\sigma_{Bl}, \sigma_{Bs} \tag{7.1.9}$$

Can obtain:

$$y, \sigma_0 \to B_u + B_d \tag{7.1.10}$$

Need:

$$z = \frac{B_u^{(N)} - B_s^{(N)}}{B_d^{(N)} - B_s^{(N)}}, \quad \text{or} \quad B_u^{(N)}/B_d^{(N)} \tag{7.1.11}$$

According to Ref. [15], the leading order contribution comes from the proton matrix elements, $B_q^{(p)}$, which gives

$$z \approx 1.49. \tag{7.1.12}$$

However this should change for other baryons. This allows the calculation of the ratio

$$\frac{B_d^{(N)}}{B_u^{(N)}} = \frac{2 + (z-1)y}{2z - (z-1)y} \tag{7.1.13}$$

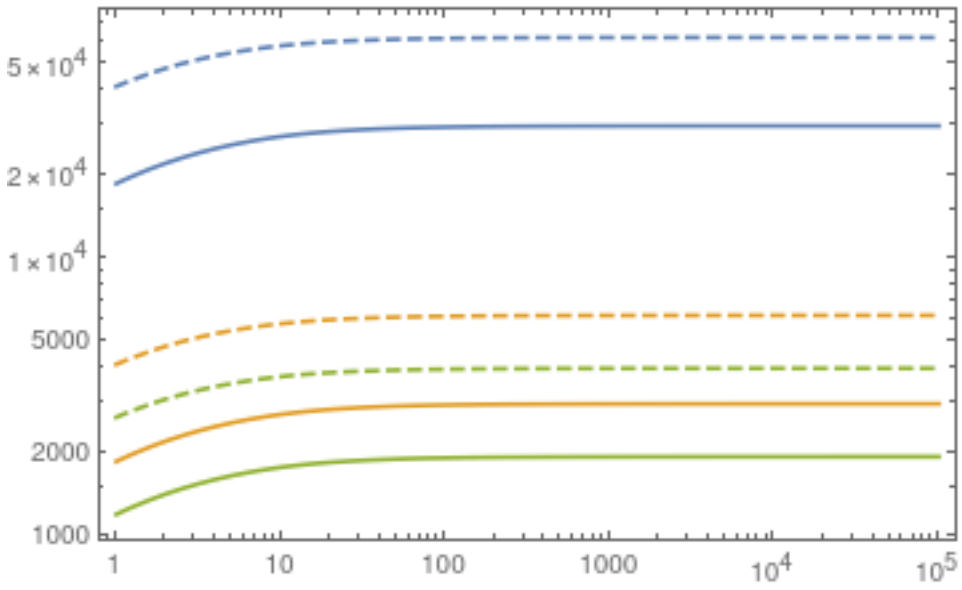

Figure 7.1: Dashed = neutron, solid = Ξ

Finally, these can be related to the $f_{T_q}^{(N)}$,

$$f_{T_u}^{(N)} = \frac{2\sigma_{Bl}}{m_N(1+\frac{m_d}{m_u})\left(1+\frac{B_d^{(N)}}{B_u^{(N)}}\right)} \tag{7.1.14}$$

$$f_{T_d}^{(N)} = \frac{2\sigma_{Bl}}{m_N(1+\frac{m_u}{m_d})\left(1+\frac{B_u^{(N)}}{B_d^{(N)}}\right)} \tag{7.1.15}$$

$$f_{T_s}^{(N)} = \frac{\left(\frac{m_s}{m_d}\right)y\sigma_{Bl}}{m_N\left(1+\frac{m_u}{m_d}\right)} \tag{7.1.16}$$

Model	$g_{\omega n}$	$g_{\rho n}$	$g_{\phi n}$
GM1A	10.617	8.198	0
GM1′B	10.558	8.198	-0.137
TM1C	12.300	9.275	-0.2897

Table 7.1: Relevant meson-neutron coupling constants for each of the models GM1A, GM1′B and TM1C

7.2 Neutron Stars Containing Hyperons

Equation of State with Hyperons

In ref. [22], the authors present several models of nucleon-hyperon matter consistent the observations of NSs with mass $\approx 2M_\odot$. [M: Describe the models] The resulting EoSs and various other thermodynamic quantities have been tabulated as functions of the baryon number density (i.e. $P(n_b), \rho(n_b)$ etc.) and are publicly available.[1] Not provided are the chemical potentials of the various species, though the authors outline the procedure to calculate them. Under beta-equilibrium, we have the following relationships between the relativistic chemical potentials for baryons of species i,

$$\mu_i = \mu_n - q_i \mu_e, \quad \mu_e = \mu_\mu, \tag{7.2.1}$$

where q_i is the charge of the baryon. And so to obtain the chemical potentials of the other particles, one needs only the electron and neutron values. These are given by

$$\mu_e = \sqrt{(p_e^F)^2 + m_e^2} \tag{7.2.2}$$

$$\mu_n = g_{\omega n}\omega^0 + g_{\rho n} I_{3n} \rho_3^0 + g_{\phi n}\phi^0 + m_n^*, \tag{7.2.3}$$

where p^F is the Fermi momentum of the species, I_{3i} the third component of the baryon isospin, the g's are coupling constants between the baryons and the mesons, and m_i^* is the Landau effective mass of the baryon i, given by

$$m_i^* = \sqrt{(p_i^F)^2 + (m_i - g_{\sigma i}\sigma - g_{\sigma^* i}\sigma^*)^2}. \tag{7.2.4}$$

For electrons, we can express the Fermi momentum in terms of their number density,

$$p_e^F = (3\pi^2 n_e)^{1/3} \tag{7.2.5}$$

Approximate Structure of the Crust

The EoSs presented in ref. [22] are not unified ones, and so do not provide information about the crust of a NS with a core containing hyperons. Nonetheless, we can obtain an approximate description for the crust layer by following the procedure laid out in ref. [44]. As the crust only constitutes a small fraction of the entire NS mass, we assume that $M_{crust} \ll M_\star$, and so we can simplify the TOV equation to

$$\frac{dP}{dr} = -\frac{GM_\star}{r^2}\left[\rho(r) + \frac{P(r)}{c^2}\right]\left[1 - \frac{2GM_\star}{c^2 r}\right]^{-1}. \tag{7.2.6}$$

The radial profiles for the crust are obtained from integrating Eq. 7.2.6 form the crust-core boundary $P(r_{cc} = P_{cc}$, to the point where $P = 0$. Eq. 7.2.6 can also be used to to arrive at an expression relating the star's radius to the radius of the core, given the baryon chemical potential at the surface ($\mu_{b,0}$) and at the crust-core interface ($\mu_{b,cc}$). This quantity is determined by assuming thermodynamic equilibrium, such that

$$\mu_b = \frac{\partial \epsilon}{\partial n_b} = \frac{P + \rho c^2}{n_b} \tag{7.2.7}$$

[1] These are available at http://www.ioffe.ru/astro/NSG/heos/hyp.html

The surface value for cold catalysed matter is $\mu_{b,0} = 930.4$ MeV for iron ^{56}Fe. Then, following ref. [44], for two radii r_1 and r_2

$$\frac{\sqrt{1-2GM_\star/r_1c^2}}{\sqrt{1-2GM_\star/r_2c^2}} = \frac{\mu_b(r_2)}{\mu_b(r_1)} \tag{7.2.8}$$

Specifically, we set $r_1 = R_\star$ and $r_2 = R_c$, one obtains

$$\frac{\sqrt{1-2GM_\star/R_\star c^2}}{\sqrt{1-2GM_\star/R_c c^2}} = \frac{\mu_{b,cc}}{\mu_{b,0}}, \tag{7.2.9}$$

which leads to the following expression for the radius of the star

$$R_\star = \frac{R_c}{1-(\alpha-1)(R_c c^2/2GM-1)}, \tag{7.2.10}$$

$$\alpha = \left(\frac{\mu_{b,cc}}{\mu_{b,0}}\right). \tag{7.2.11}$$

The authors of ref. [44] also derive an approximation for the mass of the crust,

$$M_{crust} = \frac{4\pi P_{cc} R_c^4}{GM_c}\left(1-\frac{2GM_c}{R_c c^2}\right) \tag{7.2.12}$$

$$\sim 7.62\times 10^{-2} M_\odot \left(\frac{P_{cc}}{\text{MeV fm}^{-3}}\right)\left(1-\frac{2GM_c}{R_c c^2}\right)\left(\frac{R_c}{10\text{ km}}\right)^4\left(\frac{M_c}{M_\odot}\right)^{-1} \tag{7.2.13}$$

from which the total mass of the star can be obtained as $M_\star = M_c + M_{crust}$.

The other input we need is where the crust-core transition occurs. This is a somewhat model dependent input, though a reasonable approximation is that the transition occurs when the baryon density drops to about half the nuclear saturation density, $n_b(r_{cc}) = 0.5 n_{b,0} \approx 0.16$ fm^{-3}.

TOV and Radial Profiles

Solving the TOV coupled with the EoSs parameterised by the baryon number density, one obtains the mass-radius relations shown in Fig. 7.2. We show the relation considering only the core as well as the inclusion of the crust.

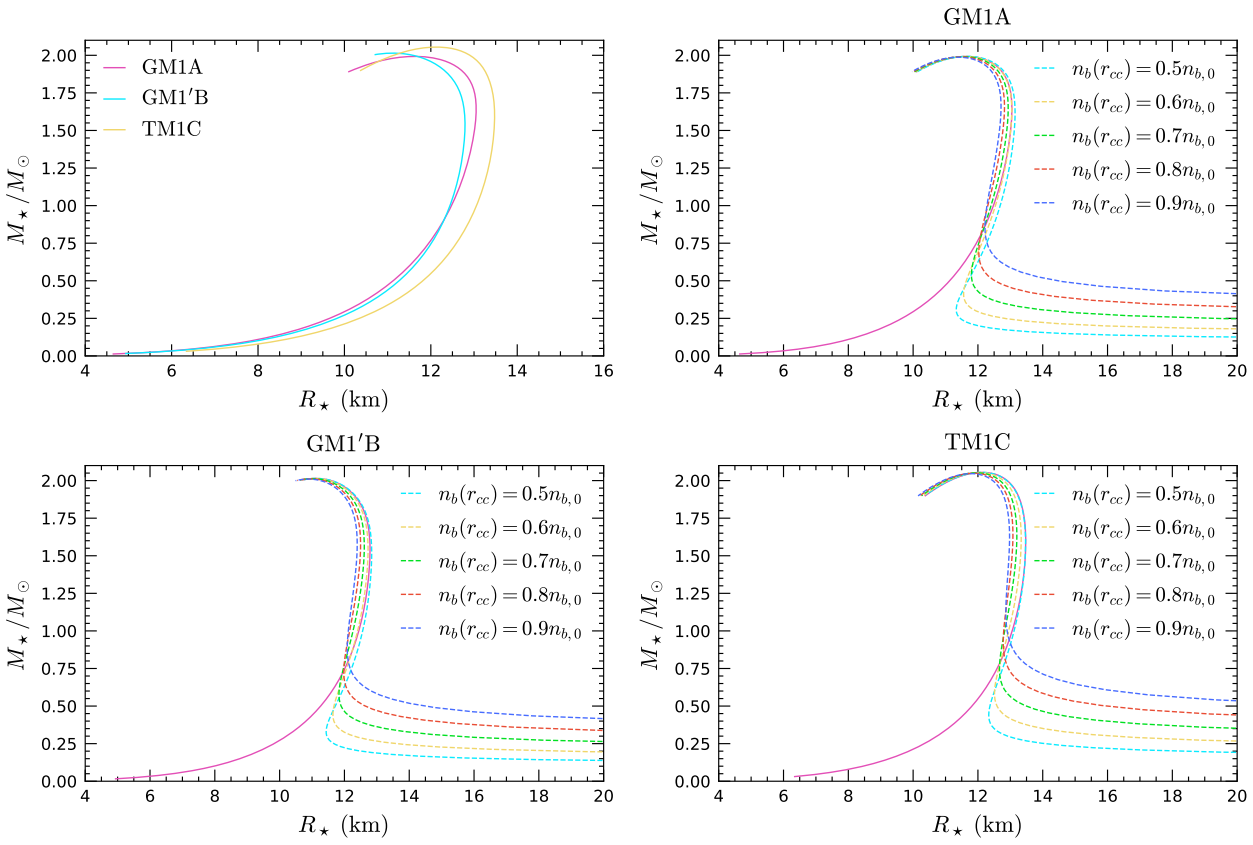

Figure 7.2: Mass-Radius relation for the NS EoS including hyperons. Solid lines represent solutions only for the core, while dashed include the crust for different crust-core transition conditions.

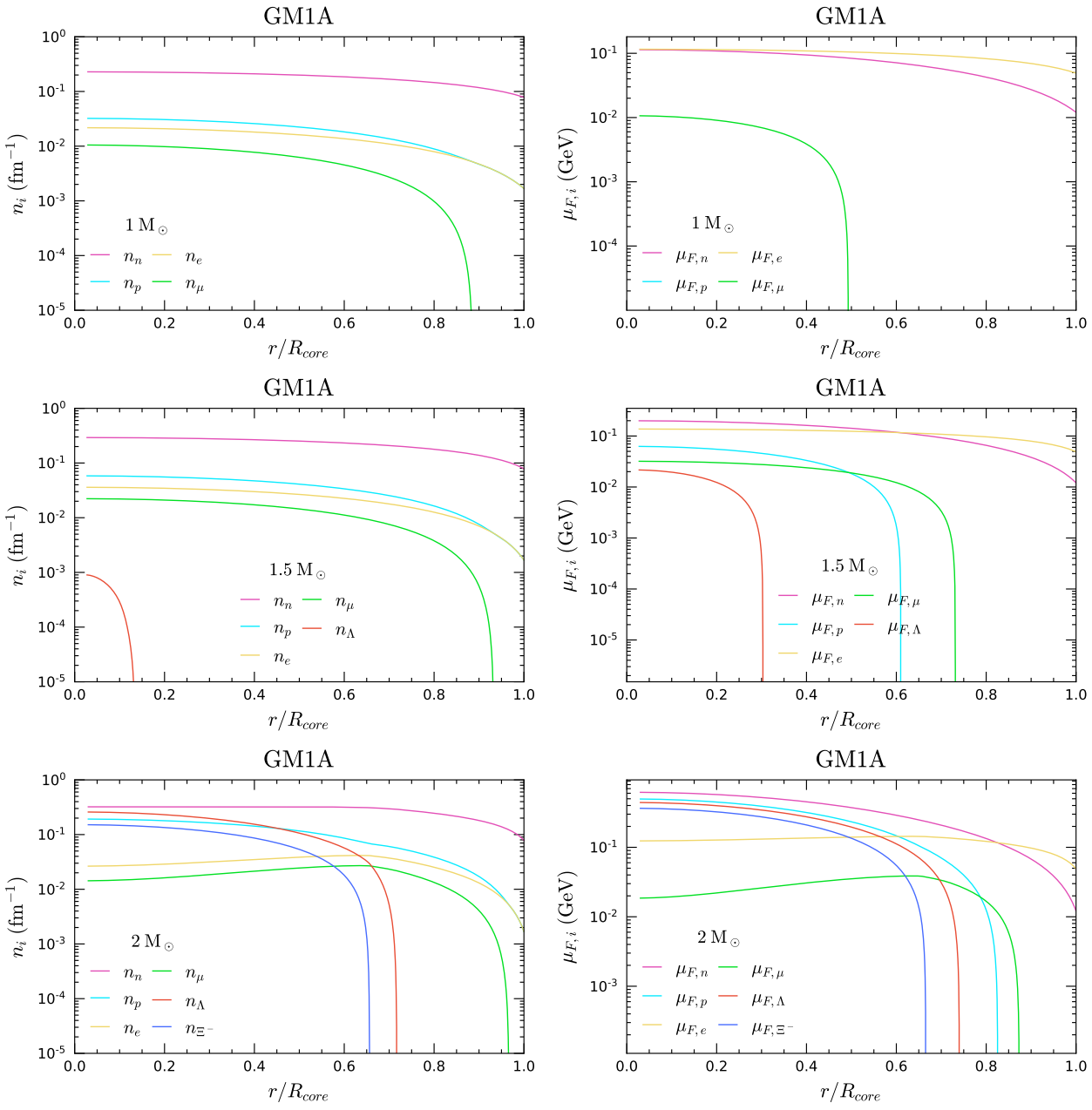

Figure 7.3: Radial profiles for the number density (left) and chemical potentials (right) for the EoS model GM1A

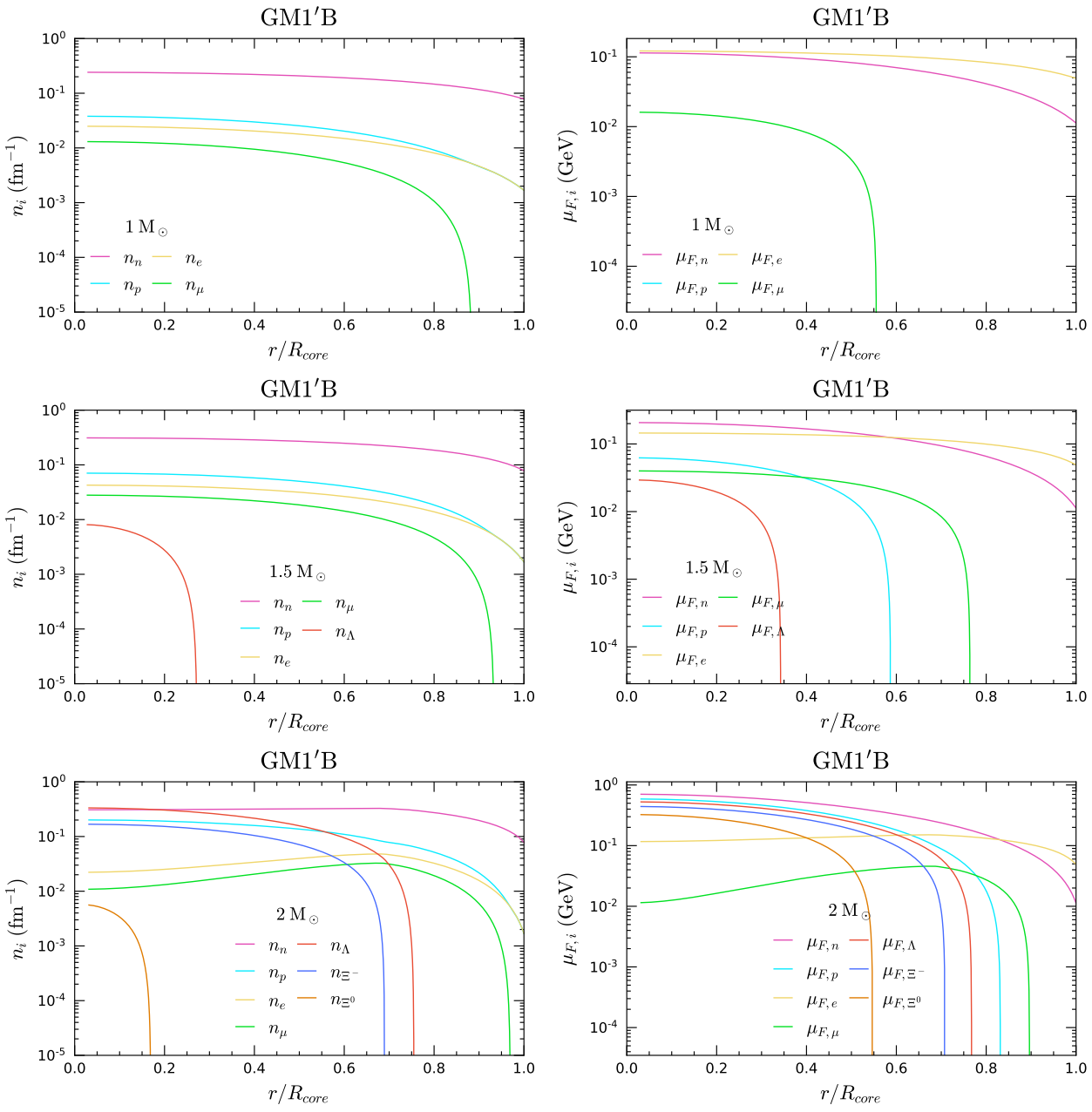

Figure 7.4: Radial profiles for the number density (left) and chemical potentials (right) for the EoS model GM1′B

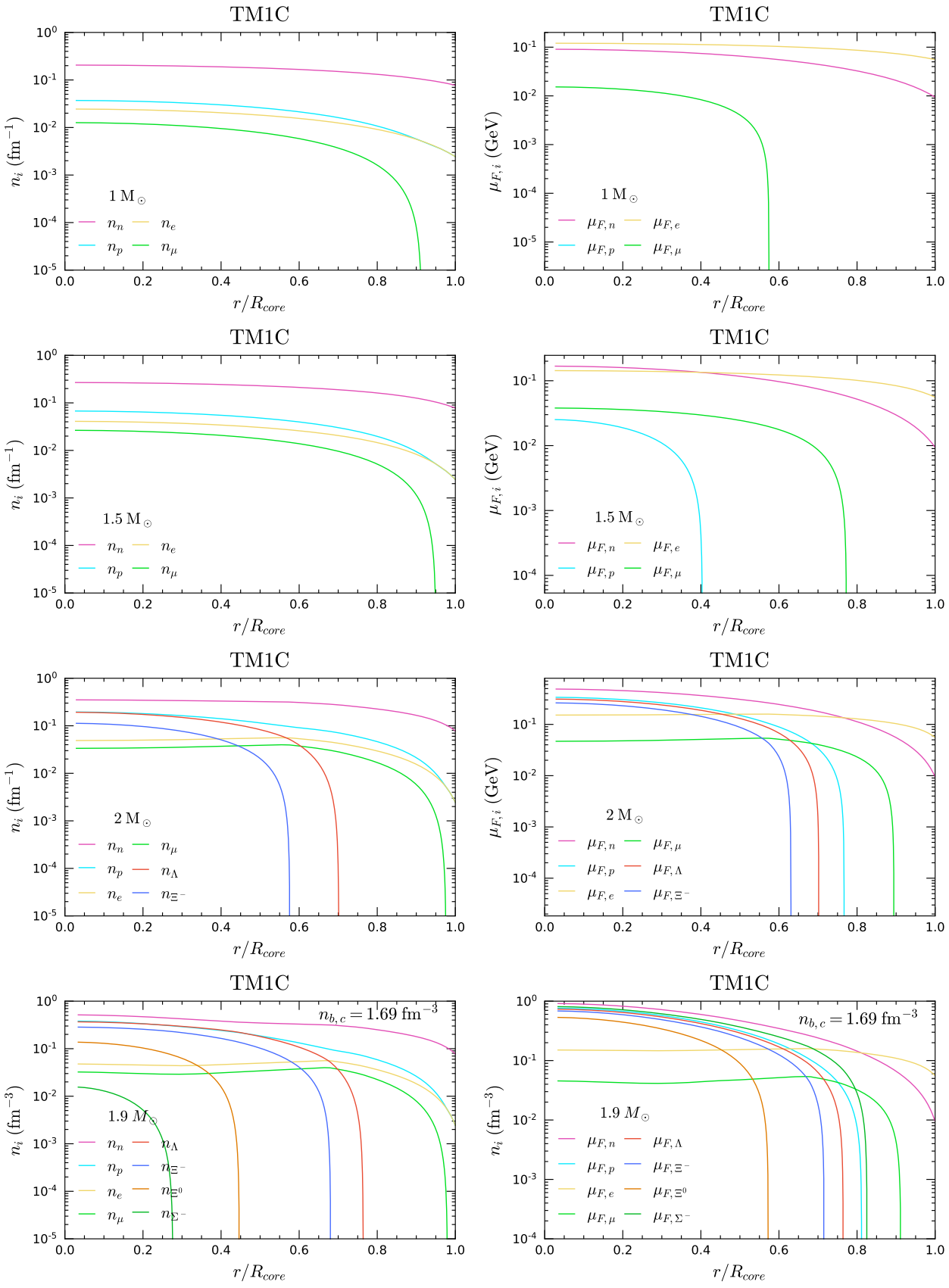

Figure 7.5: Radial profiles for the number density (left) and chemical potentials (right) for the EoS model TM1C

Chapter 8

Applications

8.1 Review

8.1.1 Super Heavy DM

1. **Ref.** [21] (1805.07381) on super SHDM ($m_\chi > 10^{22}$ GeV) inducing type Ia supernovae in WDs. Unlike ref. [1], the SN is induced by DM induced runaway fusion, rather than [M: asymmetric DM forming a BH].

   Intro:

   - If DM can substantially heat the WD, it can lead to SN with sub-Chandrasekhar WDs as their progenator.
   - SM particle production is the means of ignition for the SN.
   - Constraints are then placed from observations of specific long lived WDs, or by comparing the observed rate of type Ia SN with that expected due to DM.
   - constraints are placed on generic DM which can produce SM particles through DM-SM scattering, DM-DM interactions or DM decays, as well as being applied to a specific Q-ball model.

   WD Runaway fusion:

   - Energy deposited in region of linear size L_0, total kinetic energy $\mathcal{E}_0$ and temperature T_0
   - Fusion occurs for temperatures greater than critical value T_f for which ions overcome Coulomb barrier.
   - Cooling may reduce $T_0 < T_f$, so timescales for cooling must be longer than that of fusion energy being released.
   - As cooling timescales increase with region size, while heating from fusion is independent of size, once a region with $T_0 > T_f$ reaches a critical size, λ_T, runaway fusion begins.
   - They estimate the minimum required energy that needs to be deposited heat a region of volume $\sim \lambda_T^3$ to temperature T_f and trigger runaway fusion to be $\sim 10^{16} - 10^{23}$ GeV depending on the WD mass.
   - They use a simplified calculation to determine this critical energy in their work

   $$\mathcal{E} = \lambda_T^3 (n_{ion} T_f + n_e^{2/3} T_f^2 + T_f^4) \tag{8.1.1}$$

   Particle Heating of WD

   -

2. **Ref.** [17] 2106.09033 consider macroscopic DM in an "asteroid-like" mass range. When these pass through stars, the shock waves will result in X-ray or UV emission, which in dense globular clusters will occur more frequently than the expected flare background.

3. **Bramante Ref.** [1] (1904.11993) consider asymmetric DM igniting type Ia supernova in WDs. The thermalised DM sphere grows in mass as more DM is captured, until self gravitation is achieved. The subsequent gravitational collapse will heat the WD interior through nuclear elastic scattering, which can then trigger runaway thermonuclear reactions which preceed the type I1 supernova.

   Limits obtained depend on:

   - Time to accumulate critical mass of DM
   - DM thermalisation time
   - Timescale for gravitational collapse to occur

- Energy transferred through DM collapse via its scattering off the WD constituents.

Limits are set by requiring that the timescales of the the first three points take longer than the age of a known WD which has not yet exploded. Additionally, ignition may occur if the DM forms a black hole which can heat the interior through Hawking radiation.

DM Collapse:

- In order for gravitational collapse to occur, there are two conditions that are required:
  1) The DM must be self-gravitating, with the DM's self gravity being greater than the WD's gravitational potential. This is achieved if the density of the DM sphere is greater than the WD density.
  2) The DM must satisfy the Jeans instability condition.

Ignition:

- Requirements for ignition:
  1) DM must heat WD faster than it cools
  2) A localised region of the WD needs to be heated above a critical temperature.

8.1.2 DM Self-Capture

Issues to address:

- Timescale for thermalisation needs to be less than the other timescales in the problem.
- Incoming DM may impart enough energy to eject already captured DM, adding an additional source of evaporation.

1. **Refs.** [18] (2006.10773) mainly look at models with light mediators, but also include the possibility of self interactions. The DM is taken to be asymmetric with repulsive self-interactions. These effects weaken the limits they obtain due to gravitational collapse.

The number of DM within the star is determined by the equation

$$\frac{dN_\chi}{dt} = C_{\chi n} + C_{\chi\chi} N_\chi - E_\chi N_\chi - A_\chi N_\chi^2 \tag{8.1.2}$$

where $C_{\chi n}$ is the capture rate from scattering off stellar constituents, $C_{\chi\chi} N_\chi$ is the capture rate from self-interactions, E_χ is the DM evaporation rate, and $A_\chi N_\chi^2$ is the DM annihilation coefficient. The solution to this is then

$$N_\chi(t) = \frac{C_{\chi n}\tau \tanh(\kappa t/\tau)}{\kappa + \frac{1}{2}(E_\chi - C_{\chi\chi})\tanh(\kappa t/\tau)} \tag{8.1.3}$$

$$\tau = \frac{1}{\sqrt{C_{\chi n} A_\chi}} \tag{8.1.4}$$

$$\kappa = \sqrt{1 + \frac{\tau^2}{4}(C_{\chi\chi} - E_\chi)^2} \tag{8.1.5}$$

If evaporation can be neglected, capture annihilation equilibrium is reached in timescales $\tau \sim 1/\sqrt{C_{\chi n} A_\chi + C_{\chi\chi}^2/4}$.

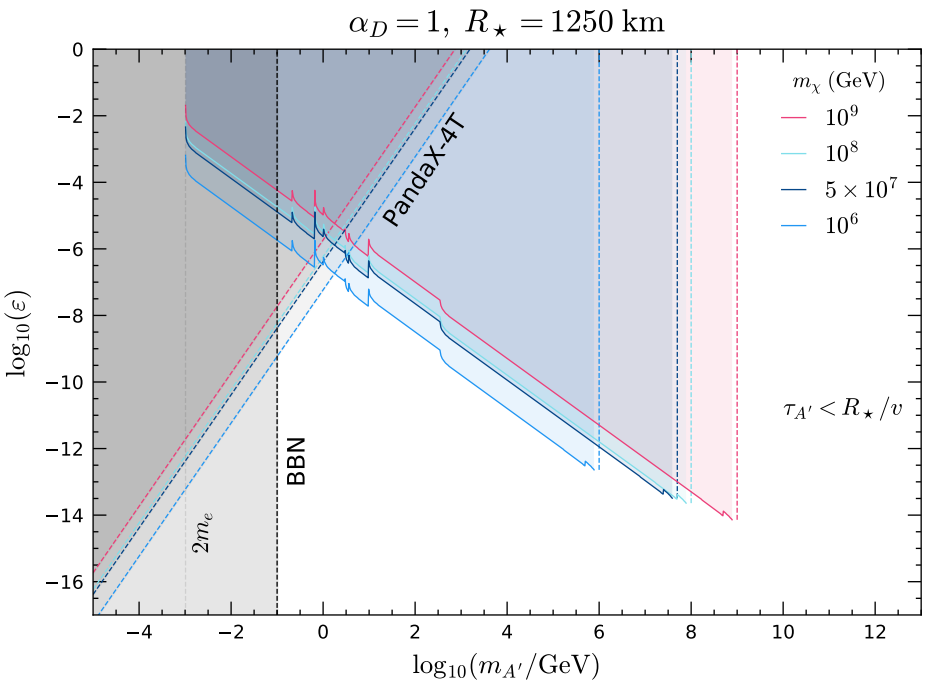

Figure 8.1: Regions of ε-$m_{A'}$ parameter space for which the dark photon decays within the WD. The BBN constraint is for THUMP DM under the assumption $m_\chi^i = 2m_{A'}$ Only PandaX-4T limits are shown as those from XENON are very similar.

8.2 THUMP Dark Matter

For DM scattering off SM fermions, we have

$$|\overline{\mathcal{M}}|^2_{\chi T} = \frac{32\pi^2\epsilon^2\alpha_{EM}\alpha_D(2(s - m_\chi^2 - m_T^2)^2 + 2st + t^2)}{(t - m_{A'}^2)^2 + m_{A'}^2\Gamma_{A'}^2} \tag{8.2.1}$$

where $\Gamma_{A'}$ is the width of the dark photon (Currently, I haven't included this. Need to figure out how to program it...).

Need to calculate m^* for this matrix element, as currently I'm using D5.

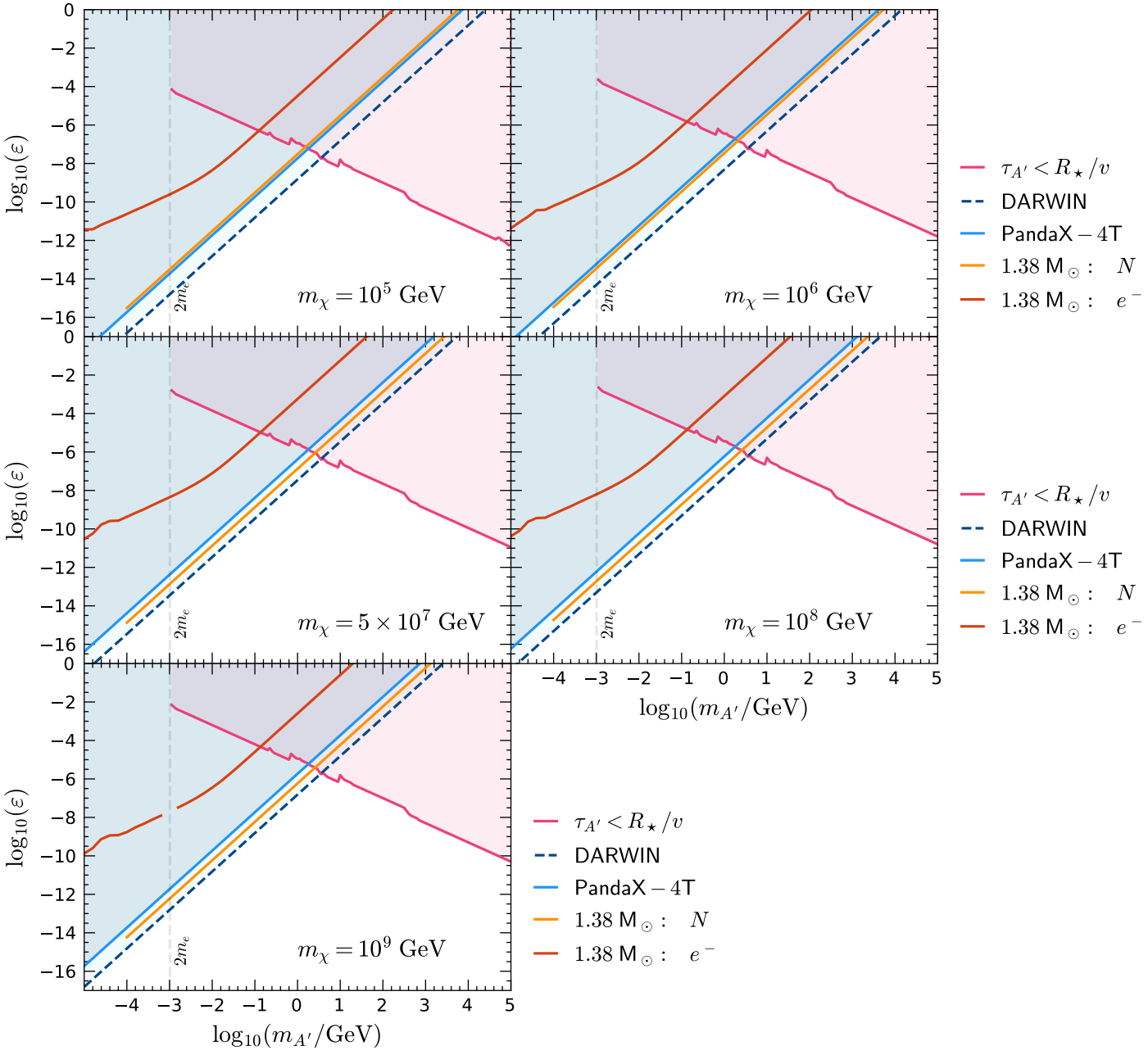

Figure 8.2: Constraints on THUMP dark photon parameter space. The WD constraint is due to a 1.38 $\mathcal{M}_\odot$ Carbon WD with radius 1250 km. The Panda-4T and DARWIN lines are extrapolated from current results. The BBN line is for the initial condition that $m_\chi^i = 2m_{A'}$.

8.3 Ignition of type Ia supernova in White Dwarfs

8.3.1 Thermalisation

The interaction rate for DM scattering off non-relativistic ions is given by [14],

$$\Omega^-(w) = \int_{w\frac{|\mu_-|}{\mu_+}}^{w} dv R^-(w \to v) \tag{8.3.1}$$

$$R^- = \int_0^\infty ds \int_0^\infty dt \frac{32\mu_+^4}{\sqrt{\pi}} k^3 n_I \frac{d\sigma}{d\cos\theta} \frac{vt}{w} e^{-k^2 v_N^2} \Theta(t+s-w)\Theta(v-|t-s|) \tag{8.3.2}$$

where the lower terminal corresponds to the minimum velocity allowed by kinematics. We then define the thermalisation time as the sum of the average times between scatterings [11]

$$\tau_{th} = \sum_{n=0}^{N} \frac{1}{\Omega^-(w_n)}, \tag{8.3.3}$$

$$\tag{8.3.4}$$

where the summation ends after the DM has reached the thermal velocity of

$$w_N = \sqrt{\frac{2T_\star}{m_\chi}}. \tag{8.3.5}$$

The velocity after n scattering events, w_n, is calculated as the average final velocity the DM with initial velocity w_{n-1} can obtain. This is achieved by weighting the differential interaction rate $R^-(w \to v)$ by the final velocity v, and integrating over all possible v, and normalising the result to the full interaction rate,

$$w_n = \frac{1}{\Omega^-(w_{n-1})} \int dv\, v R^-(w_{n-1} \to v). \tag{8.3.6}$$

As the ions we are scattering off comprise a Coulomb lattice, we must carefully account for this additional structure. This is done by modifying the scattering cross section to include the structure function of the lattice, $S(q_{tr})$, leading to the replacement [26]

$$\frac{d\sigma_{T\chi}}{d\cos\theta} \to S(q_{tr}) \frac{d\sigma_{T\chi}}{d\cos\theta}. \tag{8.3.7}$$

The Coulomb structure factor has been calculated [26, 6, 5], and is expressed as the sum the contributions from elastic Bragg scattering and inelastic phonon scattering/absorption. In the low momentum transfer limit relevant to thermalisation, the former process does not contribute to the structure factor, and so we only need to consider the inelastic contribution [1]. Thus the structure factor can be approximated to be

$$S(q_{tr}) \approx 1 - e^{-2W(q_{tr})}, \tag{8.3.8}$$

where $W(q_{tr})$ is the Debye-Waller factor[1], which can be approximated for cubic lattices as [41, 4]

$$W(q_{tr}) = \frac{\langle r_T^2 \rangle q_{tr}^2}{6} \approx \frac{7 m_T T_\star q_{tr}^2}{12\pi Z^2 e^2 \rho_\star} = \frac{1}{2}\frac{q_{tr}^2}{q_{sup}^2}, \tag{8.3.9}$$

$$q_{sup}^2 = \frac{6\pi Z^2 e^2 \rho_\star}{7 m_T T_\star} \approx 2.58 \times 10^{-5}\ \text{GeV}^2 \left(\frac{Z}{8}\right)\left(\frac{16\ \text{GeV}}{m_T}\right)\left(\frac{\rho_\star}{5.23\times 10^6\ \text{g cm}^{-3}}\right)\left(\frac{10^7\ \text{K}}{T_\star}\right) \tag{8.3.10}$$

where $\langle r_T^2 \rangle$ the the mean-squared displacement of the ions, and we have introduced q_{sup} to parameterise the scale at which the interaction rate is suppressed. For carbon WDs of interest, with temperatures $\sim 10^5$ K, this scale can range from ~ 40 MeV to ~ 12 GeV.

[1] Note that Bramante [1] absorb the factor of 2 into their definition. I keep it to stay consistent with the solid state literature.

With this structure factor in $R^-(w \to v)$, we calculate the thermalisation time for the EFT operators, assuming that the cutoff scale Λ is such that the luminosity of the star is generated by the annihilating DM. We find that there is an increase of ~ 8 orders of magnitude in the thermalisation time due the the phonon interactions, however the longest time to thermalise wsa $\sim 10^4$ yrs, well within the age of the WDs we consider.

An important special case is that of a constant DM-nucleus cross section, i.e. $d\sigma = \sigma_0/2$. Calculating the thermalisation time for such interactions yields the following scaling with DM mass:

$$\tau_{th} \propto m_\chi, \quad m_\chi \lesssim m_T, \tag{8.3.11}$$

$$\tau_{th} \propto m_\chi^{3/2}, \quad m_\chi \gtrsim m_T. \tag{8.3.12}$$

This growth/decline in thermalisation times disagrees with the results of [1], which state that the thermalisation time should grow as m_χ^2.

First, consider the case of constant cross section in the $T \to 0$ limit approximation of the interaction rate, for which we have

$$R^-(w \to v) = \frac{4\mu_+^2}{\mu} n_I \frac{v}{w} \frac{\sigma}{2} \tag{8.3.13}$$

$$\Omega^-(w) = n_I w \sigma \tag{8.3.14}$$

$$q_{tr}^2 = m_T^2 \mu (w^2 - v^2) \tag{8.3.15}$$

$$\Delta E_\chi = \frac{1}{2} m_T \mu (w^2 - v^2) \tag{8.3.16}$$

$$w_n = \left(\frac{2(\mu_+^3 - |\mu_-|^3)}{3\mu\mu_+} \right)^n w_0 \tag{8.3.17}$$

$$= \left(\frac{1 + 3\mu^2}{3\mu(1+\mu)} \right)^n w_0, \quad m_\chi > m_T \tag{8.3.18}$$

$$\langle \Delta E_\chi \rangle = 2 \frac{\mu}{(1+\mu)^2} E_\chi \tag{8.3.19}$$

where w_0 is the initial velocity of the DM. The thermalisation time in this case is

$$\tau_{th} \approx \frac{3\mu^{3/2}(1+\mu)}{n_I \sigma (3\mu - 1)} \sqrt{\frac{2T_\star}{m_T}} \tag{8.3.20}$$

$$\tau_{th} \sim 83.67 \times 10^{-6} \text{ yrs} \frac{\mu^{3/2}}{(1+\mu)^2} \left(\frac{1\text{pm}^{-3}}{n_I} \right) \left(\frac{10^{-39}\text{cm}^2}{\sigma} \right) \left(\frac{10^5 \text{K}}{T_\star} \right)^{1/2} \tag{8.3.21}$$

[M: update these] where in the second line we have assumed more than ~ 10 scatterings have taken place. For cross sections dependent on v_r and q_{tr}, the thermalisation times for hydrogen are

$$\tau_{th}^{v_r^2} \sim 13.3 \text{ yrs} \frac{\mu^{5/2}}{(1+\mu)^2} \left(\frac{1\text{pm}^{-3}}{n_I} \right) \left(\frac{10^{-39}\text{cm}^2}{\sigma} \right) \left(\frac{10^5 \text{K}}{T_\star} \right)^{3/2} \left(\frac{v_0}{0.1c} \right)^2 \tag{8.3.22}$$

$$\tau_{th}^{v_r^4} \sim 6.24 \times 10^6 \text{ yrs} \frac{\mu^{7/2}}{(1+\mu)^2} \left(\frac{1\text{pm}^{-3}}{n_I} \right) \left(\frac{10^{-39}\text{cm}^2}{\sigma} \right) \left(\frac{10^5 \text{K}}{T_\star} \right)^{5/2} \left(\frac{v_0}{0.1c} \right)^4 \tag{8.3.23}$$

$$\tau_{th}^{q_{tr}^2} \sim 14.1 \text{ yrs} \frac{\mu^{5/2}}{(1+\mu)^2} \left(\frac{1\text{pm}^{-3}}{n_I} \right) \left(\frac{10^{-39}\text{cm}^2}{\sigma} \right) \left(\frac{10^5 \text{K}}{T_\star} \right)^{3/2} \left(\frac{q_{tr,0}}{80\text{MeV}} \right)^2 \tag{8.3.24}$$

$$\tau_{th}^{q_{tr}^4} \sim 6.8 \times 10^6 \text{ yrs} \frac{\mu^{7/2}}{(1+\mu)^2} \left(\frac{1\text{pm}^{-3}}{n_I} \right) \left(\frac{10^{-39}\text{cm}^2}{\sigma} \right) \left(\frac{10^5 \text{K}}{T_\star} \right)^{5/2} \left(\frac{q_{tr,0}}{80\text{MeV}} \right)^4 \tag{8.3.25}$$

where I have used

$$\frac{d\sigma_{v_r^n}}{d\cos\theta} = \sigma \left(\frac{v_r}{v_0}\right)^n \tag{8.3.26}$$

$$\frac{d\sigma_{q_{tr}^n}}{d\cos\theta} = \sigma \left(\frac{q_{tr}}{q_{tr,0}}\right)^n \tag{8.3.27}$$

$$\tag{8.3.28}$$

Including the structure factor approximate as $S^{''} \approx q_{tr}^2/q_{sup}^2$, we get

$$R^-(w \to v) = \frac{2\mu_+^2 m_T^2 n_I \sigma}{q_{sup}^2} \frac{v}{w}(w^2 - v^2) \tag{8.3.29}$$

$$\Omega^-(w) = \frac{m_T^2 n_I \sigma w^3}{2q_{sup}^2} \left(\frac{\mu}{\mu_+}\right)^2 \tag{8.3.30}$$

$$w_n = \left(\frac{4}{15\mu^2\mu_+}(2\mu_+^5 - 5\mu_+^2|\mu_-|^3 + 3|\mu_-|^5)\right)^n w_0 \tag{8.3.31}$$

$$= \left(\frac{(1 + 5\mu - 5\mu^2 + 15\mu^3)}{15\mu^2(1+\mu)}\right)^n w_0, \quad m_\chi > m_T \tag{8.3.32}$$

$$\langle \Delta E_\chi \rangle = \frac{8}{3}\frac{\mu}{(1+\mu)^2} E_\chi \tag{8.3.33}$$

The thermalisation time is then

$$\tau_{th} = \frac{q_{sup}^2 \mu}{8 m_T^2 n_I \sigma} \left(\frac{m_\chi}{2T}\right)^{3/2} \tag{8.3.34}$$

$$\sim 1.25 \times 10^5 \text{ yrs} \left(\frac{m_\chi}{10^6 \text{ GeV}}\right) \tag{8.3.35}$$

8.4 Numerical Calculation

Instead of continuing with the discrete sum approach, we switch to the continuum approximation. This is well justified as the fraction of energy lost each collision is minuscule. The energy of the DM then follows

$$\frac{dE_\chi}{dt} = -\Omega^- \langle \Delta E_\chi \rangle \tag{8.4.1}$$

$$= -\int dv R^-(w \to v) \Delta E_\chi \tag{8.4.2}$$

$$\implies \tau_{th} = -\int_{w_0}^{w_{th}} \frac{m_\chi w}{\int dv R^-(w \to v) \Delta E_\chi} dw \tag{8.4.3}$$

Note that as ΔE_χ with in general depend on s and t, this needs to be included within these integrals inside $R^-(w \to v)$. As the integration interval over v is small, we can approximate this integral as

$$\int dv f(v) \approx \frac{w}{\mu}(f(w) + f(w\frac{\mu_-}{\mu_+})) \approx \frac{2w}{\mu} f(w) \tag{8.4.4}$$

However this is still not numerically great, as the denominator is still a 2D integral in general.

Form Factors

In order to translate the form factors of Catena [**Catena**] one inverts from the isoscalar/isovector basis to the n/p basis through [**Fitzpatrick**]

$$F_{i,j}^{(p,p)} = F_{i,j}^{00} + F_{i,j}^{01} + F_{i,j}^{10} + F_{i,j}^{11} \tag{8.4.5}$$

$$F_{i,j}^{(n,p)} = F_{i,j}^{00} + F_{i,j}^{01} - F_{i,j}^{10} - F_{i,j}^{11} \tag{8.4.6}$$

$$F_{i,j}^{(p,n)} = F_{i,j}^{00} - F_{i,j}^{01} + F_{i,j}^{10} - F_{i,j}^{11} \tag{8.4.7}$$

$$F_{i,j}^{(n,n)} = F_{i,j}^{00} - F_{i,j}^{01} - F_{i,j}^{10} + F_{i,j}^{11} \tag{8.4.8}$$

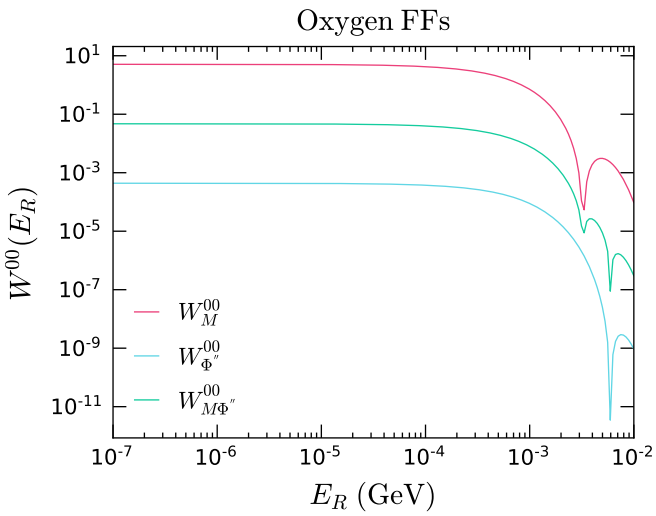

Figure 8.3: Form factors for oxygen targets as a function of the recoil energy.

The form factors are paramaterised by the dimensionless quantity $y = (bq/2)^2$, with

$$b = \sqrt{41.467/(45A^{-1/3} - 25A^{-2/3})}\ \text{fm} \tag{8.4.9}$$

We plot the non-zero form factors for oxygen in fig. 8.3, where we see that they are in effect until the recoil energy drops below ~ 100 keV. Note that the FFs will always be slowly changing, though this change is rather slow ($W_M^{00}(10^{-6}\ \text{GeV}) \sim 5.0835$ while $W_M^{00}(10^{-9}\ \text{GeV}) \sim 5.0929$), this results in the (slower) decrease in the fractional of energy lost per scatter, $\Delta E/E$. I have checked that without the inclusion of the form factors, the fractional energy loss is constant with respect to the DM energy for D1, D5 (constant cross sections).

Chapter 9

Model Building

9.1 Notes to myself

- **From Celine's Simplified model paper:** Need to solve Boltzmann equation to get correct abundance on a model by model basis, i.e. tune parameters to get right result. Maybe easier to numerically scan over param space rather than doing anything analytic.
- N_R is a Weyl fermion. This can be embedded into a bispinor as $N_R = (0, N_R)^T$.

$SU(2)$ **indices:**

From John's thesis. An $SU(2)$ doublet carries a single raised index, i.e. L^i for the lepton doublet. When it comes to neutrino masses, we need an operator of the form $\overline{L}H^\dagger N_R$. But the conjugated fields have lowered $SU(2)$ indices, $(L^i)^\dagger = (L^\dagger)_i$, similarly for $H^\dagger$. So in order to contract the indices and make a singlet, we need to raise the index of one of the fields (not sure if it matters which, probably a convention that it's the Higgs but could also be a summation convention like with 2-component fermions). To do this, we use the ϵ^{ij} tensor, such that $\epsilon^{ij}(H^\dagger)_j \equiv \tilde{H}^i$. This tells us that an $SU(2)$ doublet with a tilde over its name is the conjugated field with its index raised. Thus $\overline{L}_i \tilde{H}^i N_R$ is a singlet term.

9.2 Relation to EFTs

For t-channel real scalar mediator with Lagrangian

$$\mathcal{L} \supset \frac{1}{2}(\partial_\mu \phi)^2 - \frac{1}{2}m_\phi^2 \phi^2 - \lambda \overline{\chi} N \phi - \lambda \overline{N} \chi \phi \tag{9.2.1}$$

EoM for ϕ

$$(\Box + m_\phi^2)\phi + \lambda(\overline{\chi}N + \overline{N}\chi) = 0 \tag{9.2.2}$$

$$\implies \phi \sim -\frac{\lambda}{m_\chi^2}\left(1 + \mathcal{O}\left(\frac{\Box}{m_\phi^2}\right)\right)(\overline{\chi}N + \overline{N}\chi) \tag{9.2.3}$$

Subbing this back gives

$$\mathcal{L} \supset \frac{\lambda^2}{m_\chi^2}(\overline{\chi}N)(\overline{\chi}N + \overline{N}\chi) + \frac{\lambda^2}{m_\phi^2}(\overline{N}\chi)(\overline{\chi}N + \overline{N}\chi) \tag{9.2.4}$$

$$= \frac{2\lambda^2}{m_\phi^2}(\overline{\chi}N)(\overline{N}\chi) + \frac{\lambda^2}{m_\phi^2}(\overline{N}\chi)(\overline{N}\chi) + h.c. \tag{9.2.5}$$

We can rewrite the first term using a Fierz transformation such that

$$(\overline{\chi}N)(\overline{N}\chi) = \frac{1}{4}((\overline{\chi}\chi)(\overline{N}N) + (\overline{\chi}\gamma^5\chi)(\overline{N}\gamma^5 N) + (\overline{\chi}\gamma^\mu\chi)(\overline{N}\gamma_\mu N) + (\overline{\chi}\gamma^\mu\gamma^5\chi)(\overline{N}\gamma_\mu\gamma^5 N) + (\overline{\chi}\sigma^{\mu\nu}\chi)(\overline{N}\sigma_{\mu\nu}N)) \tag{9.2.6}$$

Instead, for only right handed neutrinos we instead have the much simpler expression

$$(\overline{\chi_L}N_R)(\overline{N_R}\chi_L) = \frac{1}{2}(\overline{\chi_L}\gamma^\mu\chi_L)(\overline{N_R}\gamma_\mu N_R) \tag{9.2.7}$$

using the results from ref. [9].

Channel	Mediator	Refs.
s	Scalar	[25]
t	Scalar	[35, 23, 12, 7, 13]
t	Vector	[16]

Table 9.1: Dirac Fermion Dark Matter

Channel	Mediator	Refs.
s	Scalar	[10]
t	Scalar	[35, 23, 12, 7, 13]

Table 9.2: Scalar Dark Matter

9.3 Models

9.3.1 Complex χ, complex scalar ϕ

Assuming χ is odd under an additional $\mathbb{Z}_2$, the most general Lagrangian for this field content is

$$\begin{aligned}
\mathcal{L} \supset & |\partial_\mu \chi|^2 + |\partial_\mu \phi|^2 + i\overline{N_R}\partial\!\!\!/ N_R && (9.3.1)\\
& - m_\chi^2 |\chi|^2 - m_\phi^2 |\phi|^2 - \frac{m_R}{2}\overline{N_L^c} N_R && (9.3.2)\\
& - \lambda_\chi |\chi|^2 \phi - \lambda_N \overline{N_L^c} N_R \phi + h.c. && (9.3.3)\\
& - \kappa |H|^2 \phi + h.c. && (9.3.4)\\
& - \mu_4 |H|^2 |\chi|^2 - \mu_5 |H|^2 |\phi|^2 - \mu_6 (|H|^2 \phi^2 + h.c.) && (9.3.5)\\
& - y_\nu \overline{L} \tilde{H} N_R + h.c. && (9.3.6)
\end{aligned}$$

with the notation $N_L^c \equiv (N^c)_L = (N_R)^c$

9.3.2 Dirac χ, complex scalar ϕ

Without introducing a $\mathbb{Z}_2$ symmetry, the Lagrangian will be

$$\begin{aligned}
\mathcal{L} \supset & i\overline{\chi}\partial\!\!\!/ \chi + i\overline{N_R}\partial\!\!\!/ N_R + |\partial_\mu \phi|^2 && (9.3.7)\\
& - m_\chi \overline{\chi}\chi - m_\phi^2 |\phi|^2 - \frac{m_R}{2}\overline{N_L^c} N_R && (9.3.8)\\
& - \lambda_{\chi N} \overline{\chi_L} N_R \phi - \lambda_\chi \overline{\chi}\chi\phi - \lambda_N \overline{N_L^c} N_R \phi + h.c. && (9.3.9)\\
& - y_\chi \overline{L} \tilde{H} \chi_R - y_\nu \overline{L} \tilde{H} N_R && (9.3.10)\\
& - \kappa (|H|^2 \phi + h.c.) - \mu_5 |H|^2 |\phi|^2 - \mu_6 (|H|^2 \phi^2 + h.c.) && (9.3.11)
\end{aligned}$$

If χ is odd under a $\mathbb{Z}_2$ symm. then the t-channel term is disallowed and only s-channel is viable. If both χ and ϕ are odd, then s-channel is disallowed. If there is no $\mathbb{Z}_2$, then the DM can simply decay to a SM neutrino and Higgs.

For the $HH\phi$ terms, after EWSB there will be a term linear in ϕ which corresponds to a tadpole diagram, leading to ϕ obtaining a vev

9.4 Categories

Follow Linder: DM type -> Ann channel -> mediator type

Exotic models:[34] for semi-annihilating scalar DM, [31] for νTHDM (neutrinophilic 2HDM).

Appendix A

Kinematics

Here I detail the derivations of some of the important kinematic quantities used throughout this work.

Final energy in 2 body scattering

A key ingredient when considering Pauli blocking in compact objects is the final energy of the target particle. As we work in the frame of the compact object, rather than the lab frame, we need to account for the motion of the target prior to the collision. The kinematics of this problem are shown in Fig. A.1, where we are free to set one of the incoming particles to lie on the x-axis. As the collision is assumed to be elastic, we take $m_1 = m_3$, $m_2 = m_4$. Applying the usual energy and momentum conservation

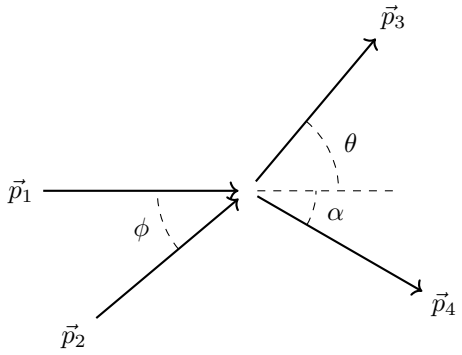

Figure A.1: Kinematics of $2 \to 2$ scattering.

$$E_1 + E_2 = E_3 + E_4 \tag{A.0.1}$$
$$\vec{p}_1 + \vec{p}_2 = \vec{p}_3 + \vec{p}_4 \tag{A.0.2}$$
$$\tag{A.0.3}$$

Momentum conservation gives

$$\vec{p}_4 = \vec{p}_3 - \vec{p}_1 - \vec{p}_2 \tag{A.0.4}$$
$$p_4^2 = p_1^2 + p_2^2 + p_3^2 + 2\vec{p}_1 \cdot \vec{p}_2 - 2\vec{p}_1 \cdot \vec{p}_3 - 2\vec{p}_2 \cdot \vec{p}_3 \tag{A.0.5}$$

We then replace the remaining dot products with the Mandelstam variables through

$$2\vec{p}_1 \cdot \vec{p}_2 = m_1^2 + m_2^2 + 2E_1E_2 - s \tag{A.0.6}$$
$$2\vec{p}_1 \cdot \vec{p}_3 = t - m_1^2 - m_3^2 + 2E_1E_3 \tag{A.0.7}$$

For the remaining product, some care is needed. We start by writing the angle between $\vec{p}_2$ and $\vec{p}_3$ as

$$\cos(\theta_{23}) = \cos(\theta - \phi) = \cos\theta\cos\phi - \sin\theta\sin\phi \tag{A.0.8}$$

Then again using the Mandelstam variables above,

$$\cos\phi = \frac{1}{2p_1p_2}(m_1^2 + m_2^2 + 2E_1E_2 - s) \tag{A.0.9}$$
$$\cos\theta = \frac{1}{2p_1p_3}(t - m_1^2 - m_3^2 + 2E_1E_3) \tag{A.0.10}$$

Appendix B

Phonons

B.1 Structure Factors for Coulomb Lattice

The (time inverse Fourier transform) inelastic structure function per ion is given by [6]

$$F^{''}(\vec{q},t) = e^{-2W(q)} \sum_{jl} e^{i\vec{q}\cdot(\vec{R}_j - \vec{R}_l)} \left\{ \exp\left[-\frac{1}{2MN} \sum_{\nu} \frac{(\vec{q}\cdot\vec{e}_\nu)^2}{\omega_\nu} \left(\alpha_{jl,\nu}(\bar{n}_\nu + 1) + \alpha^*_{jl,\nu}\bar{n}_\nu \right) \right] - 1 \right\} \tag{B.1.1}$$

$$\alpha_{jl,\nu} = \exp\Big(i\vec{k}\cdot(\vec{R}_j - \vec{R}_l) + i\omega_\nu t \Big) \tag{B.1.2}$$

$$\bar{n}_\nu = (e^{z_\nu} - 1)^{-1} \tag{B.1.3}$$

$$z = \omega_\nu / T \tag{B.1.4}$$

where $\nu = (\vec{k}, s)$ labels the phonon modes, with $s = 1, 2, 3$ enumerates the polarisation. [M: I think there is a typo in [6], which have $-i\omega_\nu t$ in $\alpha_{ij,\nu}$. This gives the wrong δ-functions later.] Expanding in a power series, keeping only leading term in q^2 and doing some stuff leaves

$$F^{''}(\vec{q},t) = \frac{V^* e^{-2W}}{2M} \sum_{\nu} \frac{(\vec{q}\cdot\vec{e}_\nu)^2}{\omega_\nu} \left[(\bar{n}_\nu + 1) e^{i\omega_\nu t} \sum_{\vec{G}} \delta(\vec{q} + \vec{k} - \vec{G}) + \bar{n}_\nu e^{-i\omega_\nu t} \sum_{\vec{G}} \delta(\vec{q} - \vec{k} - \vec{G}) \right] \tag{B.1.5}$$

where V^* is the volume of a primitive cell in reciprocal space and $\vec{G}$ is a reciprocal lattice vector. This is the single phonon interaction approximation. For larger momentum transfers, the full expression can be computed at least approximately which is what is given in [1]. For $q < q_B$ (momentum transfers within the Brillouin zone), only keep $\vec{G} = 0$. The δ-functions then set $\vec{k} = -\vec{q}$ in the first term and $\vec{k} = \vec{q}$ in the second. However, as the dispersion relation is only dependent on the magnitude of $\vec{k}$, the two are equivalent.

$$F^{''}(\vec{q},t) = \frac{V^* e^{-2W}}{2M} \sum_{s} \frac{(\vec{q}\cdot\vec{e}_s)^2}{\omega_q} \left[(\bar{n}_q + 1) e^{i\omega_q t} + \bar{n}_q e^{-i\omega_q t} \right] \tag{B.1.6}$$

We can assume for simplicity, that the polarisation of the phonon is in the same direction as the momentum transfer (i.e. only consider the longitudinal phonons) leaving

$$F^{''}(\vec{q},t) = \frac{V^* e^{-2W}}{2M} \frac{q^2}{\omega_q} \left[(\bar{n}_q + 1) e^{i\omega_q t} + \bar{n}_q e^{-i\omega_q t} \right] \tag{B.1.7}$$

We can then recover the usual structure function Fourier transforming the above, giving

$$S(\vec{q},\omega) = \frac{1}{2\pi} \int_{-\infty}^{\infty} dt\, e^{-i\omega t} F^{''}(\vec{q},t) \tag{B.1.8}$$

$$= \frac{V^* e^{-2W}}{4\pi M} \frac{q^2}{\omega_q} \left[(\bar{n}_q + 1)\delta(\omega - \omega_q) + \bar{n}_q \delta(\omega + \omega_q) \right] \tag{B.1.9}$$

The first term corresponds to the emission of a phonon, with energy being deposited into the lattice, while the second term accounts for the absorption of a phonon, with the delta function enforcing that energy is transferred to the incoming particle . For thermalistion, we can neglect the latter, which in fact is vanishing for low temperatures. The dispersion relation for the longitudinal mode is given by [41]

$$\omega^2(q) = \frac{\Omega_p^2}{1 + \kappa_{sc}^2/q^2} \tag{B.1.10}$$

$$\Omega_p^2 = \frac{4\pi n_I Z^2 e^2}{m_I} \sim 1.72 \times 10^{-11}\ \text{GeV}^2 \left(\frac{n_I}{0.216\ \text{pm}^{-3}} \right) \left(\frac{Z}{8} \right)^2 \left(\frac{16\ \text{GeV}}{m_I} \right) \tag{B.1.11}$$

$$\kappa_{sc}^2 \approx \frac{6\pi Z e^2 n_I}{E_F} \sim 9.08 \times 10^{-8}\ \text{GeV}^2 \left(\frac{n_I}{0.216\ \text{pm}^{-3}} \right) \left(\frac{Z}{8} \right) \left(\frac{0.3\ \text{MeV}}{E_F} \right) \tag{B.1.12}$$

where Ω_p is the ion plasma frequency, κ_{sc}^{-1} is a screening scale and E_F is the Fermi energy of the neutralising electron gas. for $q \ll \kappa_{sc}$, this simplifies to $\omega(q) \approx \Omega_p q/\kappa_{sc} = c_s q$ with c_s the speed of sound ~ 0.0138 for the above values. These scales should be compared to the Brillouin zone for the lattice, which is

$$q_B = \left(6\pi^2 n_I\right)^{1/3} \sim 2.7 \times 10^{-3} \text{ GeV} \left(\frac{n_I}{0.216 \text{ pm}^{-3}}\right)^{1/3} \tag{B.1.13}$$

We are only in this small momentum limit when the momentum transfer falls below q_B. As $\kappa_{sc} \sim 3{\times}10^{-}4$ GeV, we are only outside of the $q \ll \kappa_{sc}$ limit for only a small fraction of the time, and so the approximate dispersion relation for a Debeye solid should be valid.

$$S(\vec{q}, \omega) = \frac{2\pi^2 n_I e^{-2W}}{M} \frac{q^2}{\omega(q)} \frac{\delta(\omega - \omega(q))}{1 - \exp\left(-\omega(q)/T\right)} \tag{B.1.14}$$

$$S(\vec{q}) = \frac{2\pi^2 n_I e^{-2W}}{M} \frac{q}{c_s} \frac{\delta(\omega - c_s q)}{1 - \exp\left(-c_s q/T\right)} \tag{B.1.15}$$

$$\tag{B.1.16}$$

This is in somewhat agreement with [11], up to a factor of 2π and e^{-2W}, which is close to one for low momentum transfers. Rewriting in terms of the final velocity we get

$$S(\vec{q}, \omega) = \frac{2\pi^2 n_I e^{-2W}}{M} \frac{q}{c_s} \frac{1}{1 - \exp\left(-c_s q/T\right)} \left[\frac{2\delta\left(v - \sqrt{w^2 - \frac{4c_s^2}{\mu}}\right)}{m_T \mu \sqrt{w^2 - \frac{4c_s^2}{\mu}}}\right] \tag{B.1.17}$$

From this, we can see that the DM will only scatter through single phonon emission until its speed falls bellow $\sim 2c_s/\sqrt{\mu}$. In this light DM regime, the thermal velocity is much smaller than this value, and so another scattering process is required in order for the DM to thermalise.

In general, it may be the case that single phonon emission/absorption is no longer kinematically viable, i.e. the DM cannot generate momentum tranfers large enough to satisfy the phonon dispersion relation, $\omega(q)$. When this happens, the next leading process will be the multi-phonon processes such as scattering. If the system contains a trilinear phonon coupling, then it is no longer linear and things get messy.

Need to make sure we are below the melting temperature, as around there the single phonon approximation breaks down and need to go to larger number of phonon exchanges.

Appendix C

Collective Effects

C.1 Thermal Field Theory Redux

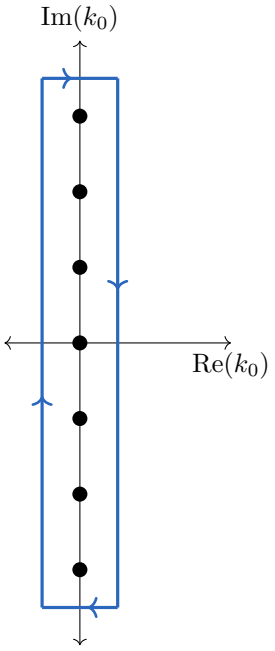

(a) Contour for Boson Matsubara sums

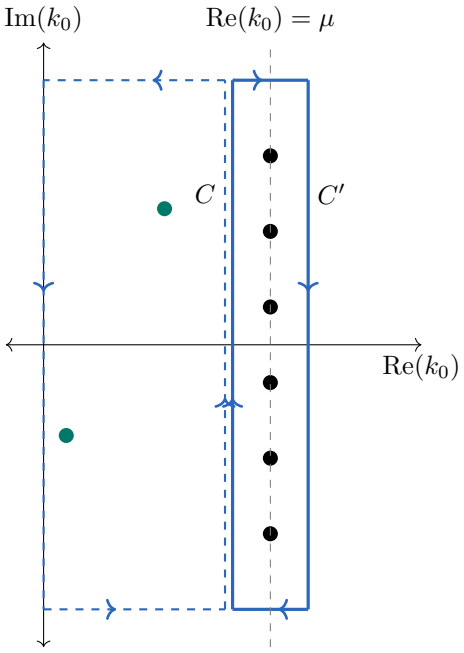

(b) Contours for Fermion Matsubara sums. Green dots are possible poles of $f(k_0)$.

Figure C.1: Contours for evaluating the integral. Notice that (b) does not encompass the pole at $i\delta$.

For fermions, the sum can be performed by using the fact that $1/(\exp(\beta(k_0-\mu))+1)$ has poles at $k_0 = (2n+1)\pi i T + \mu$. Then as before, the sum over the Matsubara modes can be written as

$$T\sum_n f(i\omega_n+\mu) = \frac{1}{2\pi i}\oint_{C'} \frac{f(k_0)dk_0}{\exp(\beta(k_0-\mu))+1} \tag{C.1.1}$$

$$= \frac{1}{2\pi i}\int_{-i\infty+\mu-\epsilon}^{i\infty+\mu-\epsilon} \frac{f(k_0)dk_0}{\exp(\beta(k_0-\mu))+1} + \frac{1}{2\pi i}\int_{i\infty+\mu+\epsilon}^{-i\infty+\mu+\epsilon} \frac{f(k_0)dk_0}{\exp(\beta(k_0-\mu))+1} \tag{C.1.2}$$

$$= \frac{1}{2\pi i}\int_{-i\infty+\mu-\epsilon}^{i\infty+\mu-\epsilon} \left(f(k_0) - \frac{f(k_0)}{\exp(\beta(\mu-k_0))+1}\right) dk_0 - \frac{1}{2\pi i}\int_{-i\infty+\mu+\epsilon}^{i\infty+\mu+\epsilon} \frac{f(k_0)dk_0}{\exp(\beta(k_0-\mu))+1} \tag{C.1.3}$$

$$= \frac{1}{2\pi i}\left[\oint_C - \int_{i\infty}^{-i\infty}\right] f(k_0)dk_0 - \frac{1}{2\pi i}\int_{-i\infty+\mu-\epsilon}^{i\infty+\mu-\epsilon} \frac{f(k_0)dk_0}{\exp(\beta(\mu-k_0))+1} - \frac{1}{2\pi i}\int_{-i\infty+\mu+\epsilon}^{i\infty+\mu+\epsilon} \frac{f(k_0)dk_0}{\exp(\beta(k_0-\mu))+1} \tag{C.1.4}$$

$$= \frac{1}{2\pi i}\int_{-i\infty}^{i\infty} f(k_0)dk_0 + \frac{1}{2\pi i}\oint_C f(k_0)dk_0 \tag{C.1.5}$$

$$- \frac{1}{2\pi i}\left[\int_{-i\infty+\mu-\epsilon}^{i\infty+\mu-\epsilon} \frac{f(k_0)dk_0}{\exp(\beta(\mu-k_0))+1} + \int_{-i\infty+\mu+\epsilon}^{i\infty+\mu+\epsilon} \frac{f(k_0)dk_0}{\exp(\beta(k_0-\mu))+1}\right] \tag{C.1.6}$$

where the first term is the zero-temperature, zero-density contribution, the second now accounts for finite densities, and the last two terms account for particle and anti-particle contributions at finite temperatures and densities.

Appendix D

Misc. Notes

D.1 To Do List

D.1.1 List

- Look into axions in NS magnetic fields, is there room to expand with our capture formalism?
- Look into cooling codes for NS/WD (Sandra has one for WDs) that can be modified to include DM effects

D.1.2 DM Annihilation

Should change/compare the annihilation rates using the relativistic expressions for thermal average

$$\langle \sigma_{ann} v \rangle = \frac{1}{8 m_\chi^4 T K_2^2(m_\chi/T)} \int_{4m_\chi^4}^{\infty} ds\ (s - 4m_\chi^2) \sqrt{s} \sigma_{ann} K_1(\sqrt{s}/T) \tag{D.1.1}$$

where the K_i are modified Bessel functions of order i.

References

[1] Javier F. Acevedo and Joseph Bramante. "Supernovae Sparked By Dark Matter in White Dwarfs". In: *Phys. Rev. D* 100.4 (2019), p. 043020. DOI: 10.1103/PhysRevD.100.043020. arXiv: 1904.11993 [hep-ph].

[2] Stephen L. Adler. "Planet-bound dark matter and the internal heat of Uranus, Neptune, and hot-Jupiter exoplanets". In: *Phys. Lett. B* 671 (2009), pp. 203–206. DOI: 10.1016/j.physletb.2008.12.023. arXiv: 0808.2823 [astro-ph].

[3] Kaustubh Agashe et al. "(In)direct Detection of Boosted Dark Matter". In: *JCAP* 10 (2014), p. 062. DOI: 10.1088/1475-7516/2014/10/062. arXiv: 1405.7370 [hep-ph].

[4] D. A. Baiko and D. G. Yakovlev. "Thermal and electric conductivities of Coulomb crystals in neutron stars and white dwarfs". In: *Astron. Lett.* 21 (1995), p. 709. arXiv: astro-ph/9604164.

[5] D. A. Baiko et al. "Coulomb crystals in the harmonic lattice approximation". In: *Phys. Rev. E* 61 (2 Feb. 2000), pp. 1912–1919. DOI: 10.1103/PhysRevE.61.1912. URL: https://link.aps.org/doi/10.1103/PhysRevE.61.1912.

[6] D. A. Baiko et al. "Ion structure factors and electron transport in dense Coulomb plasmas". In: *Phys. Rev. Lett.* 81 (1998), pp. 5556–5559. DOI: 10.1103/PhysRevLett.81.5556. arXiv: physics/9811052.

[7] Brian Batell et al. "Thermal Dark Matter Through the Dirac Neutrino Portal". In: *Phys. Rev. D* 97.7 (2018), p. 075016. DOI: 10.1103/PhysRevD.97.075016. arXiv: 1709.07001 [hep-ph].

[8] Nicole F. Bell et al. "Improved Treatment of Dark Matter Capture in Neutron Stars". In: *JCAP* 09 (2020), p. 028. DOI: 10.1088/1475-7516/2020/09/028. arXiv: 2004.14888 [hep-ph].

[9] Nicole F. Bell et al. "W/Z Bremsstrahlung as the Dominant Annihilation Channel for Dark Matter". In: *Phys. Rev. D* 83 (2011), p. 013001. DOI: 10.1103/PhysRevD.83.013001. arXiv: 1009.2584 [hep-ph].

[10] Jeffrey M. Berryman et al. "Lepton-Number-Charged Scalars and Neutrino Beamstrahlung". In: *Phys. Rev. D* 97.7 (2018), p. 075030. DOI: 10.1103/PhysRevD.97.075030. arXiv: 1802.00009 [hep-ph].

[11] Bridget Bertoni, Ann E. Nelson, and Sanjay Reddy. "Dark Matter Thermalization in Neutron Stars". In: *Phys. Rev.* D88 (2013), p. 123505. DOI: 10.1103/PhysRevD.88.123505. arXiv: 1309.1721 [hep-ph].

[12] Bridget Bertoni et al. "Constraints and consequences of reducing small scale structure via large dark matter-neutrino interactions". In: *JHEP* 04 (2015), p. 170. DOI: 10.1007/JHEP04(2015)170. arXiv: 1412.3113 [hep-ph].

[13] M. Blennow et al. "Neutrino Portals to Dark Matter". In: *Eur. Phys. J. C* 79.7 (2019), p. 555. DOI: 10.1140/epjc/s10052-019-7060-5. arXiv: 1903.00006 [hep-ph].

[14] Giorgio Busoni et al. "Evaporation and scattering of momentum- and velocity-dependent dark matter in the Sun". In: *JCAP* 10 (2017), p. 037. DOI: 10.1088/1475-7516/2017/10/037. arXiv: 1703.07784 [hep-ph].

[15] Hai-Yang Cheng. "Scalar and Pseudoscalar Higgs Couplings with Nucleons". In: *Nucl. Phys. B Proc. Suppl.* 246-247 (2014). Ed. by W.-Y. Pauchy Hwang and Guey-Lin Lin, pp. 109–115. DOI: 10.1016/j.nuclphysbps.2013.10.073.

[16] John F. Cherry, Alexander Friedland, and Ian M. Shoemaker. "Neutrino Portal Dark Matter: From Dwarf Galaxies to IceCube". In: (Nov. 2014). arXiv: 1411.1071 [hep-ph].

[17] Anirban Das et al. "Stellar Shocks From Dark Matter". In: (June 2021). arXiv: 2106.09033 [hep-ph].

[18] Basudeb Dasgupta, Aritra Gupta, and Anupam Ray. "Dark matter capture in celestial objects: light mediators, self-interactions, and complementarity with direct detection". In: *JCAP* 10 (2020), p. 023. DOI: 10.1088/1475-7516/2020/10/023. arXiv: 2006.10773 [hep-ph].

[19] Savas Dimopoulos et al. "Getting a Charge Out of Dark Matter". In: *Phys. Rev. D* 41 (1990), p. 2388. DOI: 10.1103/PhysRevD.41.2388.

[20] John R. Ellis, Keith A. Olive, and Christopher Savage. "Hadronic Uncertainties in the Elastic Scattering of Supersymmetric Dark Matter". In: *Phys. Rev. D* 77 (2008), p. 065026. DOI: 10.1103/PhysRevD.77.065026. arXiv: 0801.3656 [hep-ph].

[21] Peter W. Graham et al. "White Dwarfs as Dark Matter Detectors". In: *Phys. Rev. D* 98.11 (2018), p. 115027. DOI: 10.1103/PhysRevD.98.115027. arXiv: 1805.07381 [hep-ph].

[22] M.E. Gusakov, P. Haensel, and E.M. Kantor. "Physics input for modelling superfluid neutron stars with hyperon cores". In: *Mon. Not. Roy. Astron. Soc.* 439.1 (2014), pp. 318–333. DOI: 10.1093/mnras/stt2438. arXiv: 1401.2827 [astro-ph.HE].

[23] Syuhei Iguro, Shohei Okawa, and Yuji Omura. "Light lepton portal dark matter meets the LHC". In: (Aug. 2022). arXiv: 2208.05487 [hep-ph].

[24] M. Kawasaki, H. Murayama, and T. Yanagida. "Can the strongly interacting dark matter be a heating source of Jupiter?" In: *Prog. Theor. Phys.* 87 (1992), pp. 685–692. DOI: 10.1143/PTP.87.685.

[25] Kevin J. Kelly et al. "Probing neutrino-portal dark matter at the Forward Physics Facility". In: *Phys. Rev. D* 105.7 (2022), p. 075026. DOI: 10.1103/PhysRevD.105.075026. arXiv: 2111.05868 [hep-ph].

[26] Charles Kittel and Ching-yao Fong. *Quantum theory of solids*. Vol. 5. Wiley New York, 1963.

[27] Lawrence M. Krauss, Mark Srednicki, and Frank Wilczek. "Solar System Constraints and Signatures for Dark Matter Candidates". In: *Phys. Rev. D* 33 (1986), pp. 2079–2083. DOI: 10.1103/PhysRevD.33.2079.

[28] Rebecca K. Leane and Tim Linden. "First Analysis of Jupiter in Gamma Rays and a New Search for Dark Matter". In: (Apr. 2021). arXiv: 2104.02068 [astro-ph.HE].

[29] Rebecca K. Leane and Juri Smirnov. "Exoplanets as Sub-GeV Dark Matter Detectors". In: *Phys. Rev. Lett.* 126.16 (2021), p. 161101. DOI: 10.1103/PhysRevLett.126.161101. arXiv: 2010.00015 [hep-ph].

[30] Rebecca K. Leane et al. "Celestial-Body Focused Dark Matter Annihilation Throughout the Galaxy". In: *Phys. Rev. D* 103.7 (2021), p. 075030. DOI: 10.1103/PhysRevD.103.075030. arXiv: 2101.12213 [astro-ph.HE].

[31] Ang Liu et al. "Sterile Neutrino Portal Dark Matter in νTHDM". In: (May 2022). arXiv: 2205.11846 [hep-ph].

[32] R. Mertig, M. Böhm, and A. Denner. "Feyn Calc - Computer-algebraic calculation of Feynman amplitudes". In: *Computer Physics Communications* 64.3 (1991), pp. 345–359. ISSN: 0010-4655. DOI: https://doi.org/10.1016/0010-4655(91)90130-D. URL: https://www.sciencedirect.com/science/article/pii/001046559190130D.

[33] Saibal Mitra. "Uranus' anomalously low excess heat constrains strongly interacting dark matter". In: *Phys. Rev. D* 70 (2004), p. 103517. DOI: 10.1103/PhysRevD.70.103517. arXiv: astro-ph/0408341.

[34] Takumi Miyagi and Takashi Toma. "Semi-annihilating dark matter coupled with Majorons". In: *JHEP* 07 (2022), p. 027. DOI: 10.1007/JHEP07(2022)027. arXiv: 2201.05412 [hep-ph].

[35] Shohei Okawa and Yuji Omura. "Light mass window of lepton portal dark matter". In: *JHEP* 02 (2021), p. 231. DOI: 10.1007/JHEP02(2021)231. arXiv: 2011.04788 [hep-ph].

[36] Hiren H. Patel. "Package-X: A Mathematica package for the analytic calculation of one-loop integrals". In: *Comput. Phys. Commun.* 197 (2015), pp. 276–290. DOI: 10.1016/j.cpc.2015.08.017. arXiv: 1503.01469 [hep-ph].

[37] Michael Rotondo et al. "The Relativistic Feynman-Metropolis-Teller theory for white dwarfs in general relativity". In: *Phys. Rev. D* 84 (2011), p. 084007. DOI: 10.1103/PhysRevD.84.084007. arXiv: 1012.0154 [astro-ph.SR].

[38] Irina Sagert et al. "Compact stars for undergraduates". In: *Eur. J. Phys.* 27 (2006), pp. 577–610. DOI: 10.1088/0143-0807/27/3/012. arXiv: astro-ph/0506417 [astro-ph].

[39] P.E. Shanahan, A.W. Thomas, and R.D. Young. "Scale setting, sigma terms and the Feynman-Hellman theorem". In: *PoS* LATTICE2012 (2012). Ed. by Derek Leinweber et al., p. 165. DOI: 10.22323/1.164.0165. arXiv: 1301.3231 [hep-lat].

[40] P.E. Shanahan, A.W. Thomas, and R.D. Young. "Sigma terms from an SU(3) chiral extrapolation". In: *Phys. Rev. D* 87 (2013), p. 074503. DOI: 10.1103/PhysRevD.87.074503. arXiv: 1205.5365 [nucl-th].

[41] S. L. Shapiro and S. A. Teukolsky. *Black holes, white dwarfs, and neutron stars: The physics of compact objects*. 1983. ISBN: 978-0-471-87316-7.

[42] Vladyslav Shtabovenko, Rolf Mertig, and Frederik Orellana. "FeynCalc 9.3: New features and improvements". In: *Comput. Phys. Commun.* 256 (2020), p. 107478. DOI: 10.1016/j.cpc.2020.107478. arXiv: 2001.04407 [hep-ph].

[43] Vladyslav Shtabovenko, Rolf Mertig, and Frederik Orellana. "New Developments in FeynCalc 9.0". In: *Comput. Phys. Commun.* 207 (2016), pp. 432–444. DOI: 10.1016/j.cpc.2016.06.008. arXiv: 1601.01167 [hep-ph].

[44] J.L. Zdunik, M. Fortin, and P. Haensel. "Neutron star properties and the equation of state for the core". In: *Astron. Astrophys.* 599 (2017), A119. DOI: 10.1051/0004-6361/201629975. arXiv: 1611.01357 [astro-ph.HE].

[45] Andrew R. Zentner and Andrew P. Hearin. "Asymmetric Dark Matter May Alter the Evolution of Low-mass Stars and Brown Dwarfs". In: *Phys. Rev. D* 84 (2011), p. 101302. DOI: 10.1103/PhysRevD.84.101302. arXiv: 1110.5919 [astro-ph.CO].